OPTICAL WAVE PROPAGATION

Bruno Crosignani

California Institute of Technology

Lecture notes for EE/APh 131 , Winter 2013

Reference texts : (1) A. Yariv, "Optical Electronics in Modern Communications", Oxford Press 1997 , (2) A. Yariv and P. Yeh, "Photonics: Optical Electronics in Modern Communications", Oxford Press, 2007, and (3)S. Solimeno, B. Crosignani and P. Di Porto, "Guiding, Diffraction and Confinement of Optical Radiation", Academic Press, 1986.

1 Deterministic electromagnetic fields

1.1 Microscopic Maxwell's equations
1.2 The general problem
1.3 Propagation of EM field in the absence of charges and currents
1.4 Monochromatic fields
1.5 Paraxial approximation
1.6 Energy Flux
1.7 The paraxial Gaussian beam
1.8 The parabolic equation
1.9 The general non-paraxial case
1.10 Diffraction by an aperture
1.11 Non diffracting fields
1.12 Propagation of EM fields in matter, macroscopic Maxwell's equations
1.13 Propagation in non-homogeneous media
1.14 Light confinement in optical resonators

2 EM field as a statistical variable

2.1 Introduction

2.2 Spatial and temporal coherence of EM fields
2.3 Application to stellar interferometry
2.4 Laser spectrum

3 Guided Optical propagation

3.1 Simple geometric optics approach
3.2 Physical optics approach
3.3 Modal dispersion
3.4 Chromatic dispersion
3.5 Optical communication: Single-mode and multimode fibers
3.6 Single-mode regime
3.7 Graded-index fibers
3.8 Planar dielectric waveguides

4 Nonlinear Optics

4.1 Second-harmonic generation
4.2 Optical Kerr-effect
4.3 Soliton propagation

1 Introduction

What is a wave? Is out there a supporting medium? Why "optical"? Actually, if one considers propagation in vacuum, that is in empty space, in the absence of any charge or current, there is no difference between propagation of light or radio-waves (vacuum does not possesses any intrinsic space or time scale). Things are different if propagation takes place in the presence of a material medium, be it discrete or continuous, since the radiation-matter interaction is frequency dependent.
Propagation in vacuum has a fundamental character; conversely, propagation in a standard material medium, made up of a large number of atoms is mostly described in a phenomenological way, being based on the introduction of macroscopic quantities, like the *dielectric constant* and the *refractive index* (or index of refraction), which results from having taken spatial averages over volumes of suitable dimensions.
However, if energy dissipation associated with interaction between electromagnetic waves and matter can be neglected, and for monochromatic waves, a general description of propagation is still possible. This is no longer the case for polychromatic fields, resulting in different velocities of propagation for different frequencies (chromatic dispersion).

1.1 Microscopic Maxwell's equations

A marvelous synthesis of a number of apparently uncorrelated experimental observations, from the strange properties of amber (ελεκτρον, from which the name electricity) to Faraday's experiments, has been obtained by James Clerk Maxwell. Unlike the laws of mechanics, which Newton formulated as axioms and which successively explained a great number of natural phenomena, Maxwell's equations were the arrival-point of centuries of research.
All electromagnetic phenomena are described by two vector fields, $\mathbf{E}(\mathbf{r},t)$ (*electric field*) and $\mathbf{B}(\mathbf{r},t)$ (*magnetic induction*, which actually

would deserve to be called *magnetic field*). In the MKS system of units (Meter, Kilogram, Second and Coulomb) they read (in the beautiful formalism introduced by Oliver Heaviside)

$$\varepsilon_0 \nabla \cdot \mathbf{E} = \rho(\mathbf{r},t)$$
$$\nabla \cdot \mathbf{B} = 0$$
$$\nabla \times \mathbf{E} = -\frac{\partial \mathbf{B}}{\partial t} \qquad (1)$$
$$\nabla \times \mathbf{B} = \mu_0 \mathbf{j}(\mathbf{r},t) + \frac{1}{c^2}\frac{\partial \mathbf{E}}{\varepsilon \partial t}$$

where ∇ , the so-called "nabla" operator is (in Cartesian coordinates)

$$\nabla = \hat{\mathbf{x}}\partial_x + \hat{\mathbf{y}}\partial_y + \hat{\mathbf{z}}\partial_z .$$

In the above equations, c is the velocity of light in vacuum, ε_0 and μ_0 (such that $\varepsilon_0\mu_0 = 1/c^2$) the *electric* and *magnetic permeability* of vacuum (to be found experimentally), while ρ and **j** are the *charge* and *current* densities (see Eq.(3)). In particular, one has $\varepsilon_0 = (e^2/2\alpha hc)$, where e is the electron charge, h the Planck constant and α the fine-structure constant.

The physical meaning of **E** and **B** is provided by their relation with the force **F** exerted on a point-like charge q (Lorentz force), that is

$$\mathbf{F}(\mathbf{r},t) = q\mathbf{E}(\mathbf{r},t) + \frac{q}{c}\mathbf{v} \times \mathbf{B}(\mathbf{r},t) \ , \quad (2)$$

where **r** is the position and **v** is the velocity of the point-like charge.

1.2 The general problem

The general problem one has to face is to find the solution of the set of Eqs.(1) in the presence of a given set of charged particles subject to the

influence of an electromagnetic field to which they are exposed and which they also generate.
One writes

$$\rho(\mathbf{r},t)=\sum_i q_i \delta[\mathbf{r}-\mathbf{r}_i(t)], \quad \mathbf{j}(\mathbf{r},t)=\sum_i q_i \dot{\mathbf{r}}_i(t)\delta[\mathbf{r}-\mathbf{r}_i(t)], \quad (3)$$

where $\delta(\mathbf{r})$ is the Dirac delta-function, q_i being the charge of the i-th particle and $\mathbf{r}_i(t)$ its trajectory under the influence of the Lorentz force, the trajectories having to obey Newton's equation of motion.
The solution of this problem presents enormous difficulties and simplifying hypotheses are required in order to be able to deal with it.
Before proceeding, it is important to notice that Maxwell's equations are consistent with *charge conservation*. In fact, by taking the divergence of both sides of Eq.$(1)_4$ and recalling the vector identity

$$\nabla \cdot \nabla \times \mathbf{A} = 0 \,, \qquad (4)$$

one has (see Fig.1)

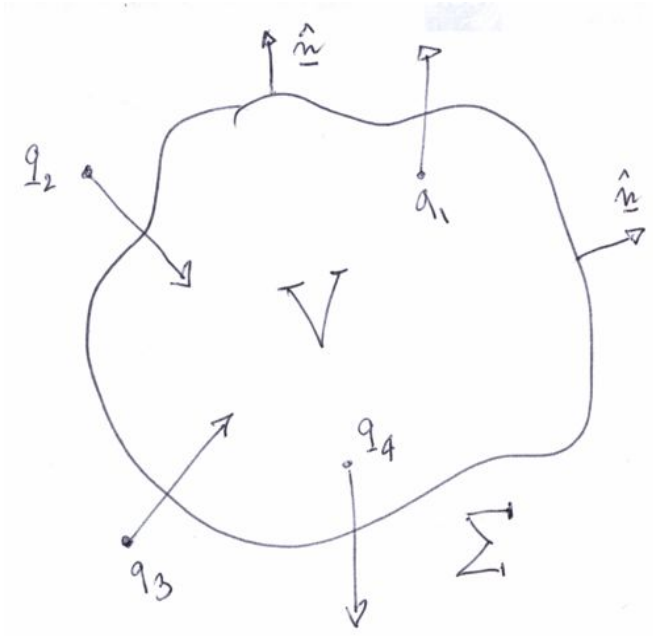

Fig. 1 Charge conservation

$$\nabla \cdot \mathbf{j} + \frac{\partial \rho}{\partial t} = 0 \,, \quad (5)$$

which implies charge conservation, as it can be easily proved by recalling *Gauss theorem*

$$\int_V \nabla \cdot \mathbf{A}\, d\mathbf{r} = -\int_\Sigma \mathbf{A} \cdot \hat{\mathbf{n}}\, d\sigma \ , \quad (6)$$

which, if applied to Eq.(5), implies

$$\frac{\partial}{\partial t}\int_V \rho\, d\mathbf{r} = -\int_\Sigma \mathbf{j} \cdot \hat{\mathbf{n}} d\sigma \ , \quad (7)$$

which expresses indeed charge conservation.

It is worth to note that the number of unknowns in the set of Eqs.(1), that is E_x , E_y , E_z , B_x , B_y and B_z , is less than the number of equations (eight, two vectorial plus two scalars).
Actually, for non-stationary situations ($\partial / \partial t \neq 0$), the number of unknowns is equal to the number of independent equations since the two "divergence" equations are a consequence of the two 'curl" equations.
In the stationary case ($\partial / \partial t = 0$), Maxwell's equations decouple in two separate set of equations for **E** and **B** which describes *Electrostatics* and *Magnetostatics*.

ELECTROSTATICS

$$\nabla \times \mathbf{E} = 0 \ \rightarrow \ \mathbf{E} = -\nabla\phi$$

$$\rho = \varepsilon_0 \nabla \cdot \mathbf{E} = -\varepsilon_0 \nabla \cdot \nabla\phi = -\varepsilon_0 \nabla^2 \phi \qquad (8)$$

$$\nabla^2 \phi = -\rho / \varepsilon_0 \quad \text{(Poisson equation)}$$

MAGNETOSTATICS

$$\nabla \cdot \mathbf{B} = 0 \;\rightarrow\; \mathbf{B} = \nabla \times \mathbf{A}$$
$$\mu_0 \mathbf{j} = \nabla \times (\nabla \times \mathbf{A}) = \nabla \nabla \cdot \mathbf{A} - \nabla^2 \mathbf{A} \qquad (9)$$

or, after choosing $\nabla \cdot \mathbf{A} = 0$,

$$\nabla^2 \mathbf{A} = -\mu_0 \mathbf{j}.$$

FOURIER TRANSFORM

The Fourier transform is a mathematical tool which allows to represent a wide class of summable functions as a superposition of sines and cosines. Given, within this class, a generic function f(t), real or imaginary, of a real variable t, the Fourier transform is defined for real values of ω (the sign of the exponential and the coefficient in front of the integral can be chosen arbitrarily) as

$$\tilde{f}(\omega) = \frac{1}{2\pi} \int_{-\infty}^{+\infty} e^{i\omega t} f(t) dt . \qquad (10)$$

It is possible to prove that Eq.(10) can be inverted to give

$$f(t) = \int_{-\infty}^{+\infty} e^{-i\omega t} \tilde{f}(\omega) d\omega . \qquad (11)$$

In particular, if f(t)=δ(t), δ(t) being the Dirac delta-function , equal to zero for t different to zero but such that its integral over t from -∞ to +∞ is equal to one, one has

$$\tilde{\delta}(\omega) = \frac{1}{2\pi} \quad , \quad \delta(t) = \frac{1}{2\pi} \int_{-\infty}^{+\infty} e^{-i\omega t} d\omega . \qquad (12)$$

In general $\tilde{f}(\omega)$ is complex also if f(t) is real. However, if this is the case, it can be easily proved that $\tilde{f}^*(\omega)=\tilde{f}(-\omega)$, so that the information about the Fourier transform is contained either in the values $\omega \geq 0$ or in the values $\omega \leq 0$. This suggests to introduce a new function, called the "analytic signal" which contains the same information as f(t), defined as

$$\hat{f}(t) = 2\int_0^{+\infty} e^{-i\omega t}\tilde{f}(\omega)d\omega, \quad (13)$$

which allows to express f as the real part of the analytic signal, that is

$$f(t)=\frac{1}{2}[\hat{f}(t)+\hat{f}^*(t)] \ . \quad (14)$$

For example,

$$f(t) = \cos(\omega_0 t) \ \rightarrow \ \tilde{f}(\omega)=\frac{1}{2}[\delta(\omega-\omega_0)+\delta(\omega+\omega_0)]$$

$$\hat{f}(t) = e^{-i\omega_0 t} \quad \text{(complex representation).}$$

The concept of Fourier transform can be straightforwardly generalized to more that one dimension.
A remarkable property of the Fourier transform, very useful in the frame of linear processes, is the convolution theorem:

$$\textit{if} \quad f(t)=\int_{-\infty}^{+\infty} g(t')h(t-t')dt' \ ,$$

$$\text{then,} \quad \tilde{f}(\omega)=2\pi\tilde{g}(\omega)\tilde{h}(\omega) \ . \quad (15)$$

1.3 Propagation of EM fields in the absence of charges and currents (vacuum)

The set of Maxwell's equations in a region hosting no charge and currents is linear and reads

$$\nabla \cdot \mathbf{E} = 0$$
$$\nabla \cdot \mathbf{B} = 0 , \qquad (16)$$
$$\nabla \times \mathbf{E} = -\frac{\partial \mathbf{B}}{\partial t} \qquad c = 1/\sqrt{\varepsilon_0 \mu_0}$$
$$\nabla \times \mathbf{B} = \frac{1}{c^2}\frac{\partial \mathbf{E}}{\partial t} . \quad (17)$$

The linearity of the system suggests to perform the time Fourier - transform of the above set of equations, thus getting

$$\nabla \cdot \tilde{\mathbf{E}}(\mathbf{r},\omega) = 0$$
$$\nabla \cdot \tilde{\mathbf{B}}(\mathbf{r},\omega) = 0 , \quad (18)$$

$$\nabla \times \tilde{\mathbf{E}}(\mathbf{r},\omega) = i\omega \tilde{\mathbf{B}}(\mathbf{r},\omega)$$
$$\nabla \times \tilde{\mathbf{B}}(\mathbf{r},\omega) = -i\frac{\omega}{c^2}\tilde{\mathbf{E}}(\mathbf{r},\omega) . \quad (19)$$

Finding a particular (specific) solution of the above linear system of equations requires either boundary conditions or initial conditions , that is knowledge of the field at all times in some region of space or at a specific time in the whole space. In the present context, having particularly in mind the propagation of *transversely-localized* fields, we assume to know the electromagnetic field on a plane (e.g., z=0) at all times and also require it to go to zero sufficiently fast in the direction transverse to z.
Applying the operator $\nabla\times$ to both sides of Eq. $(18)_1$, exploiting the vector identity

$$\nabla \times (\nabla \times \mathbf{A}) = \nabla\nabla \cdot \mathbf{A} - \nabla^2 \mathbf{A} \quad , \quad (20)$$

(valid for any vector **A**) and using Eq. $(19)_2$ one finally obtains

$$\nabla^2 \tilde{\mathbf{E}} - \nabla(\nabla \cdot \tilde{\mathbf{E}}) = -\frac{\omega^2}{c^2} \tilde{\mathbf{E}}(\mathbf{r},\omega) \quad , \quad (21)$$

which, recalling Eq. $(18)_1$, becomes the celebrated Helmholtz equation

$$\left(\frac{\partial^2}{\partial x^2} + \frac{\partial^2}{\partial y^2} + \frac{\partial^2}{\partial z^2}\right)\tilde{\mathbf{E}}(\mathbf{r},\omega) + \frac{\omega^2}{c^2}\tilde{\mathbf{E}}(\mathbf{r},\omega) = \nabla^2 \tilde{\mathbf{E}}(\mathbf{r},\omega) + \frac{\omega^2}{c^2}\tilde{\mathbf{E}}(\mathbf{r},\omega) = 0 \quad . \quad (22)$$

Equation (22) is a *scalar* one and involves separately the x, y, and z components of the electric field. Once solved, the magnetic field can be worked out from Eq. $(19)_1$, that is

$$\tilde{\mathbf{B}}(\mathbf{r},\omega) = \frac{1}{i\omega} \nabla \times \tilde{\mathbf{E}}(\mathbf{r},\omega) \quad . \quad (23)$$

Helmholtz equation can be rewritten, after introducing the wave number k and the wavelength λ defined by the relations

$$k = \frac{\omega}{c} = \frac{2\pi}{\lambda} \quad , \quad (24)$$

as

$$\nabla^2 \tilde{\mathbf{E}}(\mathbf{r},\omega) + k^2 \tilde{\mathbf{E}}(\mathbf{r},\omega) = 0 \quad . \quad (25)$$

Once this equation is solved, one has to impose *a posteriori* the solenoidal condition dictated by Eq.$(18)_1$, that is

$$\nabla \cdot \tilde{\mathbf{E}}(\mathbf{r},\omega) = 0 \quad . \quad (26)$$

We look for a solution of the form

$$\tilde{\mathbf{E}}(\mathbf{r}_\perp, z, \omega) = \int_{-\infty}^{+\infty} d\mathbf{k}_\perp e^{i\mathbf{k}_\perp \cdot \mathbf{r}_\perp} \mathbf{F}(\mathbf{k}_\perp, z, \omega) \quad , (27)$$

where $\mathbf{k}_\perp \equiv (k_x, k_y)$ and $\mathbf{r}_\perp \equiv (x,y)$, which requires, for the very existence of the Fourier transform, the electric field to vanish fast enough for $r_\perp \to \infty$. We have also privileged the z-axis since we assume to know the field on the plane z=0. Inserting Eq. (27) into Eq.(25) yields

$$\frac{\partial^2}{\partial z^2}\mathbf{F} + (k^2 - k_\perp^2)\mathbf{F} = 0 \quad , \quad (28)$$

whose solution reads

$$\mathbf{F}(\mathbf{k}_\perp, z, \omega) = \mathbf{F}^{(+)}(\mathbf{k}_\perp, \omega) e^{iz\sqrt{k^2 - k_\perp^2}} + \mathbf{F}^{(-)}(\mathbf{k}_\perp, \omega) e^{-iz\sqrt{k^2 - k_\perp^2}} , \quad (29)$$

both for $k_\perp^2 \le k^2$ and $k_\perp^2 \ge k^2$. By inserting it into Eq. (27), we get the general solution of Helmholtz equation in the form

$$\tilde{\mathbf{E}}(\mathbf{r}_\perp, z, \omega) = \int_{-\infty}^{+\infty} d\mathbf{k}_\perp e^{i\mathbf{k}_\perp \cdot \mathbf{r}_\perp} [\mathbf{F}^{(+)}(\mathbf{k}_\perp, \omega) e^{iz\sqrt{k^2 - k_\perp^2}} + \mathbf{F}^{(-)}(\mathbf{k}_\perp, \omega) e^{-iz\sqrt{k^2 - k_\perp^2}}]$$

(30)

By inspecting Eq. (30) we can check that $\tilde{\mathbf{E}}^{(+)}(\mathbf{r}_\perp, z, \omega)$, $\tilde{\mathbf{E}}^{(-)}(\mathbf{r}_\perp, z, \omega)$ are made up, for $k_\perp^2 \le k^2$, of forward and backward *propagating waves* , respectively, while, for $k_\perp^2 \ge k^2$, these waves, the so-called *evanescent waves*, are either attenuated or amplified along the z-axis. The dependence of the field on $\mathbf{r}_\perp$ is contained in the factor

$$e^{i\mathbf{k}_\perp \cdot \mathbf{r}_\perp} = e^{ik(\mathbf{k}_\perp / k) \cdot \mathbf{r}_\perp} = e^{2\pi i(\mathbf{k}_\perp / \lambda k) \cdot \mathbf{r}_\perp}$$

whose spatial period $\lambda k/|\mathbf{k}_\perp|)l$ in the transverse plane x,y is much larger or much smaller than l according whether $|\mathbf{k}_\perp| << k$ or $|\mathbf{k}_\perp| >> k$. As a result, those of the plane waves making up the *wave-packet* such that $|\mathbf{k}_\perp| << k$ are responsible for "carrying" the spatial details larger than λ, those with $|\mathbf{k}_\perp| >> k$, corresponding to $\sqrt{k^2 - k_\perp^2}$ imaginary, for "carrying" details smaller than λ.

Let us consider the case in which only the forward traveling field $\tilde{\mathbf{E}}^{(+)}$ is excited, so that

$$\tilde{\mathbf{E}}(\mathbf{r}_\perp, z, \omega) = \tilde{\mathbf{E}}^{(+)}(\mathbf{r}_\perp, z, \omega) = \int_{-\infty}^{+\infty} d\mathbf{k}_\perp e^{i\mathbf{k}_\perp \cdot \mathbf{r}_\perp + iz\sqrt{k^2 - k_\perp^2}} \mathbf{F}^{(+)}(\mathbf{k}_\perp, \omega). \quad (31)$$

By requiring Eq.(31) to obey the divergence equation expressed by Eq. $(19)_1$ implies

$$\mathbf{k}_\perp \cdot \mathbf{F}_\perp^{(+)} + \sqrt{k^2 - k_\perp^2} F_z^{(+)} = 0 \rightarrow F_z^{(+)} = -\frac{\mathbf{k}_\perp \cdot \mathbf{F}_\perp^{(+)}}{\sqrt{k^2 - k_\perp^2}} . \quad (32)$$

Accordingly, the solution of Helmholtz equation which also satisfies Maxwell's equations is (omitting for sake of simplicity the superfix (+))

$$\tilde{\mathbf{E}}_\perp(\mathbf{r}_\perp, z, \omega) = \int_{-\infty}^{+\infty} d\mathbf{k}_\perp e^{i\mathbf{k}_\perp \cdot \mathbf{r}_\perp + iz\sqrt{k^2 - k_\perp^2}} \mathbf{F}_\perp(\mathbf{k}_\perp, \omega)$$

$$\tilde{E}_z(\mathbf{r}_\perp, z, \omega) = -\int_{-\infty}^{+\infty} d\mathbf{k}_\perp e^{i\mathbf{k}_\perp \cdot \mathbf{r}_\perp + iz\sqrt{k^2 - k_\perp^2}} \frac{\mathbf{k}_\perp \cdot \mathbf{F}_\perp(\mathbf{k}_\perp, \omega)}{\sqrt{k^2 - k_\perp^2}} . \quad (33)$$

In the time domain the electric field **E**, a real physical quantity, is thus given by the *wave-packet*

$$\mathbf{E}_\perp(\mathbf{r}_\perp, z, t) = \int_{-\infty}^{+\infty} d\omega\, e^{-i\omega t} \int_{-\infty}^{+\infty} d\mathbf{k}_\perp e^{i\mathbf{k}_\perp \cdot \mathbf{r}_\perp + iz\sqrt{k^2 - k_\perp^2}} \mathbf{F}_\perp(\mathbf{k}_\perp, \omega) \quad (34)$$

$$E_z(\mathbf{r}_\perp,z,t) = -\int_{-\infty}^{+\infty} d\omega\, e^{-i\omega t} \int_{-\infty}^{+\infty} d\mathbf{k}_\perp e^{i\mathbf{k}_\perp\cdot\mathbf{r}_\perp + iz\sqrt{k^2-k_\perp^2}}\, \frac{\mathbf{k}_\perp\cdot\mathbf{F}_\perp(\mathbf{k}_\perp,\omega)}{\sqrt{k^2-k_\perp^2}}. \quad (35)$$

In order to find $\mathbf{F}(\mathbf{k}_\perp,\omega)$ it is necessary to know the transverse component of the electric field on the plane z=0 at all times. Setting z=0 in Eq. (34) and inverting the resulting relation yields

$$\mathbf{F}_\perp(k_\perp,\omega) = \frac{1}{(2\pi)^3}\int_{-\infty}^{+\infty} dt\, e^{i\omega t} \int_{-\infty}^{+\infty} dr_\perp e^{-i\mathbf{k}_\perp\cdot r_\perp}\mathbf{E}_\perp(r_\perp,z=0,t), \quad (36)$$

which can be inserted in Eqs.(34)-(35) to provide the complete solution of the problem in the space-time domain.
Note that the evanescent waves, responsible for carrying the information on the spatial details smaller than the wavelength λ,that is $|\mathbf{k}_\perp|>k$, are characterized by the factor $\exp(-z\sqrt{k_\perp^2-k^2})$ so that they attenuate on a spatial scale of the order of $1/|\sqrt{k_\perp^2-k^2}$): as a consequence, the small spatial detail carried by the field only survive for short, longitudinal distances, comparable with λ, which sets a natural limit to the possibility of using optical waves for transmission of information.

1.4 Monochromatic Fields

They are characterized by a field distribution at z=0 of the kind

$$\mathbf{E}_\perp(\mathbf{r}_\perp,z=0,t) = \mathrm{Re}[\tilde{\mathbf{E}}_\perp(\mathbf{r}_\perp,z=0)e^{-i\omega_0 t}], \quad (37)$$

so that

$$\mathbf{F}_\perp(\mathbf{k}_\perp,\omega) = \frac{1}{2}[\mathbf{F}_\perp(\mathbf{k}_\perp)\delta(\omega-\omega_0) + \mathbf{F}_\perp^*(-\mathbf{k}_\perp)\delta(\omega+\omega_0)] \quad (38)$$

where

$$\mathbf{F}_\perp(\mathbf{k}_\perp) = \frac{1}{(2\pi)^2}\int_{-\infty}^{+\infty} d\mathbf{r}_\perp e^{-i\mathbf{k}_\perp\cdot\mathbf{r}_\perp}\tilde{\mathbf{E}}_\perp(r_\perp, z=0). \quad (39)$$

By recalling Eqs.(34)-(35) we have ($k_0=\omega_0/c$)

$$\tilde{\mathbf{E}}_\perp(\mathbf{r}_\perp, z) = \int_{-\infty}^{+\infty} d\mathbf{k}_\perp e^{i\mathbf{k}_\perp\cdot\mathbf{r}_\perp + iz\sqrt{k_0^2-k_\perp^2}}\mathbf{F}_\perp(\mathbf{k}_\perp) \quad (40)$$

$$\tilde{E}_z(\mathbf{r}_\perp, z) = -\int_{-\infty}^{+\infty} d\mathbf{k}_\perp e^{i\mathbf{k}_\perp\cdot\mathbf{r}_\perp + iz\sqrt{k_0^2-k_\perp^2}}\frac{\mathbf{k}_\perp\cdot\mathbf{F}_\perp(\mathbf{k}_\perp)}{\sqrt{k_0^2-k_\perp^2}} \quad (41)$$

and

$$\mathbf{E}_\perp(\mathbf{r}_\perp, z, t) = \mathrm{Re}[\tilde{\mathbf{E}}_\perp(\mathbf{r}_\perp, z)e^{-i\omega_0 t}]$$
$$E_z(\mathbf{r}_\perp, z, t) = \mathrm{Re}[\tilde{E}_z(\mathbf{r}_\perp, z)e^{-i\omega_0 t}]. \quad (42)$$

1.5 Paraxial Approximation

The above expressions for the em field are "exact" but, in a sense, too general to be really useful. We will specialize them to describe propagation of beams whose width is much larger than the wavelength λ (0.4 – 0.7 μm for optical radiation), which is typically the case for obstacles and slits encountered in the macroscopic world.
Let us label by $\delta\mathbf{r}_\perp$ the width of the beam at z=0. According to the general property of the Fourier integral, $\mathbf{F}(\mathbf{k}_\perp)$ has, in the $\mathbf{k}_\perp$ - space, a width $\delta k_\perp \approx 1/\delta r_\perp$. If $\delta r_\perp >> \lambda$, then it follows that

$$\delta k_\perp << \frac{1}{\lambda} = k/2\pi \rightarrow \delta k_\perp/k << 1. \quad (43)$$

Eq. (43) implies that only the waves propagating almost parallel to the z-axis *(paraxial waves*) substantially contribute to propagation. In fact, labeling with $\theta(k_\perp)$ the angle between $\mathbf{k}$ and $\hat{\mathbf{z}}$ one has (at z=0), since

$$k^2 = k_\perp^2 + k_z^2, \quad \mathbf{k}\cdot\hat{z} = k\cos(\theta) = \sqrt{k^2 - k_\perp^2},$$

$$tg^2(\theta) = \frac{1-\cos^2(\vartheta)}{\cos^2(\theta)} = \frac{k_\perp^2}{k^2 - k_\perp^2} \cong \frac{k_\perp^2}{k^2} \rightarrow tg(\theta) = \frac{\delta k_\perp}{k} << 1. \quad (44)$$

This is the so-called *paraxial limit*, whose assumption allows one to restrict the $\mathbf{k}_\perp$ interval appearing in Eqs.(33) to values $|\mathbf{k}_\perp| < \delta k_\perp$ and, in turn, to take advantage of the expansion, valid for $|\mathbf{k}_\perp| < \delta k_\perp << k$,

$$\sqrt{k^2 - k_\perp^2} \approx k - \frac{k_\perp^2}{2k} \quad , \quad \frac{1}{\sqrt{k^2 - k_\perp^2}} \approx \frac{1}{k} + \frac{k_\perp^2}{2k^3} \quad . \quad (45)$$

Proceeding in this way yields

$$\tilde{\mathbf{E}}_\perp(\mathbf{r}_\perp, z) = e^{ikz} \int_{-\infty}^{+\infty} d\mathbf{k}_\perp e^{i\mathbf{k}_\perp\cdot\mathbf{r}_\perp} e^{-i(k_\perp^2 z/2k)} \mathbf{F}_\perp(\mathbf{k}_\perp) \,, \quad (46)$$

$$\tilde{E}_z(\mathbf{r}_\perp, z) = -e^{ikz} \int_{-\infty}^{+\infty} d\mathbf{k}_\perp e^{i\mathbf{k}_\perp\cdot\mathbf{r}_\perp} e^{-i(k_\perp^2 z/2k)} \frac{\mathbf{k}_\perp\cdot\mathbf{F}_\perp(\mathbf{k}_\perp)}{k},$$

having extended, since $\mathbf{F}_\perp(\mathbf{k}_\perp)$ is practically zero for $|\mathbf{k}_\perp| > \delta k_\perp$, the integral to the entire $\mathbf{k}_\perp$ space

Let us now define the slowly-varying envelope of the paraxial field as

$$\mathbf{A}_\perp(\mathbf{r}_\perp, z) \equiv \int_{-\infty}^{+\infty} d\mathbf{k}_\perp e^{i\mathbf{k}_\perp\cdot\mathbf{r}_\perp} e^{-i(k_\perp^2 z/2k)} \mathbf{F}_\perp(\mathbf{k}_\perp) \quad (47)$$

and write

$$\tilde{\mathbf{E}}_\perp(\mathbf{r}_\perp,z) = e^{ikz}\mathbf{A}_\perp(\mathbf{r}_\perp,z) \quad ,$$

$$E_z(\mathbf{r}_\perp,z) = -(i/k)e^{ikz}\nabla\cdot\mathbf{A}_\perp(\mathbf{r}_\perp,z) \quad , \qquad (48)$$

where exp(ikz) represents the plane-wave carrier and $\mathbf{A}(\mathbf{r}_\perp,z)$ the information-carrying slowly-varying amplitude. Note that while the plane-wave spatial scale is $2\pi/k=\lambda$, all the plane waves making up the envelope have a spatial scale

$$2k/k_\perp^2 = (2/k)(k^2/k_\perp^2) >> \lambda .$$

The paraxial field is a carrier (the plane wave), modulated by a function $\mathbf{A}_\perp$ containing the beam spatial information. Its longitudinal component can be in general neglected since

$$|\tilde{E}_z| = \frac{1}{k}|\nabla\cdot\mathbf{A}_\perp| \cong \frac{\delta\mathbf{k}_\perp}{k}|\mathbf{A}_\perp| << |\mathbf{A}_\perp| \quad ,$$

which makes the paraxial field basically transverse to the propagation direction z.

1.6 Energy Flux

As far as the energy flux is concerned, it is described by the real part of the Poynting vector **S**, that is

$$\mathbf{S} = \frac{1}{2\mu_0}\mathrm{Re}[\tilde{\mathbf{E}} \times \tilde{\mathbf{B}}^*] = \frac{1}{2\mu_0\omega_0}\mathrm{Re}[i\tilde{\mathbf{E}} \times \nabla \times \tilde{\mathbf{E}}^*] \quad , \quad (49)$$

so that, in the paraxial regime, one gets

$$\mathbf{S} = \frac{k_0}{2\mu_0\omega}|\mathbf{A}_\perp|^2\,\hat{\mathbf{z}} \quad , \quad (50)$$

and the energy flux is parallel to the z-axis.

More in general, If one introduces the Poynting vector

$$\mathbf{S}=\frac{1}{\mu_0}\mathbf{E}\mathrm{x}\mathbf{B},$$

E and **B** being the real fields (not the analytic signals), the following relation (*Poynting's theorem*) can be proved in general, that is

$$\frac{\partial u}{\partial \mathrm{t}}+\ \nabla\cdot\mathbf{S}=-\mathbf{J}\cdot\mathbf{E}$$

(to be compared with the charge conservation equation

$$\nabla\cdot\mathbf{j}+\ \frac{\partial\rho}{\partial t}=0)$$

where **J** is the total *current density* and

$$u=\frac{1}{2}(\varepsilon_0\mathbf{E}^2+\frac{1}{\mu_0}\mathbf{B}^2)$$

the *energy density*. In the case of propagation of a monochromatic plane wave of amplitude $\mathbf{E_0}$, for which **E** and **B** are perpendicular to each other and to the propagation direction, one has that **S** points in the propagation direction and that *the time-averaged value of its modulus*, termed *intensity* (energy crossing per unit time the unit area perpendicular to the propagation direction, e.g., Watts/square meters) is given by

$$<\mathbf{S}>=\ \frac{\varepsilon_0 c}{2}|\mathrm{E}_0|^2,$$

which can be also rewritten in terms of the *fine-structure constant* a $=\mathrm{e}^2/\hbar\mathrm{c}\cong 1/137$, of the *Planck constan*t h (=6.6x10^{-34} m^2Kg/sec) and of the *electron charge* e=1.6x10^{-19} Coulomb, as

$$|\mathrm{E}_0|^2=\frac{4\alpha\mathrm{h}}{\mathrm{e}^2}<\mathbf{S}>\ .\quad (51)$$

The electric field has the dimensions of a force divided by a charge and can be, for example, expressed as Newton/Coulomb in the SI (international system of units) system or Volt/meter (Volt being the p*otential difference* between two parallel, infinite planes spaced 1 meter apart that creates an electric field of 1 Newton per Coulomb). A convenient *energy unit* is the *electron volt* (eV), that is the energy given to an electron ($e=1.6\times10^{-19}$ Coulomb) by accelerating it through 1 *volt* of electric potential , corresponding to 1.6×10^{-19}joules. The energy $\hbar\omega$ of a visible light photon is between 1.5 and 3.5 eV, to be compared with the energy levels of bound electrons in atoms, of the order of 10 eV.

1.7 The Paraxial Gaussian beam

Let us consider the specific example in which the input beam has a Gaussian shape, a problem which can be dealt in a complete explicit analytic way. This is the case for a field distribution on the plane z=0 of the kind

$$\tilde{\mathbf{E}}_{\perp}(\mathbf{r}_{\perp},z=0) = E_0\hat{\mathbf{x}}e^{-r_{\perp}^2/\sigma_0^2} \quad , \quad (r_{\perp}^2 = x^2+y^2) \quad (52)$$

polarized along the **x** axis , with a width $\delta\mathbf{r}_{\perp} = \sigma_0$.

It is at this point useful to recall the following formulae which are often recurring in the frame of em propagation:

$$\int_{-\infty}^{+\infty} e^{-(ax^2+bx)}dx = (\sqrt{\pi/a})e^{b^2/4a}, \; a>0$$

$$\int_{-\infty}^{+\infty} e^{iax^2+ibx)}dx = e^{i\pi/4(a/|a|)}\sqrt{\pi/|a|}\, e^{ib^2/4a}. \text{ (a and b real)}$$

Inserting Eq.(52) into Eq.(39) we obtain

$$\mathbf{F}(\mathbf{k}_\perp)=\frac{E_0}{(2\pi)^2}\hat{\mathbf{x}}\int_{-\infty}^{+\infty}d\mathbf{r}_\perp e^{-i\mathbf{k}_\perp\cdot\mathbf{r}_\perp}e^{-r_\perp^2/\sigma_0^2}=\frac{E_0\sigma_0^2}{4\pi}\hat{\mathbf{x}}e^{-\sigma_0^2k_\perp^2/4}\quad,\quad(53)$$

that is the angular spectrum (the Fourier transform) is also a Gaussian (a remarkable property that the Gaussian shape shares with the hyperbolic secant=1/hyperbolic cosine) of width $2/\sigma_0$. Whenever $\sigma_0 >> \lambda$, the spectral width is much less than k_0 and one can adopt paraxial approximation (Eq.46), so that

$$A_X(\mathbf{r}_\perp,z)=\int_{-\infty}^{+\infty}d\mathbf{k}_\perp e^{i\mathbf{k}_\perp\cdot\mathbf{r}_\perp}e^{-i(k_\perp^2/2k)z}\mathbf{F}_\perp(\mathbf{k}_\perp)=$$

$$E_0\frac{\sigma_0^2}{4\pi}\int_{-\infty}^{+\infty}d\mathbf{k}_\perp e^{i\mathbf{k}_\perp\cdot\mathbf{r}_\perp}e^{-k_\perp^2[\sigma_0^2/4+(iz/2k)]}=\frac{E_0}{(1+iz/\ell_D)}e^{-r_\perp^2/\sigma_0^2(1+iz/\ell_D)}=$$

$$\frac{E_0e^{-i\psi}}{\sqrt{1+(z/\ell_D)^2}}e^{-\frac{\mathbf{r}_\perp^2}{\sigma_0^2[1+(z/\ell_D)^2]}(1-iz/\ell_D)}\quad,\quad\psi=\mathrm{arctg}(z/\ell_D)\quad(54)$$

where

$$\ell_d=\frac{k\sigma_0^2}{2}=\pi\frac{\sigma_0}{\lambda}\sigma_0\quad,\quad(55)$$

is the so-called beam <u>diffraction-length</u> (as an example, for $\lambda=1\ \mu m,\ \sigma_0=1\ mm,\ \ell_d\cong 3m$).

According to to Eq.(54), the beam propagates in such a way that at any plane z=constant the intensity distribution is a <u>Gaussian beam</u> whose <u>width</u>

$$\sigma(z)=\frac{\sigma_0}{\sqrt{2}}\sqrt{1+\frac{z^2}{\ell_d^2}}\quad,$$

grows with z and eventually becomes proportional to it for $z >> \ell_d$,

$$\sigma(z) = \frac{\sigma_0}{\sqrt{2}} \frac{z}{\ell_d} \quad . \quad (56)$$

In the asymptotic limit, the divergence angle of the beam saturates to the value

$$\theta_d \cong \mathrm{tg}(\theta_d) = \frac{\sigma(z)}{z} = \frac{1}{\sqrt{2}\pi} \frac{\lambda}{\sigma_0} \quad (\underline{\text{diffraction angle}}) \quad . \quad (57)$$

The maximum of the intensity I_M decreases for increasing z,

$$\frac{I_M(z)}{I_M(z=0)} = \frac{1}{1+(z/\ell_d)^2} \quad , \qquad (58)$$

as expected according to energy conservation.

1.8 The parabolic equation

It is easy to check, by inspecting Eq.(47), that $\mathbf{A}(\mathbf{r}_\perp, z)$ obeys the *diffusion-like* equation

$$\nabla^2 \mathbf{A}(\mathbf{r}_\perp, z) + 2ik \frac{\partial}{\partial z} \mathbf{A}(\mathbf{r}_\perp, z) = 0 \quad , \quad (59)$$

also known in the literature as the <u>parabolic equation</u>. Accordingly, the paraxial situations can be treated starting directly from Eq.(59) which, by definition, admits of Eq.(47) as a general analytic solution.
Actually, Eq. (59) can also be derived in a straightforward way from Helmholtz equation (Eq.22)), following a procedure which better emphasizes the nature of the approximation. To this end, we assume the field to be <u>transverse</u> to the propagation direction z, write it in the form

$$\tilde{\mathbf{E}}(\mathbf{r}_\perp, z) \cong \tilde{\mathbf{E}}_\perp(\mathbf{r}_\perp, z) \equiv e^{ikz} \mathbf{A}(\mathbf{r}_\perp, z) \; . \quad (60)$$

and insert it in Eq.(22). By exploiting the so-called slowly-varying approximation (SVA)

$$\left|\frac{\partial^2 \mathbf{A}}{\partial z^2}\right| \ll \left|2ik\frac{\partial \mathbf{A}}{\partial z}\right| \quad , \quad (61)$$

which is tantamount to require that $\mathbf{A}(\mathbf{r}_\perp, z)$ varies slowly, as a function of z, on a scale of the order of the wavelength $\lambda = 2\pi/k$, we find Eq.(59).

A particular class of solutions of Eq.(59), very useful for applications to many physical situation, are the Hermite-Gauss polynomials. They can be obtained by looking for a solution of Eq.(59) of the kind

$$f(x,y) = \frac{1}{h(z)} e^{-[ik/2h(z)](x^2+y^2)} . \quad (62)$$

It is easy to check that this is a solution of Eq.(59), provided that

$$\frac{dh}{dz} = 1 \rightarrow \quad h(z)=z+\alpha \quad , \quad (63)$$

with $\alpha = z_0 - iL$, where the parameter L (a length) has to be real in order to assure that 1/h(z) will not diverge. With a simple change of variables one can always assume z_0=0, the solution taking then the form

$$f(x,y) = \frac{1}{z - iL} e^{-(ik/2)(x^2+y^2)/(z-iL)} = \frac{z + iL}{z^2 + L^2} e^{-k(iz+L)(x^2+y^2)/2(z^2+L^2)}$$

so that, in order to assure the convergence of the solution for $x,y \rightarrow \infty$, it is necessary that L > 0. One can then rewrite the above equation as

$$f(x,y) = \frac{z+iL}{z^2+L^2} e^{-ik(x^2+y^2)/2R(z)} \; e^{-(x^2+y^2)/w^2(z)} \quad , \quad (64)$$

where

$$R(z)=\frac{z^2+L^2}{z}=z+\frac{L^2}{z} \quad , \qquad \underline{\text{curvature radius}} \, , \quad (65)$$

$$w^2(z)=2\frac{z^2+L^2}{kL}=\frac{\lambda(z^2+L^2)}{\pi L} \quad , \; \underline{\text{spot-size}} \, , \qquad (66)$$

The interpretation of R(z) and w(z) are the following: Eq.(64) describes a field distribution of a spherical wave with curvature radius R, amplitude modulated by a Gaussian whose amplitude is reduced by a factor 1/e when $x^2+y^2=w^2$. In particular, the spot-size takes its minimum value w_0 at z=0,

$$w_0=w(z=0)=\sqrt{\frac{\lambda L}{\pi}}, \rightarrow L=\frac{\pi w_0^2}{\lambda}=\ell_d \quad , \; (\underline{\text{beam-waist}}) \; (67)$$

in term of which we can write

$$R(z)=z[1+(\frac{L^2}{z^2})]=z[1+(\frac{\pi w_0^2}{\lambda z})^2]$$

$$w^2(z)=w_0^2[1+(\frac{z}{L})^2]=w_0^2[1+(\frac{\lambda z}{\pi w_0^2})^2]. \qquad (68)$$

The first term on the RHS of Eq.(64) can be rewritten as

$$\frac{z+iL}{z^2+L^2}=i\frac{e^{-i\phi(z)}}{\sqrt{z^2+L^2}}$$

where

$$\phi(z)=\text{arctg}(z/\ell_d)=\text{arctg}(\lambda z/\pi w_0^2), \quad (69)$$

so that, apart from a multiplication factor , the solution of Eq.(59) is

$$f(x,y,z)= i\frac{w_0}{w(z)}e^{-i[kz-\phi(z)]}e^{-\{[ik/R(z)]+[1/w^2(z)]\}(x^2+y^2)}\ , (70)$$

(Gaussian beam of zero order).

A plot of the ratio $w(z)/w_0$ is reported in Fig.2.

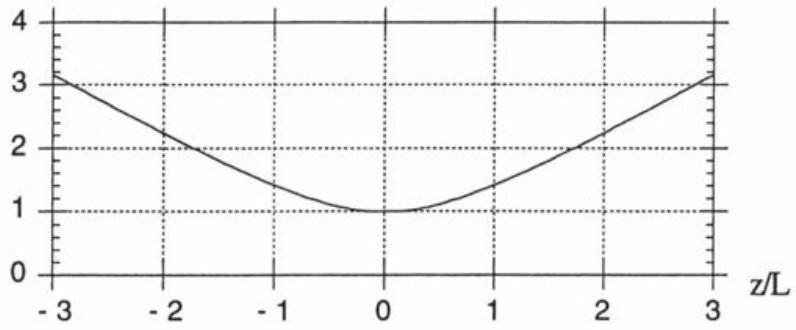

Fig.2 Beam spot-size as a function of z.

For large z (|z|>>L) we have $w(z)\cong w_0|z|/L$ so that

$$tg(\theta_d)=w(z)/|z|\cong\theta_d\cong w_0/\ell_d=\lambda/\pi w_0$$ (diffraction angle) .

Other solutions of the parabolic equation are of the form (m and n being two integers)

$$f_{n,m}(x,y,z)=f(x,y,z)e^{-i(n+m+1)\phi(z)}H_n[\sqrt{2}x/w(z)]H_m[\sqrt{2}y/w(z)],\ (71)$$

where H_n is the Hermite polynomial of n-th order defined by the relation

$$H_n(x)=(-1)^n e^{x^2}\frac{d^n}{dx^n}e^{-x^2},$$
$$H_0=1, H_1=2x, \ ..., H_{n+1}=-2nH_{n-1}+2xH_n.$$

The corresponding higher-order *Hermite-Gauss beams* are of the form

$$\frac{w_0}{w(z)} e^{i\psi_{nm}} H_n[x\sqrt{2}/w(z)] H_m[y\sqrt{2}/w(z)] e^{[ik/2R(z)-1/w^2(z)](x^2+y^2)},$$

where

$\psi_{n,m} = kz-(n+m+1)\phi(z)$.

1.9 The general non-paraxial case

Let us consider again the general solution to the propagation problem provided by Eqs.(40) -(41). The integral appearing in these expressions can be explicitly performed by using the Weyl's representation of a spherical wave, that is

$$\frac{e^{ikr}}{r} = \frac{i}{2\pi}\int_{-\infty}^{+\infty} d\mathbf{k}_\perp e^{i\mathbf{k}_\perp \cdot \mathbf{r}_\perp} \frac{e^{iz\sqrt{k^2-k_\perp^2}}}{\sqrt{k^2-k_\perp^2}}, \quad r=\sqrt{x^2+y^2+z^2}, \quad (72)$$

The integrals over $k_\perp$ in Eqs. (40-41) can be explicitly evaluated thus getting

$$\begin{aligned} \tilde{\mathbf{E}}_\perp(\mathbf{r}_\perp, z) &= -\frac{\partial}{\partial z}\int d\mathbf{r}'_\perp \left(\frac{1}{2\pi}\frac{e^{ikR}}{R}\right)\tilde{\mathbf{E}}_\perp(\mathbf{r}'_\perp, z=0) \\ \tilde{E}_z(\mathbf{r}_\perp, z) &= i\nabla\cdot\int d\mathbf{r}'_\perp \left(\frac{1}{2\pi}\frac{e^{ikR}}{R}\right)\tilde{\mathbf{E}}_\perp(\mathbf{r}'_\perp, z=0), \end{aligned} \qquad \textbf{(73)}$$

where $R=\sqrt{(x-x')^2+(y-y')^2+z^2}$.

Performing the partial z-derivative appearing in Eq.$(73)_1$ by exploiting the relation $\partial/\partial z(e^{ikr}/r) = -(\partial/\partial r)(e^{ikr}/r)(\partial r/\partial z)$ yields

$$\tilde{\mathbf{E}}_\perp(\mathbf{r}_\perp, z) = \frac{1}{2\pi}\int d\mathbf{r}_\perp \frac{e^{ikR}}{R}\left(ik-\frac{1}{R}\right)\cos(\theta)\tilde{\mathbf{E}}_\perp(\mathbf{r}'_\perp, z=0), \quad (74)$$

where cos(θ)=z/R, also known as the Rayleigh-Sommerfeld formula.

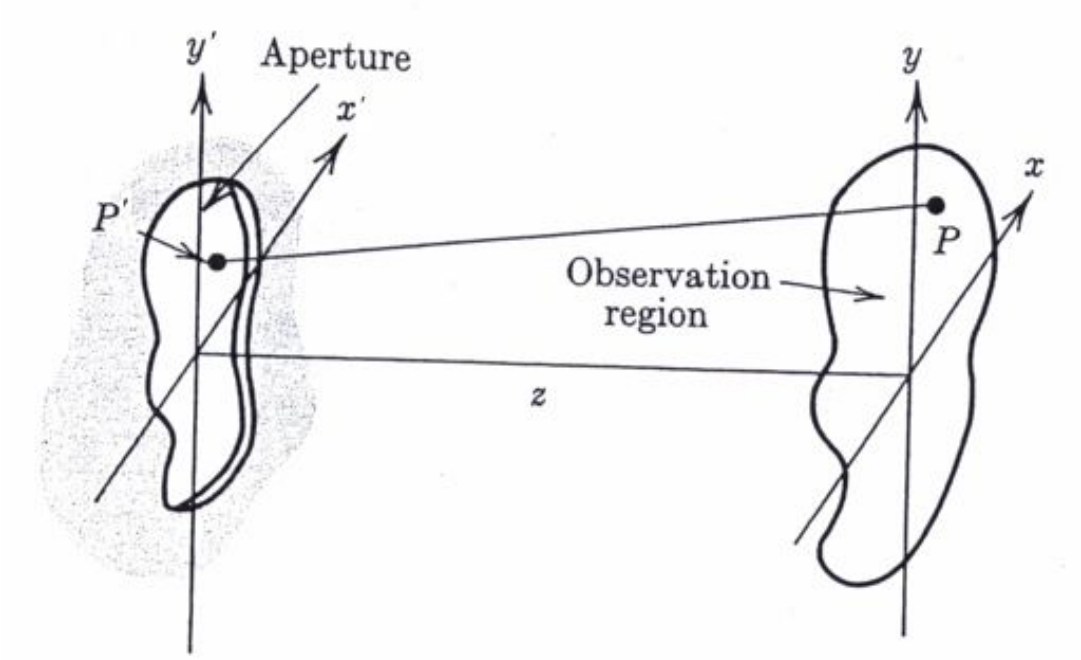

Fig.3 Diffraction by a finite aperture

Let us apply it in the geometrical context depicted in Fig.(3), which describes propagation through a finite aperture. Let us assume z>>R, that is its linear dimensions around the origin small compared with respect to z, and limit the diffraction pattern to values of x and y small with respect to z. In the limit of this approximation, we can rewrite Eq.(74) as (cos(θ) ≅ 1, k>>1/R)

$$\tilde{\mathbf{E}}_{\perp}(\mathbf{r}_{\perp},z)=\frac{ik}{2\pi z}\int d\mathbf{r}'_{\perp}\,\frac{e^{ikR}}{R}\,\tilde{\mathbf{E}}_{\perp}(\mathbf{r}'_{\perp},z=0) \quad . \quad (75)$$

The exponential term exp(ikR) appearing in Eq.(75) can be approximately written as

$$e^{ikR} \cong e^{ikz+(ik/2z)[(x-x')^2+(y-y')^2]},$$

provided that the following sufficient condition, which expresses the possibility of neglecting in the exponential the quadratic term in the expansion $\sqrt{1+\varepsilon} = 1+\varepsilon/2 - \varepsilon^2/8 + \ldots,$ is valid, that is

$$z^3 >> [(x-x')^2 + (y-y')^2]^2/8\lambda \ , \ (\lambda=2\pi/k) \ . \quad (76)$$

If this is the case, Eq. (75) becomes

$$\tilde{\mathbf{E}}_\perp(\mathbf{r}_\perp, z) = \frac{ike^{ikz}}{2\pi z} \int d\mathbf{r}'_\perp e^{\frac{ik}{2z}[(x-x')^2+(y-y')^2]} \tilde{\mathbf{E}}_\perp(\mathbf{r}'_\perp, z=0) \quad , \ (77)$$

which represents the diffracted field in the Fresnel approximation . In polar coordinate $(x'=\rho\cos\varphi \ , y'=\rho\sin\varphi \ ; x=r\cos\vartheta \ , y=r\sin\vartheta)$, the above expression becomes

$$\mathbf{W}(r,\vartheta,z) = \frac{ie^{ikz}}{\lambda z} \int_0^\infty \mathbf{W}_0(\rho,\varphi) \, e^{i(k/2z)[\rho^2+r^2-2\rho r\cos(\vartheta-\varphi)]} r d\rho d\varphi \ . \ (77)_1$$

Note that the condition associated with Eq.(76) is only a sufficient one, so that the Fresnel approximation may also be valid for values of z much lesser than those fulfilling Eq.(76).
Let us now rewrite Eq.(77) as

$$\tilde{\mathbf{E}}_\perp(\mathbf{r}_\perp, z) = \frac{ik}{2\pi z} e^{i[kz+(k/2z)(x^2+y^2)]} \int d\mathbf{r}'_\perp e^{i(k/2z)(x'^2+y'^2)-(ik/z)(xx'+yy')} \tilde{\mathbf{E}}_\perp(\mathbf{r}'_\perp, z=0)$$

and assume $(ik/2z)((x'^2+y'^2)$ to be negligible compared to $2i\pi$. In this limit, Fraunhofer approximation, the diffracted field becomes

$$\tilde{\mathbf{E}}_\perp(\mathbf{r}_\perp, z) = \frac{ik}{2\pi z} e^{i[kz+(k/2z)(x^2+y^2)]} \int d\mathbf{r}'_\perp e^{-(ik/z)(xx'+yy')} \tilde{\mathbf{E}}_\perp(\mathbf{r}'_\perp, z=0) \, . \ (78)$$

The integral appearing in Eq.(78) represents the Fourier transform of $\tilde{\mathbf{E}}_\perp(\mathbf{r}'_\perp, z=0)$ at the spatial frequencies $\chi_x = kx/z$ and $\chi_y = ky/z$.

Note that the condition for the validity of Eq.(78) can be rather stringent, that is

$$z >> (x'^2 + y'^2)/2\lambda \quad (\lambda = 2\pi/k). \quad (79)$$

As an example, for l=0.5 mm and linear dimensions of the aperture of the order of 1 cm, this corresponds to z >> 50 meters. This would make Eq.(78) not very helpful for actually evaluating Fourier's transforms if not for the fact that the distant region can be simulated by using convergent lenses.

The distance z_t of transition between the range of validity of the Fresnel region and that of the Fraunhofer approximation can be conventionally defined as $z_t = \pi a^2/\lambda$, where a is the radius of the aperture.

1.10 Diffraction by an aperture

Fresnel and Fraunhofer approaches are typically exploited to describe diffraction of a monochromatic plane wave, propagating in the z-direction, by an aperture in an otherwise opaque screen (see Figs.4 and 5), like, e.g., a rectangle or a circle, respectively described by the screen transmittance $\mathrm{rect}(\xi/a)\mathrm{rect}(\eta/b)$ and $\mathrm{circ}(\rho/a)$ (the "rect" function being a function that is 0 outside the interval [-1/2,1/2] and unity inside, the "circ" function its analogous in polar coordinates).

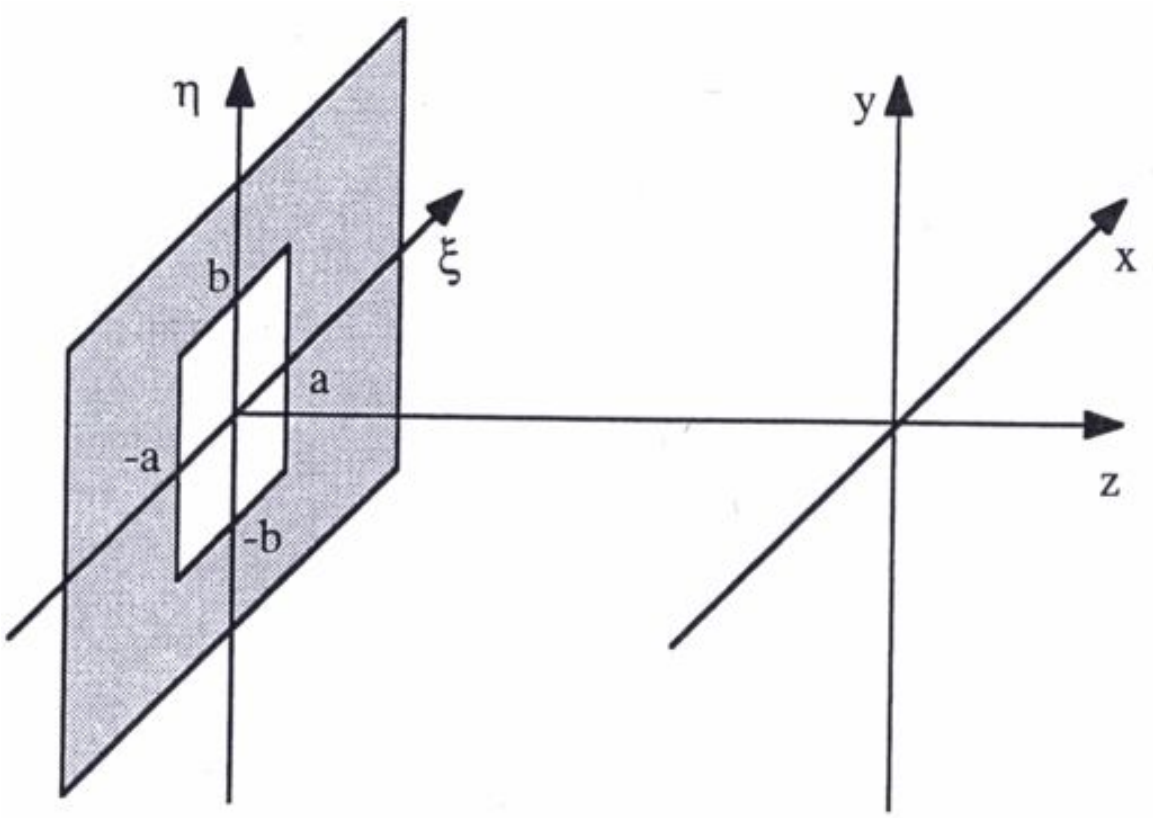

Fig.4

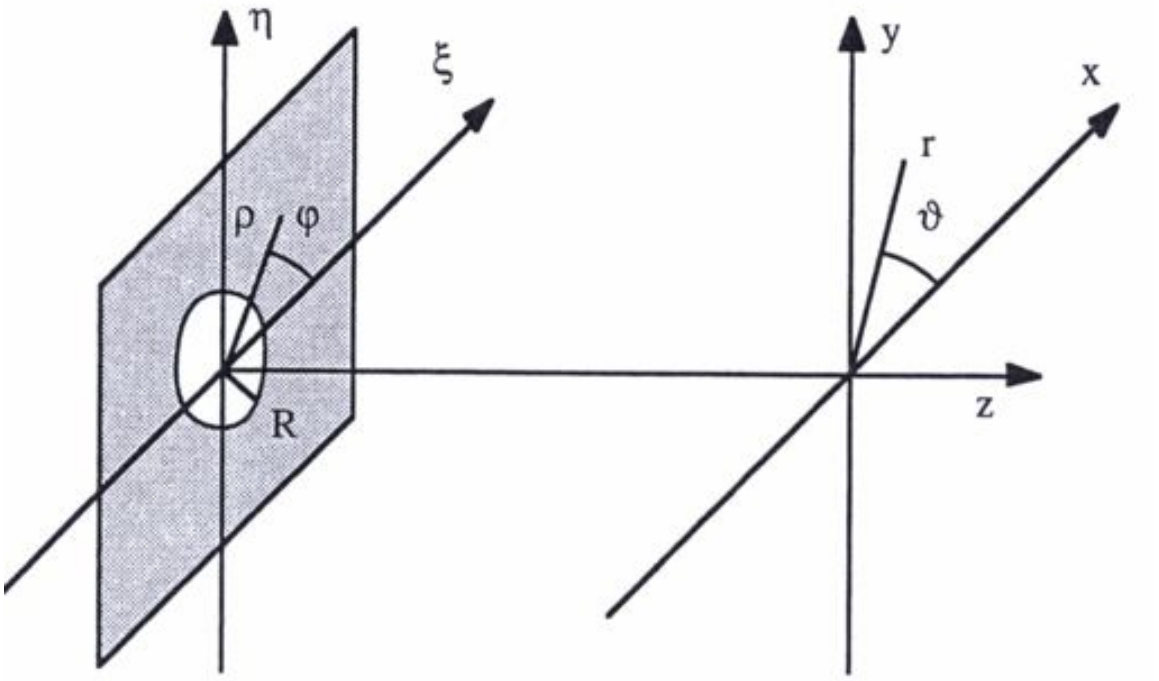

Figs. 4-5 Diffraction by a rectangular and a circular aperture

In the case of a rectangular aperture, Eq.(77) yields, for a field of amplitude A,

$$E(x,y,z)=\frac{iAe^{ikz}}{\lambda z}\int_{-a}^{a} d\xi \int_{-b}^{b} d\eta\, e^{i\frac{k}{2z}[(x-\xi)^2+(x-\eta)^2]} \quad , \quad (80)$$

which, in the Fraunhofer approximation, reads

$$E(x,y,z)=\frac{4iAabe^{i[kz+(k/2z)(x^2+y^2)]}}{\lambda z}\,\mathrm{sinc}\left(\frac{2ax}{\lambda z}\right)\mathrm{sinc}\left(\frac{2by}{\lambda z}\right) \quad , \quad (81)$$

where sinc(x)=sin(x)/x.
In the case of the circular hole, Eq.$(77)_1$ becomes

$$W(r,z)=\frac{ikA}{z}e^{ikz}\,e^{\frac{ikr^2}{2z}}\int_0^{\infty}e^{ik\rho^2/2z}J_0(k\rho r/z)\rho\,d\rho\ ,\quad (82)$$

where $r^2 = x^2 + y^2$, J_0 being the Bessel function of zero-order.

In the case described by Eq.(80), it is convenient to define the dimensionless variables

$$s=(x/a),\quad \sigma=(\xi/a),\ t=(y/b)\ ,\ \tau=(\eta/b)\,,$$

and the so-called Fresnel's numbers

$$N_{Fx}=\ (a^2/\lambda z)\ \ ,\ N_{Fy}=\ (b^2/\lambda z)\,,$$

which allows one to rewrite Eq.(80), after some manipulation, in the form

$$E(x,y,z)=\frac{iAe^{ikz}}{2}\{F[(a+x)\sqrt{\frac{2}{\lambda z}}]+F[(a-x)\sqrt{\frac{2}{\lambda z}}]\}\times\{F[(b+y)\sqrt{\frac{2}{\lambda z}}]+F[(b-y)\sqrt{\frac{2}{\lambda z}}]\}\quad (83)$$

where

$$F(\chi)=\int_0^{\chi}e^{i\frac{\pi}{2}\chi'^2}\,d\chi'=C(\chi)+iS(\chi)\quad ,\quad (84)$$

C and S being the so-called Fresnel's integrals.
The case described by Eq.(82) can be rewritten, after introducing the dimensionless variables,

$$t=r/a\ ,\ \chi=\rho/a\ \text{ and }N_F=a^2/\lambda z$$

as

$$W(at,z) = 2\pi i A N_F e^{i(kz+\pi N_F t^2)} \int_0^1 e^{i\pi N_F \chi^2} J_0(2\pi N_F \chi t)\chi d\chi \quad . \quad (85)$$

Remarkably, the above expression depends only on the parameter N_F (Fresnel number) and not on a, z and λ separately.
The Fraunhofer diffraction pattern for a rectangular and circular aperture are reported in Figs. (6) and (7).

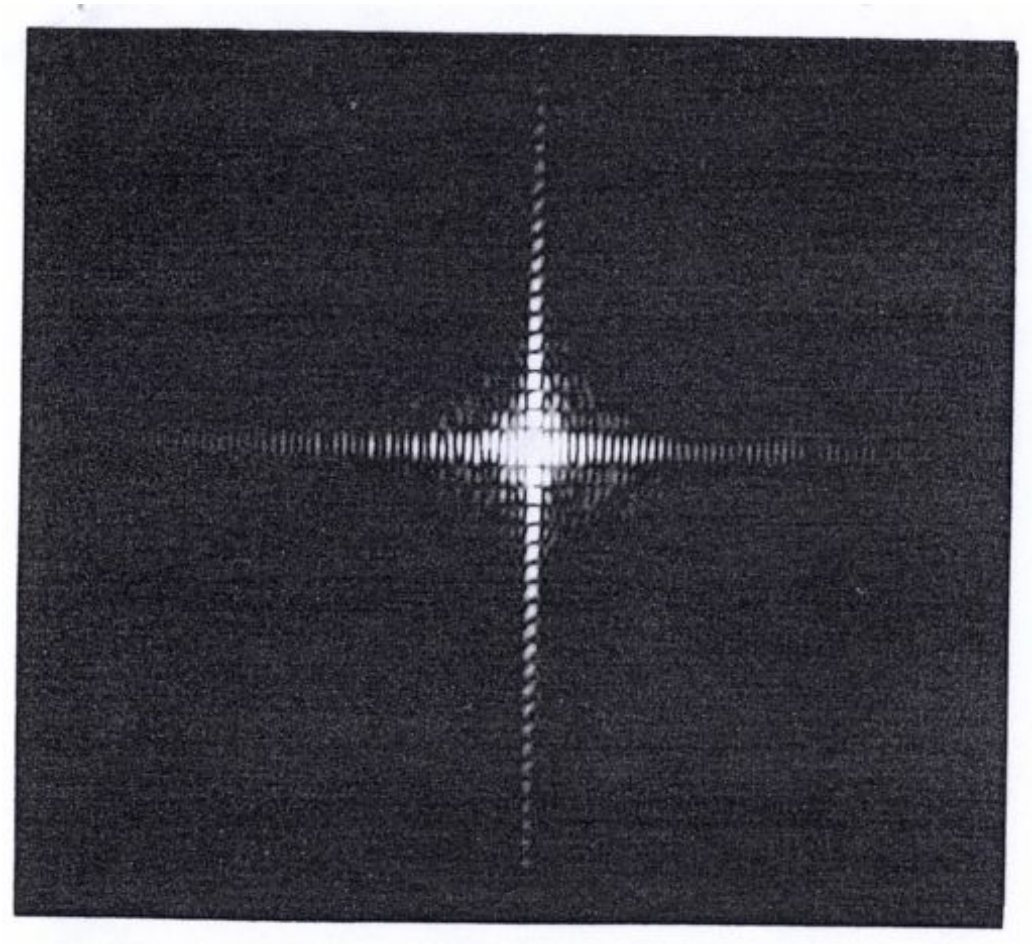

.

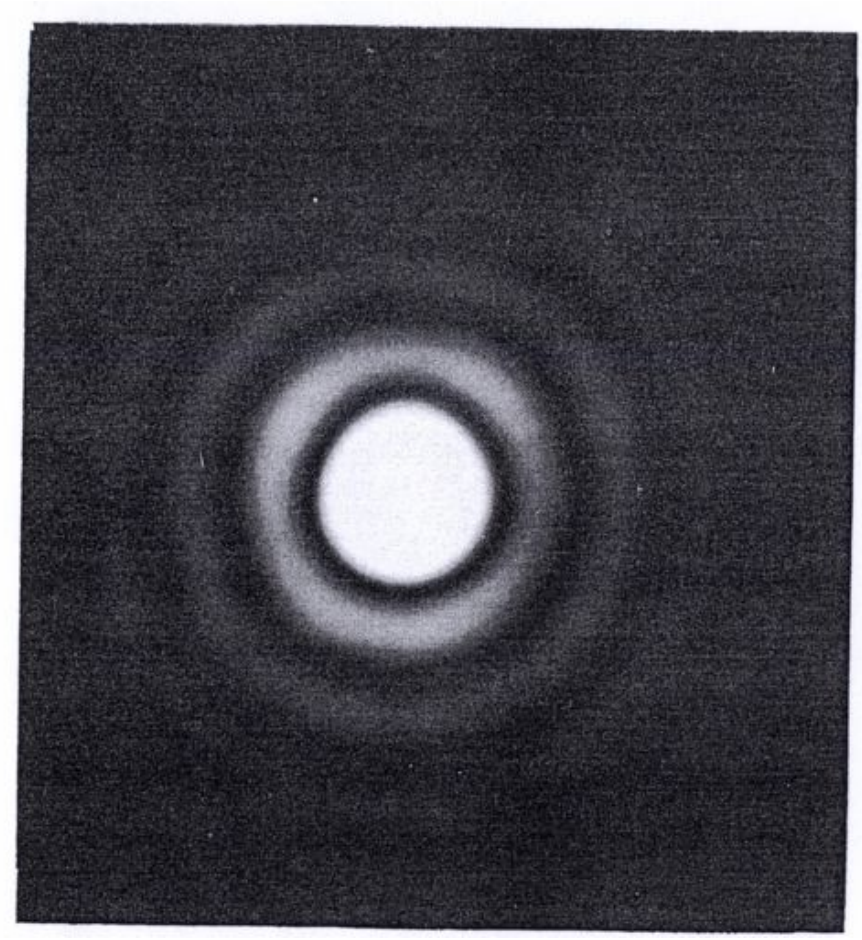

Figs. 6,7 Diffraction pattern from rectangular and circular aperture.

1.11 Nondiffracting fields

Diffraction is an ubiquitous phenomenon. However, there exist exact solutions of Maxwell's equations which propagate in space without changing (apart from a phase factor) their transverse distribution (non-diffracting or section-invariant beams). Note, however, that they are only mathematical solutions of Maxwell's equations which carry infinite power and, as such, are only models apt to describe realistic physical fields.

We start noting that the evolution of propagation is contained in the factor $\exp(iz\sqrt{k^2 - k_\perp})$ which is responsible for the dephasing of the different plane waves whose superposition generates the longitudinal dynamics of the field manifested through diffraction (see Eqs.40-41)).

Let us then assume the beam to be made up only by the plane waves which have a fixed inclination with respect to z. This requires tg(θ), where

$$\mathrm{tg}(\theta)=\frac{k_z}{|\mathbf{k}_\perp|}=\frac{\sqrt{k^2-k_\perp^2}}{|\mathbf{k}_\perp|}\quad,\quad(86)$$

to be the same for all the beam waves. This is only possible if the involved waves have the same $|\mathbf{k}_\perp|$ and, as a consequence, the same $k_z=\sqrt{k^2-k_\perp^2}$. This can be achieved by superimposing the plane waves belonging to the cone $k_z=|\mathbf{k}_\perp|\mathrm{tg}(\theta)$, which is analytically expressed in term of the δ-function as

$$\tilde{\mathbf{E}}_\perp(\mathbf{k}_\perp)=\tilde{\mathbf{E}}_{\perp 0}\delta(|\mathbf{k}_\perp|-h)\quad,\quad(87)$$

where h is a given positive number. One then has, according to Eqs.(40) and (41),

$$\tilde{\mathbf{E}}_\perp(\mathbf{r}_\perp,z)=\tilde{\mathbf{E}}_{\perp 0}\int_{-\infty}^{+\infty}d\mathbf{k}_\perp e^{i\mathbf{k}_\perp\cdot\mathbf{r}_\perp+iz\sqrt{k^2-k_\perp^2}}\delta(|\mathbf{k}_\perp|-h)$$

$$\tilde{E}_z(\mathbf{r}_\perp,z)=-i\tilde{\mathbf{E}}_{\perp 0}\cdot\nabla_\perp\int_{-\infty}^{+\infty}d\mathbf{k}_\perp e^{i\mathbf{k}_\perp\cdot\mathbf{r}_\perp+iz\sqrt{k^2-k_\perp^2}}\left[\frac{\delta(|\mathbf{k}_\perp|-h)}{\sqrt{k^2-k_\perp^2}}\right]\qquad(88)$$

or, by using polar coordinates,

$$x=r\cos(\phi)\ ,\ y=r\sin(\phi);\ k_x=k\cos(\theta),\ k_y=k\sin(\theta),$$

$$\tilde{\mathbf{E}}_\perp(r,\phi)=h\tilde{\mathbf{E}}_{\perp 0}e^{iz\sqrt{k^2-k_\perp^2}}\int_0^{2\pi}d\theta e^{ihr\cos(\theta-\phi)}\ ,\ (89)$$

and an analogous expression for $\tilde{E}_z$.
By recalling the relation

$$J_0(\xi) = \frac{1}{2\pi}\int_0^{2\pi} d\psi e^{i\xi\cos(\psi)} \quad , \quad (90)$$

where J_0 is the zero-th order Bessel function of the first kind, one can finally write

$$\tilde{\mathbf{E}}_\perp(\mathbf{r}_\perp, z) = \tilde{\mathbf{E}}_{\perp 0} 2\pi h e^{iz\sqrt{k^2-h^2}} J_0(hr)$$

$$\tilde{E}_z(\mathbf{r}_\perp, z) = -i\frac{h}{\sqrt{k^2-h^2}} e^{iz\sqrt{k^2-h^2}} \tilde{\mathbf{E}}_{\perp 0} \cdot \nabla_\perp J_0(hr) \quad (91)$$

whose square modulus does not depend on z (no diffraction) as long as $1/h > 1/k = \lambda/2\pi$ (if the opposite inequality holds, there is an exponential attenuation of the beam with z).
Note that $\int_0^\infty J_0^2(x)dx = +\infty$, so that the non-diffracting beam carries an infinite power (but so also do plane waves!).
As plane waves can represent a fair approximation for beams much larger than λ, the non-diffracting beams represents a good model apt to describe physical field possessing a very large diffracting length.
Other invariant-section beams can be obtained by selecting set of plane waves who have k_z in common but whose amplitudes and phases are completely arbitrary. The amplitude at z=0 can be obtained by Eq.(89) multiplied by a complex amplitude $A(\theta)$, which takes into account the distribution of the plane waves, and integrated between 0 and 2π, that is

$$\int_0^{2\pi} A(\theta) e^{ihr\cos(\theta-\phi)} d\theta \, . \quad (92)$$

After expanding $A(\theta)$ into the Fourier series,

$$A(\theta)=\sum_{n=-\infty}^{+\infty}A_n(\theta)e^{in\theta}\,, \quad (93)$$

Eq.(92) becomes

$$\sum_{n=-\infty}^{+\infty}A_n\int_0^{2\pi}e^{i[n\theta+hr\cos(\theta-\phi)}d\theta \quad (94)$$

which, by introducing the variable $\psi=\theta-\phi-\pi/2$, and using the integral expression for the Bessel function J_n of n-th order, reduces to the linear combination of Bessel functions

$$2\pi\sum_{n=-\infty}^{+\infty}(i)^nJ_n(hr)e^{in\phi} \quad . \quad (95)$$

1. 12 Propagation of EM field in matter: macroscopic Maxwell's equations

Up to now we have dealt with exact microscopic Maxwell equations <u>in vacuum</u>. How do we proceed when matter, that is a certain distribution of charges and currents, is present?
Let us look back at Eqs.(1) and (3) and consider that the trajectories of the charges q_i have to be found by solving the appropriate dynamical equations of motion in the presence of the Lorentz force given in Eq.(2). In general this approach presents insurmountable difficulties and one has to be content with the knowledge of the space-averaged quantities

$$<\mathbf{E}(\mathbf{r},t)>=\frac{1}{V}\int_v\mathbf{E}(\mathbf{r}',t)d\mathbf{r}' \quad , \quad <\mathbf{B}(\mathbf{r},t)>=\frac{1}{V}\int_v\mathbf{B}(\mathbf{r}',t)d\mathbf{r}' \quad , \quad (96)$$

where the integrals are extended to a suitable spatial volume V centered around the position **r**. The adjective "suitable" means that the volume has to be not too large since the scale of variation of the averaged field as a function of **r** is of the order $V^{1/3}$, nor too small since the number of

charges inside the volume has to be big enough to allow for the neglect of fluctuations.
This procedure leads to the so-called macroscopic Maxwell equations which, when dealing with diamagnetic materials, read

$$\begin{aligned}
&\varepsilon_0 \nabla \cdot < \mathbf{E}\,(\mathbf{r},t)> = <\rho(\mathbf{r},t> \,, \\
&\nabla \cdot < \mathbf{B}\,(\mathbf{r},t)> = 0, \\
&\nabla \times < \mathbf{E}\,(\mathbf{r},t)> = -\frac{\partial}{\partial t} < \mathbf{B}\,(\mathbf{r},t)> \,, \qquad (97) \\
&\nabla \times < \mathbf{B}\,(\mathbf{r},t)> = \mu_0 < \mathbf{j}\,(\mathbf{r},t)> + \frac{1}{c^2}\frac{\partial}{\partial t} < \mathbf{E}\,(\mathbf{r},t)> \,.
\end{aligned}$$

Note that the charge-conservation equation applies also to the averaged quantities , that is

$$\frac{\partial}{\partial t} < \rho(\mathbf{r},t) > \; + \nabla \cdot <\mathbf{j}(\mathbf{r},t)> = 0 \quad . \quad (98)$$

To proceed further, one introduces the polarization for unit volume $\mathbf{P}(\mathbf{r},t)$, defined as the sum of the dipole moments $\mathbf{p}_i$ induced in any single atom present in the unit volume by the electric field $\mathbf{E}$ **(r,t),**

$$\mathbf{P}(\mathbf{r},t) = \sum_i \mathbf{p}_i \,. \qquad (99)$$

It can be proved in general that

$$< \rho(\mathbf{r},t)> = -\nabla \cdot \mathbf{P}(\mathbf{r},t) \quad , \quad (100)$$

which in turn implies, according to Eq.(98),

$$< \mathbf{j}(\mathbf{r},t)> = \frac{\partial}{\partial t}\mathbf{P}(\mathbf{r},t) \quad . \quad (101)$$

By using Eqs.(100) and (101), the macroscopic Maxwell equations can be written (dropping for sake of simplicity the angular brackets, that is by labeling <$\mathbf{E}(\mathbf{r},t)$> and <$\mathbf{B}(\mathbf{r},t)$> as $\mathbf{E}(\mathbf{r},t)$ and $\mathbf{B}(\mathbf{r},t)$, in the form

$$\nabla \cdot \mathbf{E}(\mathbf{r},t) = -\frac{1}{\varepsilon_0} \nabla \cdot \mathbf{P}(\mathbf{r},t) ,$$
$$\nabla \cdot \mathbf{B}(\mathbf{r},t) = 0 ,$$
$$\nabla \times \mathbf{E}(\mathbf{r},t) = - \frac{\partial}{\partial t}\mathbf{B}(\mathbf{r},t) , \qquad (102)$$
$$\nabla \times \mathbf{B}(\mathbf{r},t) = \mu_0 \frac{\partial}{\partial t}\mathbf{P}(\mathbf{r},t) + \frac{1}{c^2}\frac{\partial}{\partial t}\mathbf{E}(\mathbf{r},t).$$

To proceed further one needs an analytic relation between **E** and **P**, which is in general a rather difficult task, unless dealing with particular simple physical models. At this point, it is customary to take a phenomenological approach, that is to assume, as a reasonable intuitive guess, the validity of a simple linear relation of the kind

$$\mathbf{P}(\mathbf{r},t) = \varepsilon_0 \int_0^{+\infty} \chi(\mathbf{r},t')\mathbf{E}(\mathbf{r},t-t')dt' \quad , (\mathbf{P}, \mathbf{E} \text{ and } \chi \text{ real!}) \quad (103)$$

which requires the field to be not too strong, the medium to be isotropic and its response local in space. The function $\chi(\mathbf{r},t)$ is termed *dielectric susceptibility* of the medium. Taking into account the necessity of the validity of the principle of cause and effect, according the which the polarization per unit volume at time t, **P**(t) can only depend on the field at times smaller than t, Eq. (103) can be more conveniently rewritten as

$$\mathbf{P}(\mathbf{r},t) = \varepsilon_0 \int_{-\infty}^{+\infty} \hat{\chi}(\mathbf{r},t')\mathbf{E}(\mathbf{r},t-t')dt' , \quad (104)$$

where $\hat{\chi}(\mathbf{r},t') = \chi(\mathbf{r},t')$ for $t'>0$ and $\hat{\chi}(\mathbf{r},t') = 0$ for $t' \le 0$.

One can now choose to work either in the time-domain or in the frequency domain.

In the first case, it is easy to derive from Eqs. (102) the following evolution equation for **E(**r,t)

$$\nabla^2\mathbf{E} + \frac{1}{\varepsilon_0}\nabla\nabla\cdot\mathbf{P} - \frac{1}{c^2}\frac{\partial^2\mathbf{E}}{\partial t^2} = \mu_0 \frac{\partial^2\mathbf{P}}{\partial t^2} \quad . \quad (105)$$

In the frequency domain, Eq. (105) becomes

$$\nabla^2\mathbf{E}_\omega + \frac{1}{\varepsilon_0}\nabla\nabla\cdot\mathbf{P}_\omega + \frac{\omega^2}{c^2}\mathbf{E}_\omega = -\mu_0\omega^2\mathbf{P}_\omega \quad , \quad (106)$$

where, recalling Eq.(15),

$$\mathbf{P}_\omega(\mathbf{r}) = \varepsilon_0\hat{\chi}_\omega(\mathbf{r})\mathbf{E}_\omega(\mathbf{r}) \quad . \quad (107)$$

Also, the Fourier transform of Eq.$(102)_1$ reads

$$\nabla\cdot\varepsilon_0(\mathbf{E}_\omega + \hat{\chi}_\omega\mathbf{E}_\omega) = \nabla\cdot\varepsilon_0[(1+\hat{\chi}_\omega)]\mathbf{E}_\omega \equiv \nabla\cdot(\varepsilon_\omega\mathbf{E}_\omega), \quad (108)$$

which , when introduced, together with Eq. (107), into Eq. (106),

allows to rewrite it as the *vectorial* equation

$$\nabla^2\mathbf{E}_\omega + 2\nabla[\mathbf{E}_\omega\cdot\nabla\ln(n_\omega)] + \frac{\omega^2}{c^2}n_\omega^2\mathbf{E}_\omega = 0 \ , \ (109)$$

The dimensionless <u>complex</u> quantities, ε_ω and n_ω, which are called *dielectric constant* and *refractive index* of the medium, respectively given by

$$\varepsilon_\omega = \varepsilon_0(1+\hat{\chi}_\omega) \ , \quad (110)$$

$$n_\omega = \sqrt{\frac{\varepsilon_\omega}{\varepsilon_0}} = \sqrt{1+\hat{\chi}_\omega} \quad , \quad (111)$$

are functions of the frequency ω and of the position **r**. They are of <u>phenomenological nature</u> and can be inferred either from experiments or by some appropriate physical model (classical or semi-classical) of the medium. If n_ω does not depend on **r**, Eq.(109) is analogous to the *scalar* one describing propagation in vacuum: the analytic approach used in vacuum can still be adopted, provided that k is replaced by

$k(\omega)=(\omega/c)n(\omega)$,

but for the presence of n_ω , a complex number, so that the field can be either attenuated or amplified. In fact, since $\hat{\chi}(t)$ is a real asymmetric function of time, its Fourier transform has an imaginary part,

$$\hat{\chi}_\omega = \hat{\chi}'_\omega + i\hat{\chi}''_\omega \quad , \quad (112)$$

so that a plane wave, propagating in the z-direction of an homogeneous medium in the presence of such a dielectric constant, will be of the form

$$e^{ik(\omega)z} = e^{i(\omega/c)(1+\hat{\chi}_\omega)^{1/2}z} \cong e^{i(\omega/c)(1+(1/2)\hat{\chi}_\omega)z} = e^{i(\omega/c)(1+\hat{\chi}'_\omega/2)z} e^{-(k\hat{\chi}''_\omega/2)z} \quad (113)$$

which predicts amplification or attenuation according to the sign of $\hat{\chi}''_\omega$ (typically, a passive medium induces attenuation while an active one, such as a laser medium, amplifies the field). However, if ω is far from the resonance frequencies of the medium, one can assume $\hat{\chi}_\omega$ to be a real quantity (see below).

A natural question is to ask what is responsible for the energy loss or gain associated with attenuation or amplification. The answer can be found in the energy expended (or gained) in the interaction between the em field and the induced dipole moment. In fact, the time average power per unit volume resulting from the interaction between field and electric polarization of the medium is (Re stands for "real part of" and one considers **E** to be parallel to **P**, that is an isotropic medium)

$$<\text{power}>/\text{volume} = <\mathbf{E}\cdot\partial\mathbf{P}/\partial t> = \text{Re}(e^{i\omega t}E_0)\,\text{Re}(i\omega e^{i\omega t}E_0\varepsilon_0\hat{\chi}_\omega) = \frac{\omega}{2}\varepsilon_0|\mathbf{E}_0|^2\,\text{Re}(i\hat{\chi}_\omega) = -\frac{\omega}{2}\varepsilon_0|\mathbf{E}_0|^2\,\hat{\chi}''_\omega \quad , \quad (114)$$

so that either losses or gain are present according to the sign of χ''_ω.

It is worthwhile to note that if one considers propagation of a non-monochromatic plane wave

$$\mathbf{E}(z,t)= \int \boldsymbol{\varepsilon}(\omega) e^{i(\omega/c)(\hat{\chi}'_\omega/2)z-(\omega/c)(\hat{\chi}''_\omega/2)z+i(\omega/c)z-i\omega t} d\omega \quad , \quad (115)$$

for a not too large frequency bandwidth Eq.(115) can be approximated by

$$\mathbf{E}(z,t)= e^{i(\omega/c)z-(\omega/c)(\hat{\chi}''_\omega/2)z} \int \boldsymbol{\varepsilon}(\omega) e^{i(\omega/c)(\hat{\chi}'_\omega/2)z-i\omega t} d\omega \quad , \quad (116)$$

so that the loss term factorizes and the temporal shape of the pulse is not greatly affected (if the carrier frequency is not too close to the resonant frequency of the medium).

From the above it is apparent that if a material medium is homogeneous and isotropic, one can use for a monochromatic field (that is in the frequency domain) the same approach to propagation used for em fields in vacuum, just replacing $k(\omega)=\omega/c$ with $k(\omega)=\omega n(\omega)/c$. However, in going back from frequency domain to time domain, the analytic approach may become quite complicated unless one is dealing with plane or quasi-plane waves (see, e.g., propagation in optical fibers), where one can use the concept of *group-velocity , group-velocity dispersion* and so on, concepts which are meaningless for an ordinary beam where a single propagation direction cannot be identified. A field propagating along the z-direction, like a plane wave in a dispersive medium, can be written as the superposition of monochromatic plane waves (*wave- packet*) in the form

$$E(z,t) = \int_{-\infty}^{+\infty} \varepsilon(\omega)\, e^{ik(\omega)z-i\omega t} d\omega =$$

$$e^{ik(\omega_0)z-i\omega_0 t} \int_{-\infty}^{+\infty} \varepsilon(\omega) e^{i[k(\omega)-k(\omega_0)]z-i(\omega-\omega_0)t} d\omega \quad , \quad (117)$$

where

$$\varepsilon(\omega) = \frac{1}{2\pi} \int_{-\infty}^{+\infty} E(z=0,t) e^{-i\omega t}\, dt \quad . \quad (118)$$

The dynamics of the evolution of the wave-packet is contained in the dependence of k on ω, resulting from the assumed theoretical model (either quantum or classical) used to describe the material medium. In any case, according to relativity, the front of the wave-packet cannot

exceed the velocity of light in vacuum c, that is the forerunners of the packet cannot arrive at a given location z=L before a time L/c. This places restrictions on the form of $k(\omega)$ which can be expressed by the behavior of its analytic continuation in the complex $\Omega = (\omega + i\gamma)$ -plane.

In general, because of the causality principle, the real and imaginary part of $k(\omega)=k'(\omega)+i\,k''(\omega)$ are not independent but need to obey the Kramers-Kronig relations. (see, e.g., Yariv (1), pg.812)

A simple theoretical model, in which the em field is interacting with atoms described by an harmonic force holding together a proton-electron system, is able to produce a simple expression for $k(\omega)$. The approach eventually allows one to write (see, e.g., Solimeno et al. (3), pg. 18)

$$\hat{\chi}'\omega = \frac{Nq^2}{m\varepsilon_0}\ \frac{\omega_0^2-\omega^2}{(\omega_0^2-\omega^2)^2+\beta^2\omega^2}$$

$$\hat{\chi}''\omega = \frac{Nq^2}{m\varepsilon_0}\ \frac{\beta\omega}{(\omega_0^2-\omega^2)^2+\beta^2\omega^2} \qquad (119)$$

where m and q are the electron charge and mass, N the number of atom per unit volume, ω_0 the associated harmonic-oscillator frequency and β some damping coefficient which takes into account the system energy loss. By making the approximation $\omega+\omega_0 \cong 2\omega_0$, Eqs. (119) can be rewritten as ($\Gamma = \beta/2$)

$$\hat{\chi}'\omega = \frac{Nq^2}{2m\varepsilon_0}\ \frac{1}{\Gamma\omega_0}\ \frac{(\omega-\omega_0)/\Gamma}{1+(\omega-\omega_0)^2/\Gamma^2}$$

$$\hat{\chi}''\omega = \frac{Nq^2}{2m\varepsilon_0}\ \frac{1}{\Gamma\omega_0}\ \frac{1}{1+(\omega-\omega_0)^2/\Gamma^2}\ , \qquad (120)$$

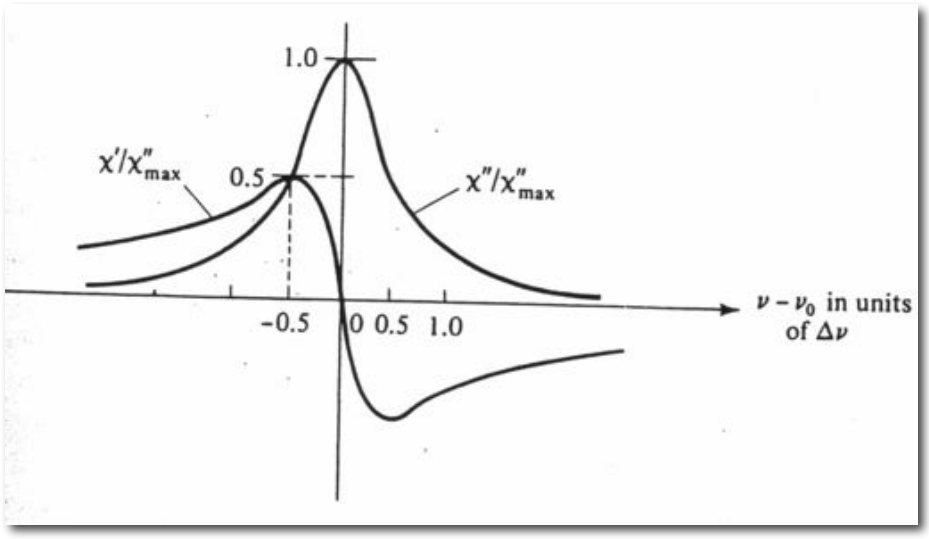

Fig. 8: Real and imaginary part of the Fourier transform of the dielectric susceptibility $\hat{\chi}_\omega = \hat{\chi}'_\omega + i\hat{\chi}''_\omega$.

Note that around the resonance frequency ω_0 there is a range of frequencies where $\hat{\chi}'_\omega$ is increasing (normal dispersion regime) and a range where $\hat{\chi}'_\omega$ is decreasing (anomalous dispersion regime), the maximum of the attenuation occurring at $\omega = \omega_0$ where $\hat{\chi}''_\omega$ has a maximum. Typically, optical propagation is concerned with transparent media, that is with ranges of frequencies where $\hat{\chi}''_\omega$ can be neglected.
Some general results about propagation can be derived from Eqs.(117) and (118) by assuming the refractive index n(ω) to be a real quantity. To this end, let us assume $\varepsilon(\omega)$ to be peaked around $\omega = \omega_0$ and consider the Taylor's expansion of $k(\omega)$

$$k(\omega) = k(\omega_0) + (dk/d\omega)_{\omega=\omega_0}(\omega-\omega_0) + \frac{1}{2}(dk^2/d\omega^2)_{\omega=\omega_0}(\omega-\omega_0)^2 + .. \equiv$$

$$k(\omega_0) + \frac{1}{V_g(\omega_0)}(\omega-\omega_0) + a_g(\omega-\omega_0)^2 + \ldots \quad , \quad (121)$$

having introduced the *group- velocity* V_g (distinct from the *phase velocity* $V_{ph} = \omega / k$) and the *group-velocity dispersion* a_g defined by the relations

$$\frac{1}{V_g} = \left(\frac{dk}{d\omega}\right)_{\omega=\omega_0}, \quad \frac{1}{a_g} = \frac{1}{2}\left(\frac{d^2k}{d\omega^2}\right)_{\omega=\omega_0} = -\frac{1}{2}\frac{1}{V_g^2(\omega_0)}\left(\frac{dV_g}{d\omega}\right)_{\omega=\omega_0} \quad (122)$$

By inserting Eq.(121) into Eq.(117) and using Eq.(122) we obtain

$$E(z,t) = e^{ik(\omega_0)z - i\omega_0 t} \int_{-\infty}^{+\infty} \varepsilon(\omega)\, e^{i[k(\omega)-k(\omega_0)]z - i(\omega-\omega_0)t} d\omega = e^{ik(\omega_0)z - i\omega_0 t} \int_{-\infty}^{+\infty} \varepsilon(\omega) e^{i[z/V_g - t](\omega-\omega_0) + iA_g z(\omega-\omega_0)^2} d\omega + \ldots \quad (123)$$

If the second and higher order terms are neglected one has

$$E(z,t) = e^{ik(\omega_0)z - i\omega_0 t} \int_{-\infty}^{+\infty} \varepsilon(\omega) e^{-i(t - z/V_g)(\omega-\omega_0)} d\omega = e^{ik(\omega_0)z - i\omega_0 t} E(z=0, t - z/V_g), \quad (124)$$

which justifies the name of group-velocity for V_g. The presence of the group-velocity dispersion eventually distorts the signal due to the dependence of the group-velocity on frequency.

1.12 Propagation in non-homogeneous media

When dealing with monochromatic fields in an isotropic non-homogeneous material, the theoretical approach becomes more complicated and, in general, it is not possible to find an exact solution to the propagation problem. However, some particular situations dealing with non-homogeneous media possessing an intrinsic scale larger than the wavelength, and exhibiting not too large deviations of the refractive

index from its average value, can be treated in the frame of a simplified approach.
In a non-homogeneous medium, the polarization **P** is a function of **r** and so are $\hat{\chi}'_\omega$, $\hat{\chi}''_\omega$ and the refractive index (see, e.g., Eq.(120), where N can be a function of the position **r**). In many cases of interest one can write

$$n_\omega(\mathbf{r}) = \sqrt{1+\hat{\chi}'_\omega(\mathbf{r})+i\hat{\chi}''_\omega(\mathbf{r})} \cong 1+\frac{\hat{\chi}'_\omega(\mathbf{r})}{2}+i\frac{\hat{\chi}''_\omega(\mathbf{r})}{2} \cong 1+\frac{\hat{\chi}'_\omega(\mathbf{r})}{2} \quad , (125)$$

having neglected the intrinsic losses of the medium.

In general, Eq.(109) can be rewritten as

$$\nabla^2\mathbf{E}_\omega + 2\nabla\{\mathbf{E}_\omega \cdot \nabla \ln[n_\omega(\mathbf{r})] + k^2 n_\omega^2(\mathbf{r})\mathbf{E}_\omega = 0 \quad , (126)$$

whose vectorial character is associated with the middle term containing the logarithm (polarization-mixing or scrambling term). If this term can be neglected, that is if

$$\frac{\lambda}{\ell}\ \frac{\Delta n}{n} << 1 \quad , \quad (127)$$

where ℓ is the typical spatial scale of variation of the refractive index and Δn its variation, Eq.(126) becomes the scalar Helmholtz equation

$$\nabla^2\mathbf{E}_\omega + \ + k^2 n_\omega^2(\mathbf{r})\mathbf{E}_\omega = 0 \quad . \quad (128)$$

It is in general impossible to find the solution of Eq.(128). However, under suitable hypotheses, it can be recast in a more convenient form. To this end, we write

$$n_\omega(\mathbf{r}) = n_{0\omega} + \delta n_\omega(\mathbf{r}) \quad , \quad (129)$$

with $|\delta n_\omega(\mathbf{r})| << n_{0\omega}$, substitute Eq.(129) into Eq.(126) and neglect the terms in $(\delta n_\omega(\mathbf{r}))^2$ thus getting

$$\nabla^2\mathbf{E}_\omega + +k^2\mathbf{E}_\omega + 2k^2\frac{\delta n(\mathbf{r})}{n_0}\mathbf{E}_\omega = 0 \ , k(\omega)=(\omega/c)n_{0\omega} \ . (130)$$

If one now writes (recall the paraxial approximation in vacuum)

$$\mathbf{E}_\omega(\mathbf{r}_\perp, z) = e^{ikz}\mathbf{A}(\mathbf{r}_\perp, z) \ ,$$

where $\mathbf{A}(\mathbf{r}_\perp, z)$ is assumed to undergo a slowly z-variation on a scale compared to 1/k, Eq.(130) becomes

$$\nabla_\perp^2\mathbf{A} + \frac{\partial^2}{\partial z^2}\mathbf{A} + 2ik\frac{\partial}{\partial z}\mathbf{A} - k^2\mathbf{A} + k^2\mathbf{A} = -2k^2\frac{\delta n}{n_0}\mathbf{A} \ ,$$

or, after neglecting the term with the second derivative with respect to z (the SVA approximation introduced in vacuum)

$$\nabla_\perp^2\mathbf{A}(\mathbf{r}_\perp, z) + 2ik\frac{\partial}{\partial z}\mathbf{A}(\mathbf{r}_\perp, z) = -2\frac{k^2}{n_0}\delta n_\omega(\mathbf{r}_\perp, z)\mathbf{A}(\mathbf{r}_\perp, z)$$

or, equivalently,

$$\left(\frac{\partial}{\partial z} + \frac{1}{2ik}\nabla_\perp^2\right)\mathbf{A}(\mathbf{r}_\perp, z) = i\frac{k}{n_0}\delta n_\omega(\mathbf{r}_\perp, z)\mathbf{A}(\mathbf{r}_\perp, z) \quad . \quad (131)$$

The form of Eq. (131) suggests to look for an approximate solution of the kind

$$\mathbf{A}(\mathbf{r}_\perp z) = \mathbf{A}_0(\mathbf{r}_\perp z) + \mathbf{A}_1(\mathbf{r}_\perp z)$$

where $\mathbf{A}_0$ and $\mathbf{A}_1$ obey the equations

$$\left(\frac{\partial}{\partial z} + \frac{1}{2ik}\nabla_\perp^2\right)\mathbf{A}_0(\mathbf{r}_\perp, z) = 0 \quad , \quad (132)$$

and

$$(\frac{\partial}{\partial z}+\frac{1}{2ik}\nabla_{\perp}^{2})\mathbf{A}_1(\mathbf{r}_{\perp},z)=i\frac{k}{n_0}\delta n_{\omega}(\mathbf{r},z)\mathbf{A}_0(\mathbf{r}_{\perp},z) \quad , \quad (133)$$

having assumed, consistently with the smallness of $\delta n / n_0$, $\mathbf{A}_1 << \mathbf{A}_0$.
The above results can be generalized to include the time domain. After setting

$$\mathbf{E}(\mathbf{r}_{\perp},z,t) = e^{ik(\omega_0)z-i\omega_0 t}\mathbf{A}(\mathbf{r}_{\perp},z,t) \quad ,$$

where ω_0 is the frequency around which the field spectrum $\varepsilon(\omega)$ is centered, the generalization of the parabolic equation (see Eq.(127)) to include the time domain can be readily obtained under the hypothesis of <u>both</u> slow z and t variations of **A** over scales of the order of $1/k_0$ and $1/\omega_0$. It has the form of a *diffusion-like* equation and reads

$$(\frac{\partial}{\partial z}+\frac{1}{V_g}\frac{\partial}{\partial t}+\frac{1}{2ik_0}\nabla_{\perp}^{2}-\frac{1}{2ia_g}\frac{\partial^2}{\partial t^2})\mathbf{A}(\mathbf{r}_{\perp},z,t) = ik_0\frac{\delta n(\mathbf{r},t)}{n_0}\mathbf{A}(\mathbf{r}_{\perp},z,t)) \quad , \quad (134)$$

where V_g and a_g are the group-velocity and the group-velocity dispersion defined in Eq.(122) and $k_0=k(\omega_0)$. By inspecting it is natural to regard <u>temporal dispersion</u> as a kind of <u>time-diffraction</u>.
Equation(134) can be written in a simpler form performing the change of variables $z'=z$, $t'=t-z/V_g$: by taking into account the relation

$$\frac{\partial}{\partial z}=\frac{\partial z'}{\partial z}\frac{\partial}{\partial z'}+\frac{\partial t'}{\partial z}\frac{\partial}{\partial t'}=\frac{\partial}{\partial z'}-\frac{1}{V_g}\frac{\partial}{\partial t'} \quad , \quad \frac{\partial}{\partial t}=\frac{\partial t'}{\partial t}\frac{\partial}{\partial t'}+\frac{\partial z'}{\partial t}\frac{\partial}{\partial z'}=\frac{\partial}{\partial t'}$$

it reads

$$(\frac{\partial}{\partial z}+\frac{1}{2ik_0}\nabla_{\perp}^{2}-\frac{1}{2ia_g}\frac{\partial^2}{\partial t'^2})\mathbf{A}(\mathbf{r}_{\perp},z,t') = ik_0\frac{\delta n(\mathbf{r},t')}{n_0}\mathbf{A}(\mathbf{r}_{\perp},z,t')) \, . \quad (135)$$

A straightforward application of the above formalism deals with propagation through a thin lens, which shows the possibility of obtaining in real time the Fourier transform of the input field. (see also Yariv (1), pg.817). To this end we note that if the diffraction term in Eq.(133) can be neglected and δn does not depend on z, it admits the solution

$$\mathbf{A}(\mathbf{r}_\perp,z) = \mathbf{A}(\mathbf{r}_\perp,z=z_0)e^{i(\omega/c)\delta n(\mathbf{r}_\perp)(z-z_0)} \quad . \quad (136)$$

If we consider now propagation through a thin lens of curvature radius R and width Δ (see Fig.9), it is not difficult to check that the phase change between z and z_0 depends on $r_\perp^2$ through the relation

$$k(n-1)(\Delta-h) = k\{\Delta-[R-\sqrt{R^2-r_\perp^2}]\} \cong k(n-1)(\Delta-r_\perp^2/2R)\,,\ (r_\perp^2 << R^2)$$

where n is the refractive index of the lens and 1 that of air. Recalling now the relation between the focal length f, the radius of curvature R and the refractive index n of a lens, that is 1/f=(n-1)/R, one can connect(see Fig.9) the field **A** on the left side of the lens in terms of the one on the right as

$$\mathbf{A}_{right}(x,y) = \mathbf{A}_{left}(x,y)e^{-i(k/2f)(x^2+y^2)} \quad (137)$$

in which the trivial factor exp[ik(n-1)Δ] can be neglected.

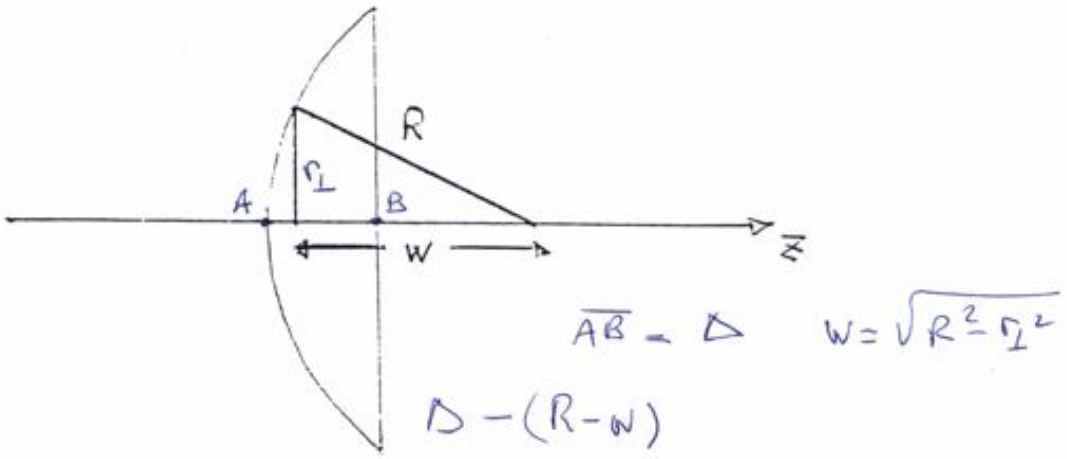

Fig. 9 . Lens geometry

Taking into account the above results, let us consider propagation of a monochromatic field **E**= **u**(x,y) exp(-iωt), **u** being the complex entrance function at the plane z=z_0=0, through the thin lens to the focal exit plane located at z+f (see Fig.(10).

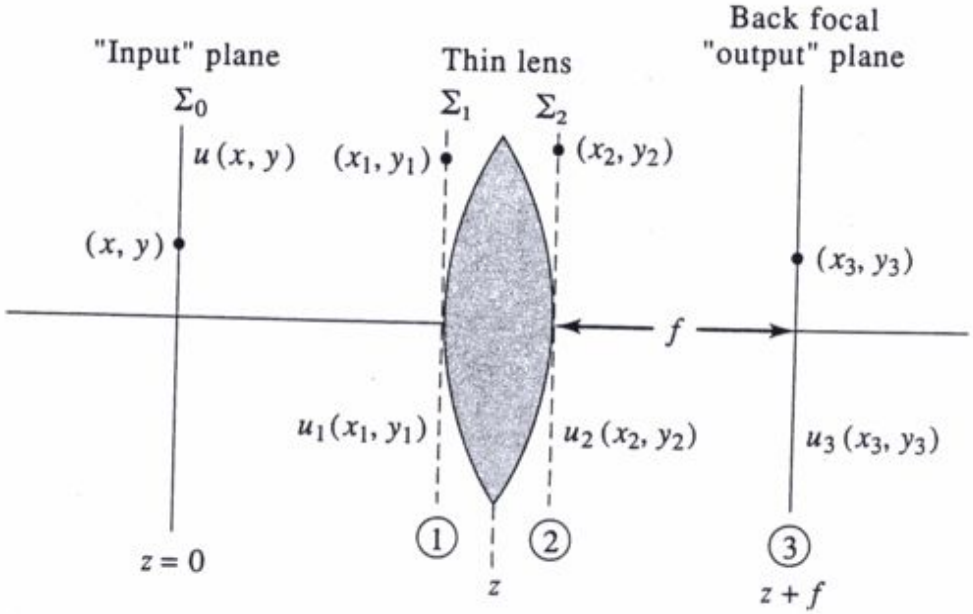

Fig. 10 Geometry of Fourier transform by a lens.

To follow the field evolution, one can employ Eq.(77), that is

$$E(x,y,z,t) = i\frac{e^{ikz-i\omega t}}{\lambda z}\int_{-\infty}^{+\infty} dx'dy'\; E(x',y')\; e^{(ik/2z)[(x-x')^2+(y-y')^2]},$$

thus getting

$$u_1(x_1,y_1) = i\frac{e^{ikz}}{\lambda z}\int_{-\infty}^{+\infty} dx\,dy\; u(x,y)\; e^{(ik/2z)[(x-x_1)^2+(y-y_1)^2]}, \quad (138)$$

and, using Eq.(137), in which the inessential factor exp[ik(n-1) Δ] is neglected,

$$u_2(x_2,y_2) = e^{-i(k/2f)(x_2^2+y_2^2)}u_1(x_2,y_2)\ .$$

Relying on the standard expression provided by Eq.(138) to propagate from the plane (x_2 ,y_2) to the plane (x_3 ,y_3) we can finally write

$$u_3(x_3,y_3) = \frac{i}{\lambda f}e^{ik(z+f)}e^{i(k/2f)(1-z/f)(x_3^2+y_3^2)}\int_{-\infty}^{+\infty} dx\,dy\; u(x,y)e^{-ik[(xx_3/f)+yy_3/f)]} \quad (139)$$

From the very definition of Fourier transform

$$\hat{u}(p,q) = \frac{1}{(2\pi)^2}\int_{-\infty}^{+\infty} dx\,dy\; e^{ipx+iqy}u(x,y)$$

it then follows that

$$u_3(x_3,y_3) = \frac{i(2\pi)^2}{\lambda f}\; e^{ik(z+f)}e^{(ik/2f)(1-z/f)(x_3^2+y_3^2)}\hat{u}(\bar{p},\bar{q}) \quad (140)$$

where

$$\bar{p} = -\frac{kx_3}{f}\quad,\quad \bar{q} = -\frac{ky_3}{f}\ .$$

In particular, if z=f , that is the input plane is the front focal plane,

$$u_3(x_3,y_3)=\frac{i(2\pi)^2}{\lambda f}\, e^{ik(z+f)}\hat{u}(\overline{p},\overline{q}) \quad , \quad (141)$$

that this the exit field is proportional to the Fourier of the input field. In particular, a plane wave is turned into a delta-function and a deltafunction into a plane wave. An example of the Fourier -transform property of a lens is shown in Fig. (11).

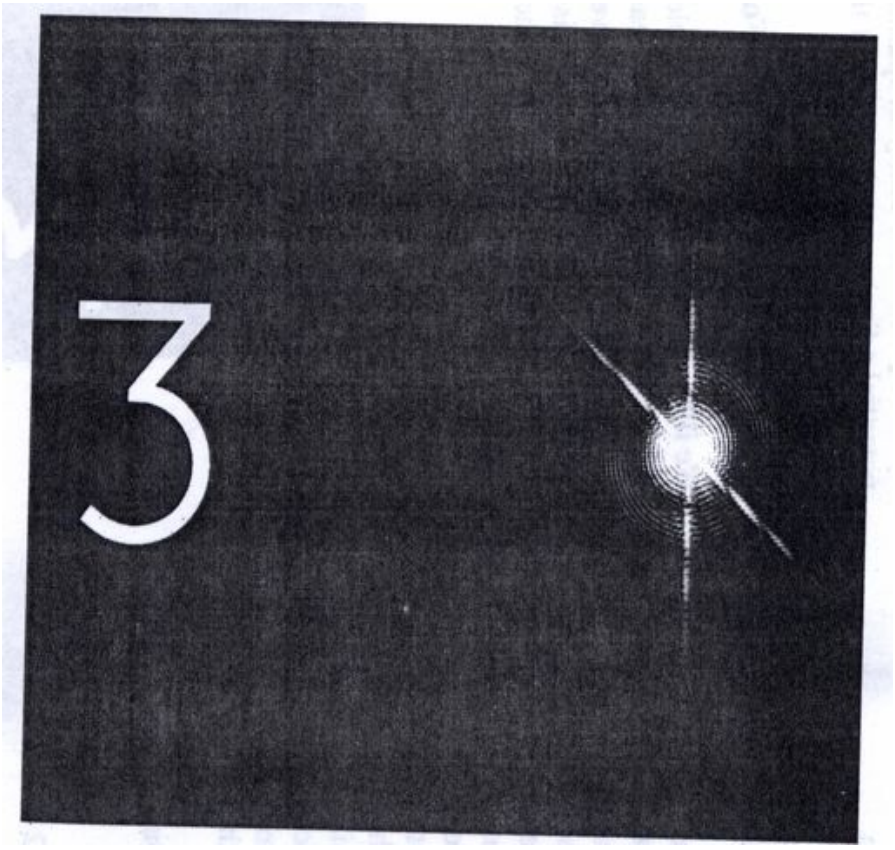

Optically obtained Fourier transform of symbol 3

1.13 Light confinement in optical resonators

The practical relevance of Gaussian beams is mainly due to the fact that in many cases they are the *modes of optical cavities* used in connection with laser operation.

Let us consider two identical Gaussian beams possessing the same waist propagating along the same axis, but in opposite direction. Let us now image to introduce two *spherical mirrors* of suitable curvature, such that the reflecting surfaces coincide with two equi-phase surfaces:
If the mirrors are perfectly reflecting and their spot-size on the mirror much smaller than the mirror dimension, it seems plausible that the Gaussian beam could start to oscillate in a stationary way between the two mirrors, producing the *mode of the resonator* made up by the two mirrors.
Keeping into account the fact that the mirrors are not perfect (their reflectivity is not, and cannot be, one) and that their extension is finite, the amplitude of the oscillating beam will decrease in time (if the mirror dimensions are large compared with the spot size, the diffraction losses can be neglected).
Given a specific *Gaussian beam*, there are infinite pairs of mirrors producing a resonator having the beam as a resonant mode. The inverse problem is more interesting: given two mirrors of curvature radius R_1 and R_2 placed at a distance d, find what Gaussian beam can eventually be a mode of the resulting resonator.
Consider two *spherical mirrors* of curvature radii R_1 and R_2 .(see Fig.1)

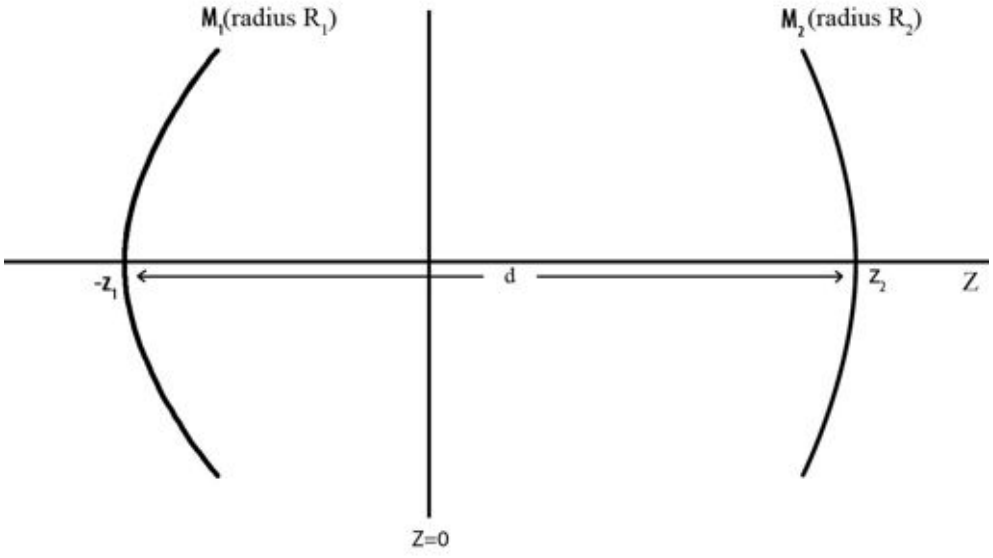

Fig.1

Assuming their extension to be much larger that the spot-size of a given Gaussian beam, can it bounce back and fourth between them producing eventually a stationary oscillation? (TEM_{nm} Gaussian modes)
In order to do that, the radii of curvature of the two beams have to be chosen equal to those of the beam wave-front at the two locations $-z_1$ and z_2 . Recalling Eqs.$(70)_1$ and (71) of the lecture notes on propagation in vacuum, the transverse field can be written as

$$i\frac{w_0}{w(z)}e^{-ik(x^2+y^2)/2R(z)}\ e^{-(x^2+y^2)/w^2(z)}H_n[\sqrt{2}x/w(z)]H_m[\sqrt{2}y/w(z)]\times$$
$$e^{ikz-i(n+m+1)\phi(z)},\quad \text{with}\quad \phi(z)=\text{arctg}(\lambda z/\pi w_0^2)\ ,\quad (1)$$

where

$$R(z) = z + \frac{z_0^2}{z}\ ,\quad (z_0 = \pi w_0^2/\lambda = \ell_d)\ .$$

Accordingly, it is necessary to satisfy the two equations between curvature radii and mirror distances from the beam waist

$$R_1 = z_1 + \frac{z_0^2}{z_1}\quad ,\quad R_2 = z_2 + \frac{z_0^2}{z_2}\quad .\quad (2)$$

From the first one we get

$$z_0^2 = R_1 z_1 - z_1^2\ ,$$

which, inserted in the second, yields

$$R_2 z_2 = z_2^2 + R_1 z_1 - z_1^2\ .$$

Taking into account the relation $z_1+z_2=d$, where d is the distance between the two mirrors, it follows

$$z_1 = d\frac{R_2\text{-}d}{R_1+R_2\text{-}2d} \quad , \quad z_2 = d\frac{R_1\text{-}d}{R_1+R_2\text{-}2d} \ . \quad (3)$$

Once z_1 (or z_2) is evaluated, Eq. (2) allows to evaluate z_0^2 and thus $w_0^2 = \lambda z_0 / \pi$.

In order to check the consistency of the above solutions, one introduces the so-called *g-parameters* of the cavity defined as

$$g_1 = 1\text{-}d/R_1 \quad , \ g_2 = 1\text{-}d/R_2 \ \rightarrow \ R_j = d/(1\text{-}g_j) \ . \quad (4)$$

According to their definition one has

$$z_1 = d\frac{g_2(1\text{-}g_1)}{g_1+g_2-2g_1g_2} \ ,$$

which inserted into Eq.(2) yields, after taking advantage of Eq.(4),

$$z_0^2 = z_1(R_1\text{-}z_1) = d\frac{g_2(1-g_1)}{g_1+g_2-2g_1g_2}\left[\frac{d}{1-g_1}\text{-}\frac{g_2(1-g_1)}{g_1+g_2-2g_1g_2}\right] = \qquad (5)$$
$$d^2 = \frac{g_1g_2(1-g_1g_2)}{(g_1+g_2-2g_1g_2)^2} > 0$$

which implies

$$0 \le g_1g_2 \le 1 \quad , \ \textit{stability condition} \ . \quad (6)$$

The g-parameters allows to associate to any cavity with spherical mirrors a point in Cartesian plane g_1, g_2,

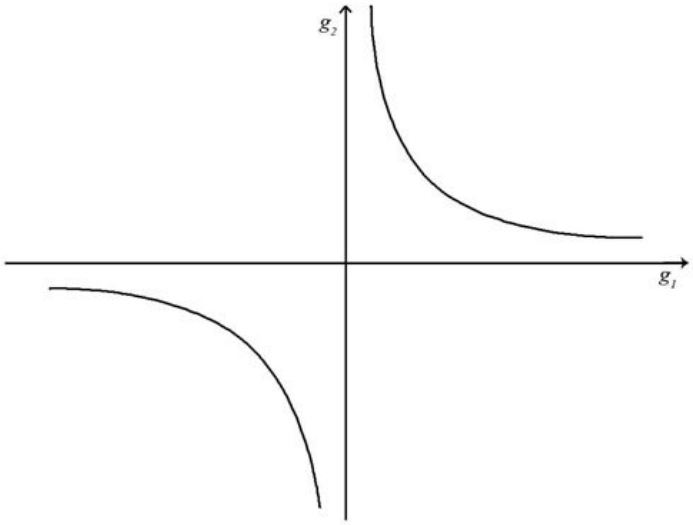

Fig.2

the stability condition being fulfilled in the crossed region. (Fig.2)

Symmetric resonators (identical mirrors)

$R_1=R_2=R=d \rightarrow z_1=z_2=d/2$.

From Eq.(2) we have

$$z_0^2 = \pi^2 w_0^4 / \lambda^2 = (2Rd-d^2)/4 \ ,$$

so that

$$w_0 = \sqrt[4]{\lambda^2(2Rd-d^2)} \qquad (7)$$

which, inserted in Eq. (66) of the lecture notes on Optical Wave Propagation in vacuo, allows to evaluate the spot-size on the mirrors (z=d/2), that is

$$w^2 = w_0^2[1+(d/2z_0)2] = w_0^2 2Rd/(2Rd-d^2) = (\lambda/\pi)\sqrt{R^2 d/(2R-d)} \ . \ (8)$$

Confocal resonators

The configurations obtained when R=d, that is the center of curvature of one mirror falls on the other mirror. According to Eq.(4)

$$z_0 = d/2$$

and, from Eq.(7),

$$w_0 = \sqrt{\lambda R/2\pi} = \sqrt{\lambda d/2\pi} \ ,$$

so that

$$w = \sqrt{\lambda R/\pi} = \sqrt{\lambda d/\pi} \ .$$

The resonators described above can also oscillate on higher-order Gaussian modes, the selection of the fundamental mode being in particular required when the oscillations are supported by an active medium in order to produce laser operation. This can be obtained by using a resonator such that the diffraction losses of the higher order modes (possessing a transverse extension larger than that of the fundamental one) are bigger than those of the fundamental mode.

We have assumed above the wavelength l of the field to be fixed. Actually, for every resonator, once the transverse configurations (*transverse mode*) of the field (see Eq.1) has been chosen, there exists an infinity number of wavelengths compatible with its oscillation. The fields oscillating at these frequencies are termed *axial modes* associated with a given transverse mode.
More in general, we have to impose the boundary condition

$$\psi_{n,m}(z_1) + \psi_{n,m}(z_2) = r\pi \ ,$$

r, m, and n being integer numbers, that is

$$2\pi d/\lambda_{r,m,n} - (n+m+1)[\mathrm{arctg}(z/z_0) - \mathrm{arctg}(z/z_1)] = \pi r \ , \quad (9)$$

where $\lambda_{r,m,n} = c/\nu_{r,m,n}$ are the oscillating wavelengths.

For a symmetric resonator ($z_2=d/2$, $z_1=-d/2$)

$$\nu_{r,m,n} = [r+(2/\pi)(m+n+1)\text{arctg}(d/2z_0)](c/2d) \quad . \quad (10)$$

The frequency separation between two *contiguous longitudinal modes* is given by

$$\Delta\nu_r = \nu_{r+1,m,n} - \nu_{r,m,n} = c/2d \ , \quad (11)$$

independently from the type of resonator. It can be compared with that of an ordinary Fabry-Perot resonator, consisting in two parallel plane mirrors separated by a distance ℓ (see Fig.3).

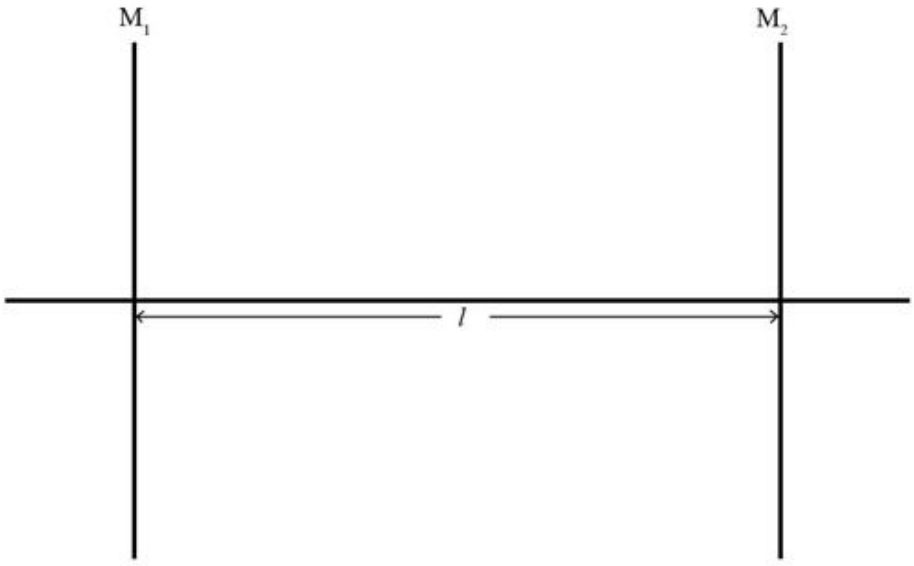

Fig.3

The transverse resonant mode inside the cavity is of the form

$$\mathbf{E}=\mathbf{E}_0\cos(\omega t)\sin(kx)$$

which is identically zero at x=0 and x=ℓ provided that

$$k\ell = n\pi \ , \quad (n=1,2,\ldots,n)$$
$$k_n = n\pi/\ell \ \rightarrow \ \nu_n = nc/2\ell \ \rightarrow \ \Delta\nu = c/2\ell. \qquad (12)$$

The separation between two *contiguous transverse modes* depends on the resonator

$$\Delta\nu = \nu_{r,n+1,m} - \nu_{r,n,m} = (c/\pi d)\,\mathrm{arctg}(d/2z_0) \ .$$

For a confocal resonator ($z_0=d/2$)

$$\Delta\nu = (c/\pi d)\,\mathrm{arctg}(1) = c/4d \ ,$$

so that two transverse modes with different m and n have the same frequency separation.

2 EM field as a statistical variable

2.1 Introduction

The theory of electromagnetic propagation introduced above applies to the case of a prescribed deterministic field. This can actually be a realistic description when the em field is generated by a macroscopic source, like an antenna, and the propagation medium can be described in terms of a deterministic refractive index. While this is often the case when dealing with long wavelength, is not generally true at optical frequencies where the field is the sum of individual fields generated by very small antennas, the atoms. The em field behaves in this case as a random variable and its description requires the introduction of a formalism able to take into account the fluctuations of the field around its average value. This formalism, usually referred to as *theory of optical coherence*, allows to describe propagation in terms of average values, correlation functions and other quantities which are usually introduced introduced when dealing with stochastic variables.

Detection of the optical field

EM fields are practically not directly observable at optical frequencies,

$\nu = c/\lambda \approx 6x10^{14}\,\mathrm{sec}^{-1}$, $\omega = 2\pi\nu \approx 3.6x10^{15}$ rad/sec .

What we actually measure at optical frequencies is the *optical intensity*, defined as

$$I(t) = \hat{\mathbf{E}}(t)\cdot\hat{\mathbf{E}}^{*}(t) = |\hat{\mathbf{E}}(t)|^{2} \quad , \quad (1)$$

averaged over the detector time-response T_D, that is

$$V_{T_D}(t) = \frac{1}{T_D}\int_{t-T_D}^{t+T_D} I(t')dt' \quad . \quad (2)$$

The involved time-scales are typically :
T_D , $1/w_0$ (w_0 being the central frequency of the field, T_M (the time scale associated with the deterministic modulation process) and a characteristic time-scale t_c associated with the stochastic nature of light. In most cases (practically always before the invention of laser), the time-scale hierarchy is

$$1/\omega_0 << t_c << T_D << T_M \quad , \quad (3)$$

T_D ranging from 1/25 sec (human eye) to hundred of picoseconds for advanced photo-detectors.
For the typical case $t_c << T_M$, the electric field can be written as

$$\hat{E}(t) = F(t)S(t) \quad , \quad (4)$$

where F(t) and S(t) are, respectively, a fast varying term whose spectrum is centered on ω_0 and a deterministic factor describing the field modulation on a time scale T_M . Accordingly,

$$V_{T_D}(t) = \frac{1}{T_D} \int_{t-T_D/2}^{t+T_D/2} |\hat{E}(t')|^2 dt' \cong |S(t)|^2 \lim_{T_D \to \infty} \int_{t-T_D/2}^{t+T_D/2} |F(t')|^2 \, dt' =$$

$$= |S(t)|^2 \, \langle |F(t)|^2 \rangle \quad , \quad (5)$$

where the angular brackets stand for "*ensemble average*" (its identity with the *time average* being justified, in the frame of stationary situations, by the validity of the so-called ergodic theorem). Thus, for $T_D >> t_c$, $V_{T_D}(t)$ is practically a *deterministic* variable, no fluctuations being present. The information contained in $V_{T_D}(t)$ would not allow to tell the difference between a laser source and a suitably filtered light bulb!
Things are different if the detection time T_D is smaller than t_c,

$$1/\omega_0 << T_D << t_c \quad . \quad (6)$$

In this case, $V_{T_D}(t)$ is a *time-dependent stochastic variable* and has to be dealt with as such, meaning that its description requires not only the knowledge of its *averaged value*

$$\langle I(t) \rangle = \lim_{T \to \infty} \frac{1}{T} \int_{t-T/2}^{t+T/2} V_{T_D}(t') \, dt' \quad , \quad (7)$$

but also of its *variance* , that is

$$\langle I^2(t) \rangle - \langle I(t) \rangle^2 \quad , \quad (8)$$

where

$$\langle I^2(t) \rangle = \lim_{T \to \infty} \frac{1}{T} \int_{t-T/2}^{t+T/2} V_{T_D}^2(t') \, dt' \, , \quad (9)$$

together with all *higher-order moments* $\langle I^n \rangle$ of the random variable.

This does not exhaust all the possible quantities necessary to describe the stochastic variable, like, e.g., the *correlation functions*, of which the lowest order one reads

$$<I(t)I(t+\tau)> = \lim_{T\to\infty} \int_{t-T/2}^{t+T/2} V_{T_D}(t')V_{T_D}(t'+\tau)dt' \ . \quad (10)$$

In particular, evaluating the moments of the stochastic variable I(t) requires the knowledge of the *distribution function* P(I) of the instantaneous intensity I(t), since

$$<I^n(t)> = \int_0^\infty P(I)I^n dI \ . \quad (11)$$

This allows one to understand the basic difference between a *chaotic* field, like the one emitted by the Sun or a light bulb), and a *laser* one:

$$P_{chaotic}(I) = \frac{1}{I_0}\exp(-I/I_0) \ \rightarrow \ <I^n(t)>=n!<I>^n \ , \ (12)$$

and

$$P_{laser}(I)=\delta(I-I_0) \ \rightarrow \ <I^n(t)>=<I>^n \ . \ (13)$$

2.2 Spatial and temporal coherence of the EM field

In general, the statistical properties of the field involve also the value of the electric field at different times and positions.
The most significant example is the famous *Young interference experiment* (see Fig.1)

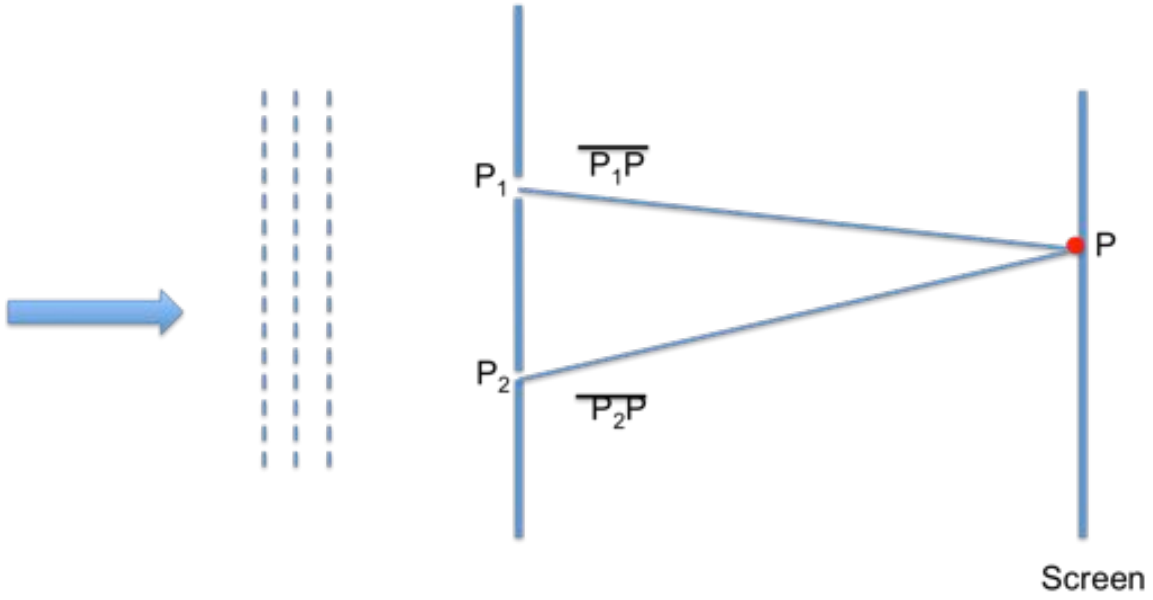

Fig. 1

The field on the screen is the sum of the two fields diffracted by the holes in P_1 and P_2, that is

$$\hat{E}(P,t)= \alpha_1 \hat{E}(P_1,t-\overline{PP_1}/c) + \alpha_2 \hat{E}(P_2,t-\overline{PP_2}/c) \quad , \quad (14)$$

where α_1 and α_2 are two geometrical factors. The intensity at a given position P on the screen can then be written as, assuming a *stationary* situation (that is independence from the choice of the origin of time)

$$I(P,t)=<|\hat{E}(P,t)|^2>=|\alpha_1|^2<|\hat{E}(P_1,t)|^2>+|\alpha_2|^2<|\hat{E}(P_2,t)|^2>+ \\ \alpha_1\alpha_2^*<\hat{E}(P_1,0)\hat{E}^*(P_2,\tau)>+\alpha_1^*\alpha_2<\hat{E}^*(P_1,0)\hat{E}(P_2,\tau)> \quad (15)$$

where $\tau = (\overline{P_1 P} - \overline{P_2 P})/c$,

the complex terms being responsible for the *interference* among the two beams (light + light = darkness!). The *correlation* between the two fields at different times and positions is associated with the *first-order correlation function*

$$G^{(1)}(\mathbf{r}_1,t_1;\mathbf{r}_2,t_2) = \langle \hat{E}^*(\mathbf{r}_1,t_1)\hat{E}(\mathbf{r}_2,t_2) \rangle \quad . \qquad (16)$$

More in general, the statistical description of the electromagnetic field requires the knowledge of its *n-order correlation functions*

$$\begin{aligned} &G^{(n)}(\mathbf{r}_1,t_1;\mathbf{r}_2,t_2;....;\mathbf{r}_n,t_n;\mathbf{r}_{n+1},t_{n+1};.....;\mathbf{r}_{2n},t_{2n}) = \\ &\langle \hat{E}^*(\mathbf{r}_1,t_1).....\hat{E}^*(\mathbf{r}_n,t_n)\hat{E}(\mathbf{r}_{n+1},t_{n+1}).....\hat{E}(\mathbf{r}_{2n},t_{2n}) \rangle . \end{aligned} \qquad (17)$$

In particular, after defining

$$\begin{aligned} &G_{1,2}(\tau) = \langle \hat{E}(P_1,0)\hat{E}^*[P_2, (\overline{P_1 P} - \overline{P_2 P})/c]) , \\ &G_{1,1}(\tau = 0) = \langle |\hat{E}(P_1,t)|^2 \rangle \equiv I_1 , \qquad (18) \\ &G_{2,2}(\tau = 0) = \langle |\hat{E}(P_2,t)|^2 \rangle \equiv I_2 \end{aligned}$$

it is convenient to introduce the *complex degree of coherence* defined as

$$\gamma_{1,2} = G_{1,2}(\tau)/[\sqrt{G_{1,1}(0)G_{2,2}(0)}] = G_{1,2}(\tau)/[\sqrt{I_1 I_2}] \quad , \quad (19)$$

which can be checked to obey the relation

$$0 < |\gamma_{1,2}(\tau)| \leq 1 \quad . \quad (20)$$

The *interference experiment* can then be described by the relation

$$I(P)=<|\hat{E}(P,t)|^2>= I_1(P)+I_2(P)+2\sqrt{I_1(P)I_2(P)}\,\mathrm{Re}\{\gamma_{1,2}(\tau)\},\quad (21)$$

where $I_1(P)$ and $I_2(P)$ are the intensities which would be present at position P if one of the two holes would be closed.

The complex degree of coherence $g_{12,}$ contains both space and time correlations. In particular, $\overline{P_1P}=s_1=\overline{P_2P}=s_2$, implies $\tau=0$ and $\gamma_{12}(0)$ describes to the lowest significant order the *spatial coherence* properties of the field. When $P_1=P_2$ (which is, e.g., the case for a Michelson interferometer) $\gamma_{1,2}(\tau)$ describe the *temporal coherence* properties.

An em field is *completely coherent* if, for any choice of P_1, P_2 and τ, one has $|\gamma_{1,2}(\tau)|=1$, while is termed *completely incoherent* if, with the exception of the case $P_1,=P_2$ and $\tau=0$, one has) $\gamma_{1,2}(\tau)=0$.

In most situations, for any fixed position P_1 there exists an ensemble of points such that over it $|\gamma_{1,2}(\tau)|\cong 1$.

In particular, if we set $P_1=P_2$, $|\gamma_{1,2}(\tau)|$ will take a value close to one for a given range of values of τ and will go to zero (not necessarily in a monotonic way) for larger values of τ : the range of values of t within which $|\gamma_{1,2}(\tau)\cong 1$ is called *coherence time* t_c.

In a similar way, for $\tau=0$ there will exist a region around P_1 such that, if P_2 is chosen within it, $|\gamma_{1,2}(\tau=0)\cong 1$: the area of this region is called *coherence area.*

As an example, let us consider the following *quasi-monochromatic* field centered around the frequency $\nu_0=\omega_0/2\pi$, that is

$$\hat{E}(P,t)= 2\int_0^\infty E_\nu(P)\exp(-2\pi i\nu t)d\nu=2\exp(-2\pi i\nu_0 t)\int_0^\infty E_\nu(P)\exp[-2\pi i(\nu-\nu_0)t]d\nu =$$
$$A(P,t)\exp[i\phi(P,t)]\exp(-2\pi i\nu_0 t)\ ,$$

where the two real functions A(P,t) and f(P,t) are slowing varying in time (with respect to $1/\nu_0$).

The fields at t=0 and at a time t such that $t\Delta\nu<<1$ will be approximately equal. Thus $\hat{E}(P,t)$ and $\hat{E}(P,t=0)$ can be different, and loose memory of each other, only if $t\Delta\nu \geq 1$, so that one can assume the coherence time t_c to be

$$t_c \cong 1/\Delta\nu . \quad (22)$$

A more rigorous general approach for determining the *coherence time* is provided by the *Wiener-Khinchin theorem* which connects the correlation function of a random stationary signal to its spectrum $S(\nu)$. In particular, the spectrum of the em field can be written as

$$S(\nu)=\frac{1}{4}\int \exp(2\pi i\nu\tau) < \hat{E}(t+\tau)\hat{E}^{*}(t)>d\tau \quad (23)$$

from whose anti-Fourier transform one can obtain t_c.

As far as *spatial coherence* is concerned, it is possible to prove the following formula connecting $G_{1,2}(\tau=0)$ on a given plane P_1 to the same quantity on a parallel plane P_2 placed at a certain distance R (see Fig.2):

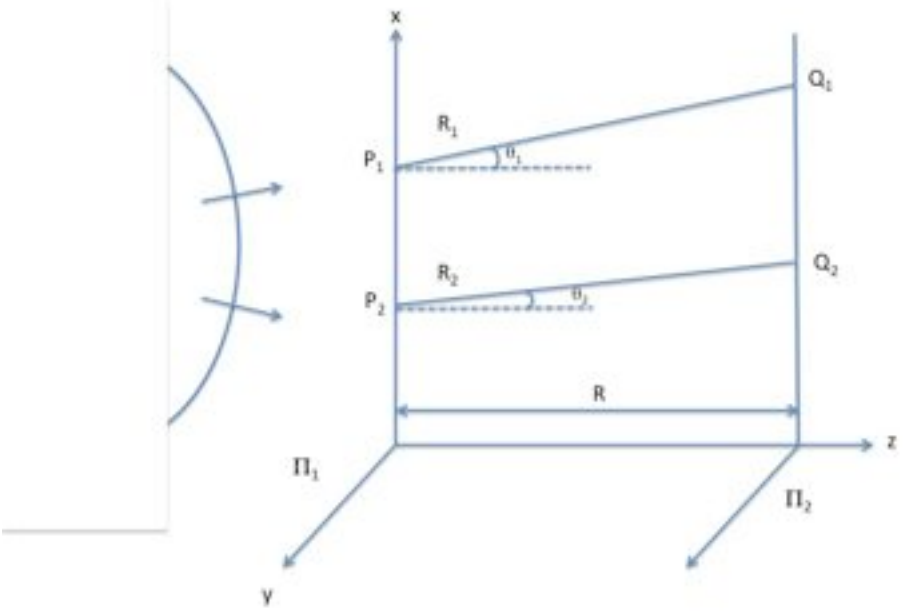

Fig. 2

$$J(Q_1,Q_2)=\frac{1}{\lambda_0^2}\int_{\pi_1} dP_1 \int_{\pi_2} dP_2 J_0(P_1,P_2)\frac{e^{ik_0(R_1-R_2)}}{R_1R_2}\cos\theta_1\cos\theta_2 \quad , (24)$$

where

$$J_0(Q_1,Q_2)\equiv<\hat{E}(Q_1,t)\hat{E}^*(Q_2,t)> \quad , \; J_0(P_1,P_2)\equiv<\hat{E}(P_1,t)\hat{E}^*(P_2,t)> \; . (25)$$

In particular, assuming Π_1 to coincide with a *completely incoherent planar source* for which

$$J_0(P_1, P_2)=I_0(P_1)\lambda_0^2\delta(P_1- P_2) \; ,$$

Eq.(24) produces the *VanCitter-Zernicke theorem*, that is

$$<E(Q_1,t)\hat{E}^*(Q_2,t)>=\int_{\pi_1} I_0(P)\frac{e^{ik_0(R_1-R_2)}}{R_1R_2}\cos\theta_1\cos\theta_2 dP \quad , (26)$$

where now R_1 and R_2 originate from the same point P of Π_1. (Fig.3)
If we now assumes the intensity to be negligible outside a region of P_1 of linear dimension $d<<R$, centered at the origin of the axis-system x,y,z=0, and consider a region on Π_2 centered on the axis-system X,Y, z=R of linear dimensions small with respect to R, one can approximately write

$$\frac{1}{R_1}\cong\frac{1}{R_2}\cong\frac{1}{R} \quad , \quad \cos\theta_1\cong\cos\theta_2\cong 1 \quad .$$

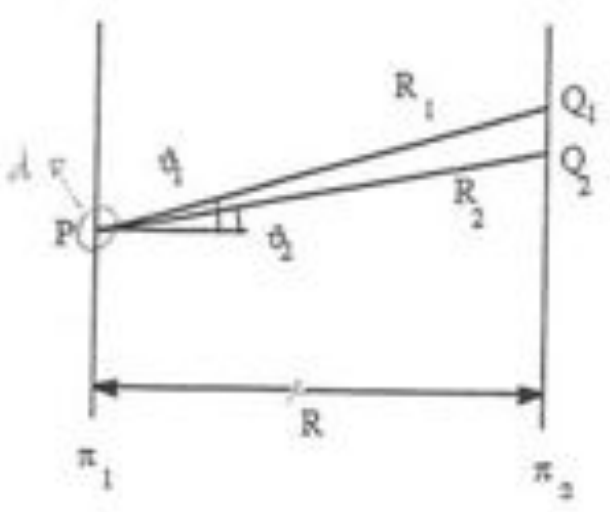

Fig. 2.2

If we set now (see fig. 2.2)

$Q_1=(X_1, Y_1, R)$, $Q_2=(X_2, Y_2, R)$, $P=(x,y)$,

we have, by using the Fresnel-like approximation,

$$R_{1,2}=[R^2+(X_{1,2}-x)^2+(Y_{1,2}-y)^2]^{1/2} \cong R+\frac{1}{2R}(X_{1,2}-x)^2+R+\frac{1}{2R}(Y_{1,2}-y)^2 .$$

By substituting these expressions in Eq.(26) we finally get

$$<E(X_1,Y_1)\hat{E}^*(X_2,Y_2)>=\frac{1}{R^2}\exp\{\frac{ik_0}{2R}[(X_1^2+Y_1^2)-(X_2^2+Y_2^2)]\}_x$$
$$\int_{\Pi_1} I_0(x,y)e^{-i(k_0/R)[(X_1-X_2)x+(Y_1-Y_2)y]}dxdy. \qquad (27)$$

Apart from a geometrical factor, the correlation function $J(P_1,P_2)$ on the plane Π_2 is *the Fourier-transform of the intensity distribution of the source on the plane* Π_1.

2.3 Application to Stellar Interferometry

By inspecting the above relation it is apparent that the radiation emitted by the source, initially completely spatially incoherent, becomes gradually spatially coherent while propagating (increasing value of R). This is the reason why the light coming from the stars exhibits quite large spatial coherence. Besides, according to the properties of the Fourier-transform, the coherence area will increase, for fixed k_0 and R, i*nversely* with the size of the source.
If we consider the case of an incoherent quasi-monochromatic circular source of radius a, centered on x=y=0 and possessing an uniform intensity $I(x,y)=I_0$, one has, after defining the "besinc" function,

$\mathrm{besinc}(x) \equiv J_1(x)/x$, $J_1(x)$ = first-order Bessel's function,

$$\mu_{1,2} \equiv \gamma_{1,2}(\tau = 0) = \mathrm{besinc}(\rho d/\lambda_0 R) = J_1(\rho d/\lambda_0 R)/(\rho d/\lambda_0 R) \quad , \quad (28)$$

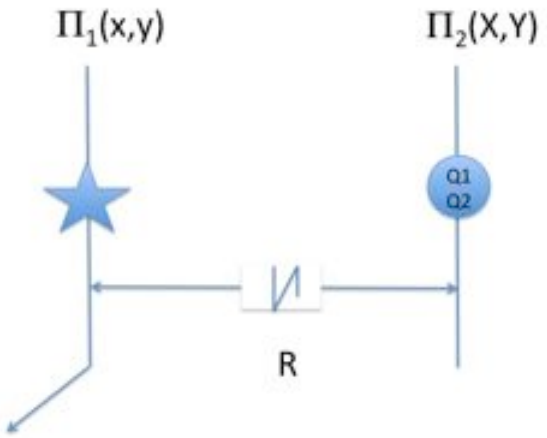

Fig. 3

where d=2a , $\rho = \overline{Q_1 Q_2}$, and $\lambda_0 = 2\pi / k_0$.

To determine the diameter of a star (see Fig.4), it is sufficient to measure $\mu_{1,2}$ on Earth as a function of ρ and find the value ρ_0 for which the besinc has its first zero, which happens when

$\rho_0 d/R\lambda_0 = 1.22$,

from which one can infer the *angular diameter* d/R of the star .
In Fig,(4) is shown a sketch of the *Michelson's stellar interferometer*.

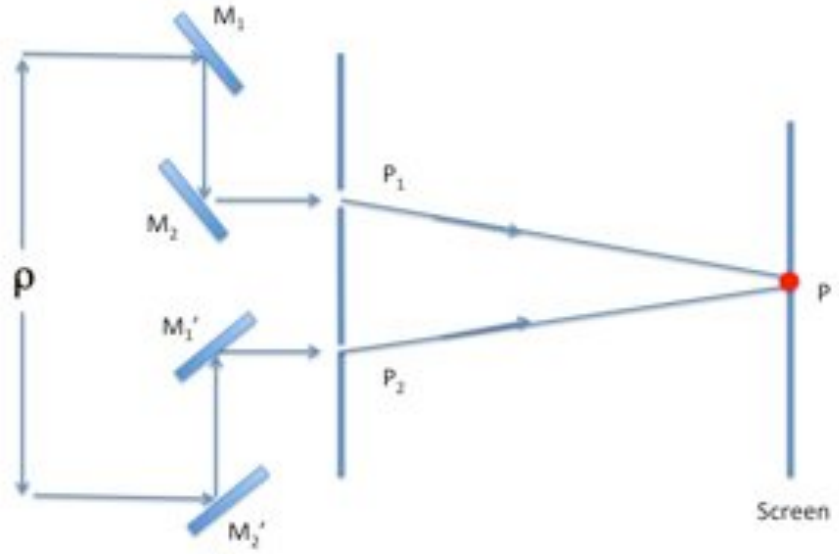

Fig. 4

For reason of mechanical instabilities and atmospheric turbulence, which can cause random movements in the interference fringes, ρ cannot exceed 10 meters, so that, assuming λ_0=0.5mm , the minimum appreciable angular diameter is (d/R)=5x10^{-8} rad.
In order to avoid these difficulties, a higher-order coherence property is measured, the *intensity correlation*, by means of the *Hanbury-Brown and Twiss* interferometer. In this device, the *intensities* of the star light are directly measured, so that phase fluctuations are eliminated: the resulting low-frequency signal, mutually retarded by an amount τ, are sent to an electronic correlator and integrator which measure the quantity $\langle I(t)I(t+\tau)\rangle$ (see Fig. (5)).

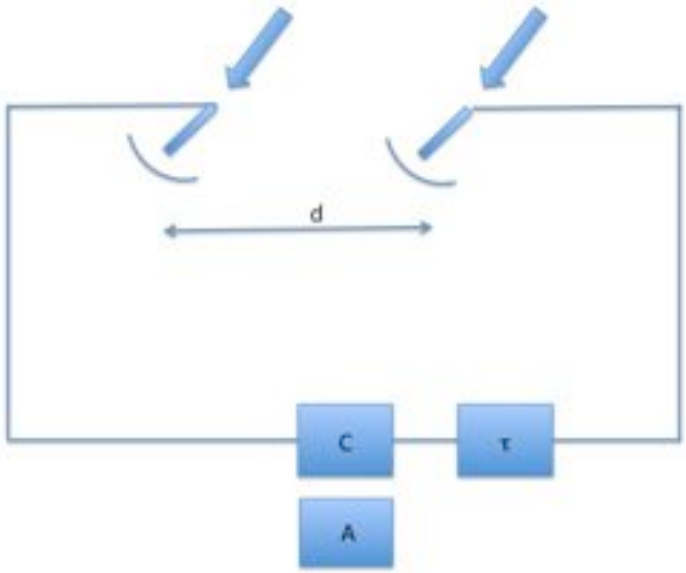

Fig. 5

For a completely chaotic source

$$<I_1(t)I_2(t+\tau)>=<I_1(t)><I_2(t>[1+|\gamma_{1,2}(\tau)|^2] \quad , \quad (29)$$

from which is possible to deduce $|\gamma_{1,2}(\tau)|$ and, from it, d/R.

2.4 Temporal coherence: the spectrum of an ideal laser

According to the Wiener-Khinchin theorem (see Eq.(23)), in order to evaluate the spectrum of a radiation field one needs to know its autocorrelation function.
For an ideal laser source, one can assume the field to be a plane wave with *constant amplitude* and *random phase*, that is

$$E(t)=E_0 e^{i\omega_0 t+i\varphi(t)} \quad . \quad (30)$$

The phase randomness may be modeled as due to *random changes of the instantaneous frequency* $\omega(t)$, that is

$$\omega(t)=\omega_0+\delta\omega(t) \quad \rightarrow \quad \varphi(t)=\int_0^t \delta\omega(t')dt' \quad , \quad (31)$$

so that the correlation function of the field reads

$$<\hat{E}(t)\hat{E}^*(t+\tau)>=|\hat{E}_0|^2 e^{-i\omega_0\tau} <e^{i\int_0^\tau \delta\omega(t')dt'}> \quad . \quad (32)$$

In particular, if dw(t) is a *Gaussian distributed* random variable,

$$<\hat{E}(t)\hat{E}^*(t+\tau)>=|\hat{E}_0|^2 e^{-i\omega_0\tau} e^{-(1/2)\int_0^\tau dt'\int_0^\tau dt''<\delta\omega(t')\delta\omega(t'')>} =$$

$$=|\hat{E}_0|^2 e^{-i\omega_0\tau} e^{-(1/2)\int_0^\tau dt'\int_0^\tau dt''<\delta\omega(0)\delta\omega(t''-t')>} \quad . \quad (33)$$

$$=|\hat{E}_0|^2 e^{-i\omega_0\tau} e^{-\int_0^\tau (\tau-\tau')<\delta\omega(0)\delta\omega(\tau')>d\tau'}$$

If t_c is the *correlation time* of the random frequency fluctuations, that is

$$<\delta\omega(0)\delta\omega(\tau')>=0 \text{ for } \tau'>\tau_c \quad , \quad (34)$$

then

$$\int_0^\tau (\tau-\tau')<\delta\omega(0)\delta\omega(\tau')>d\tau'=\tfrac{1}{2}<\delta\omega^2(0)>\tau^2 \text{ for } \tau<<\tau_c \quad (35)$$

and

$$\int_0^{\tau}(\tau-\tau')<\delta\omega(0)\delta\omega(\tau')>\mathrm{d}\tau' = A\tau \quad \text{for } \tau >> \tau_c \ , \quad (36)$$

where $A = 2\int_0^{\infty} <\delta\omega(0)\delta\omega(\tau')>\mathrm{d}\tau'$.

Accordingly, whether $t_c \to 0$ or $t_c \to \infty$, the laser spectrum tends to be respectively Gaussian or Lorentzian (in most cases the spectrum is actually Lorentzian).

3 Guided optical propagation

3.1 Simple geometrical optics approach

A simple light-guiding mechanism can be intuitively understood by looking at the figures sketched below, which schematically depict a glass cylindrical structure of refractive index n_1 (*core*) surrounded by a medium of lower refractive index n_2 (*cladding)* , a structure referred to as an *optical fiber* . By adopting a naïve geometrical optics picture, valid as long as the dimensions of the core are large compared with the wavelength of the propagating light beam, we can explain the guiding properties of the structure in terms of geometrical optics, by relying upon the *Snell law* which describes the refraction and the total reflection when a plane wave (a ray) impinges on a medium of refractive index n_2 coming from a medium of refractive index n_1. (see Fig. 1)

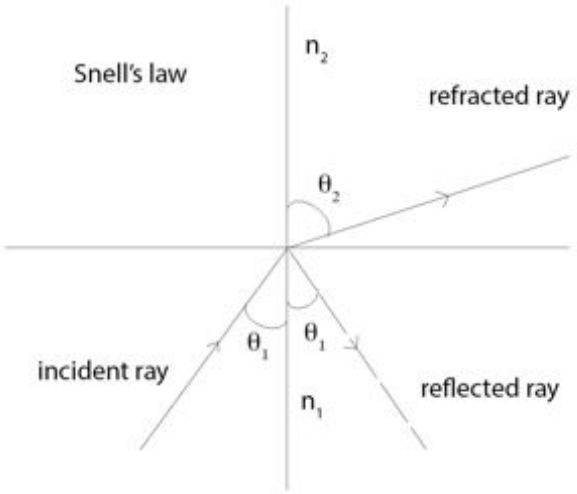

Fig. 1

Snell's law :
(angles are evaluated with respect to the normal to the separation plane)

$\theta_1=\theta'_1$; $n_1\sin\theta_1= n_2\sin\theta_2$. (1)

If $n_1> n_2$, Eq. (1) implies the existence of a *critical angle* θ_ℓ such that $\sin\theta_2 =(n_1/ n_2)\sin\theta_1$ becomes larger than one for $\theta > \theta_\ell$, which implies *no refraction* , that is *total reflection*, the angle obviously being given by the relation

$$\theta_\ell = \arcsin(n_2 / n_1) \quad . \quad (2)$$

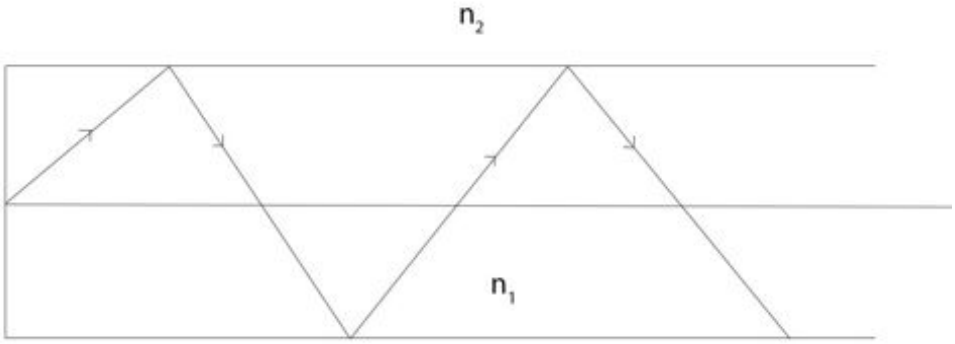

Fig. 2

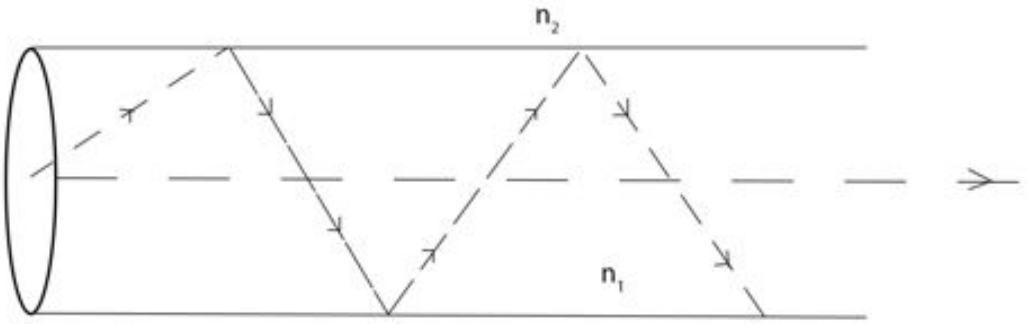

Fig. 3

By considering, for sake of simplicity, only *meridian* rays, that is the ones which remain in a plane during their propagation (the other ones being referred to as *skew* rays), one can easily understand how some rays can get trapped inside the glass cylinder. By looking at Figs.1 .2 and 3., it is obvious that the rays impinging on the surface of discontinuity, forming an angle with its normal larger than θ_ℓ are totally reflected and then proceed to propagate through successive total reflections, only hampered by the natural losses present in glass. Conversely, the other rays are only partially reflected and loose energy to the surrounding space , becoming quickly extinct.

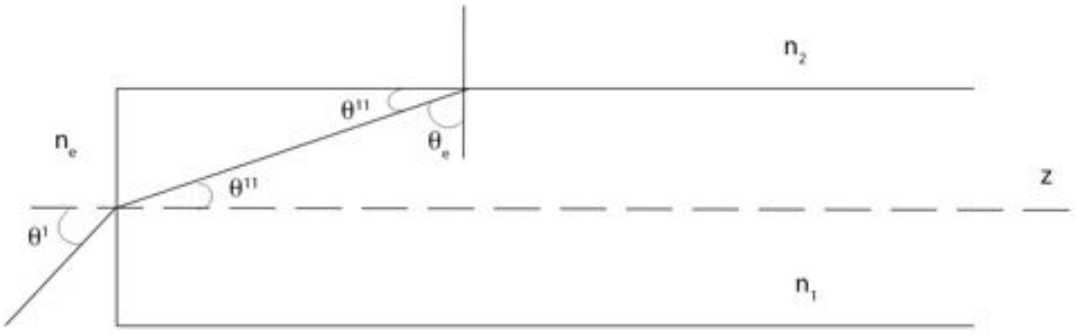

Fig. 4

By looking at Fig. 4, one can evaluate the maximum *angle of acceptance* Θ_M inside the fiber for rays coming from outside. One has

$$n_e \sin\theta' = n_1 \sin\theta'' = n_1 \sin(\frac{\pi}{2} - \theta_\ell) = n_1 \cos\theta_\ell = n_1 \sqrt{1 - n_2^2 / n_1^2} = \sqrt{n_1^2 - n_2^2}$$

and , after introducing the parameter $\Delta = (n_1^2 - n_2^2)/2n_1^2$,

$$\theta_M \cong \sin\theta_M = (n_1 / n_2)\sqrt{2\Delta} \quad , \quad NA \equiv n_e \sin\theta_M \cong n_1 \sqrt{2\Delta} \qquad ,$$

NA being referred to as the *numerical aperture.* typically of the order of some percent for telecommunication fibers.

Each family of parallel rays can be considered as a *mode of propagation* of the structure (according to this definition, there will be an infinite number of modes). Actually, all plane waves undergo diffraction so that all the rays within the diffraction angle can be assumed to belong to the same family: the number of *guided modes* N is actually finite and is given by the ratio between the *solid angles* associated with guidance and diffraction. Recalling that the *diffraction angle* is given by $\theta_d \cong \lambda / 2\pi a = 1/ka$, where k=2π/λ) one has

$$N = \frac{\pi\theta_M^2}{\pi\theta_d^2} = k^2 a^2 (n_1^2 - n_1^2) = V^2, \quad (4)$$

where

$$V = ka\sqrt{(n_1^2 - n_1^2)} \quad (5)$$

is the so-called *normalized frequency.*

(e.g., a= 20 μm , λ=0.5 μm , $n_1 \cong n_2 = 1.5$, $n_1 - n_2 = 0.01$, $N=V^2= 10^3$).

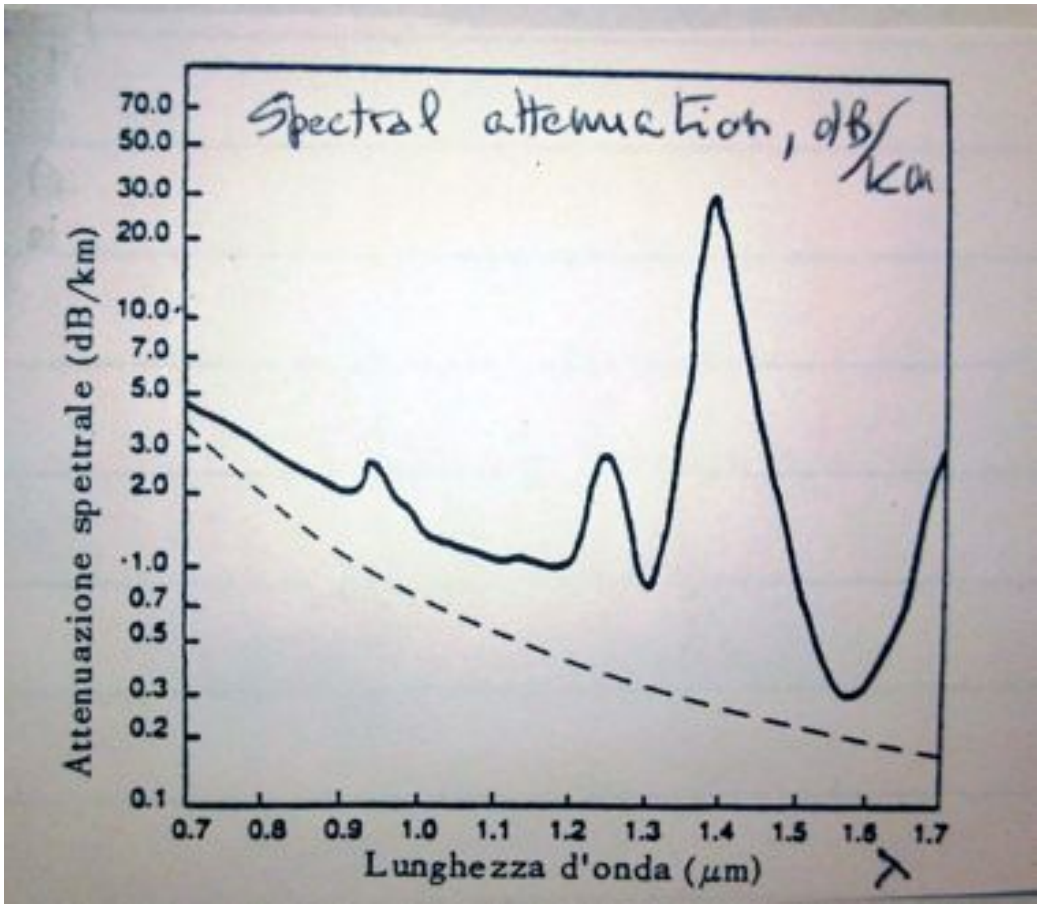

Fig. 5

Typically, the role of an optical fiber is to transfer light from one location to another, the main purpose being to transmit information suitably encoded in a light beam. To this end, several characteristics are necessary, as low attenuation of the signal at the carrier frequency (see Fig.5), minimal distortion of the encoded information and more down to earth but very important requirements, such as robustness, easiness of manipulation and, last but not least, cost.

The minimal distortion requirement is associated with the description of propagation of the electromagnetic field in the fiber. From an intuitive point of view, each guided modes carries a fraction of the field present at the fiber input along different paths, whose length varies from a minimum L (the fiber length) to a maximum $L(n_1/n_2)$, by bouncing back and forth between the surfaces separating core and cladding, loosing at each bounce part of the associated energy because of refraction. This propagation mechanism produces both losses, a generic mode typically undergoing many refraction processes over a

short traveled length, and distortion of the signal, this last shortcoming being associated with the different lengths of the paths traveled by different modes. (see Fig.6) , which in turn result in different times of arrival (L/c) and $(L/c)(n_1/n_2)$.

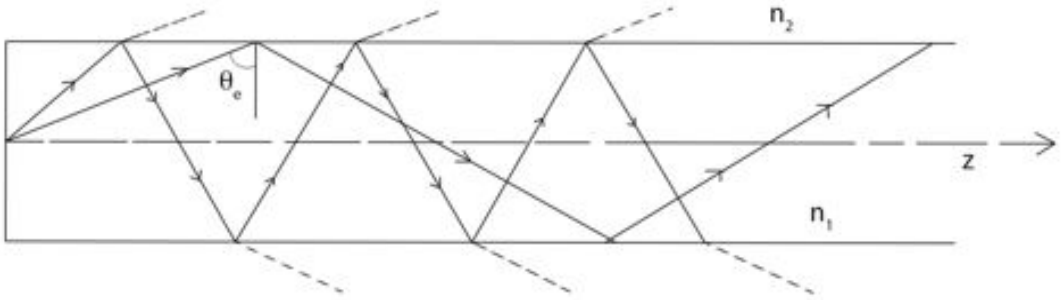

Fig. 6

The above simple intuitive geometrical-optics approach is only valid when the fiber radius is much larger than the wavelength but it is already capable to show the advantage of using a single mode, possibly the one propagating parallel to the fiber axis, to minimize distortion and losses. Also, it implies that distortion can be reduced by letting the refractive-index of the core vary with the distance from the fiber-axis in such a way that modes traveling at an angle with the fiber axis, thus traveling a longer path, see a smaller refractive index and, consequently, have a larger velocity than the ones parallel to the axis.
Fully understanding propagation in optical fibers, however, requires a physical-optics approach describing the case in which their transverse dimensions are comparable with the wavelength of the light.

3.2 Physical optics approach to propagation

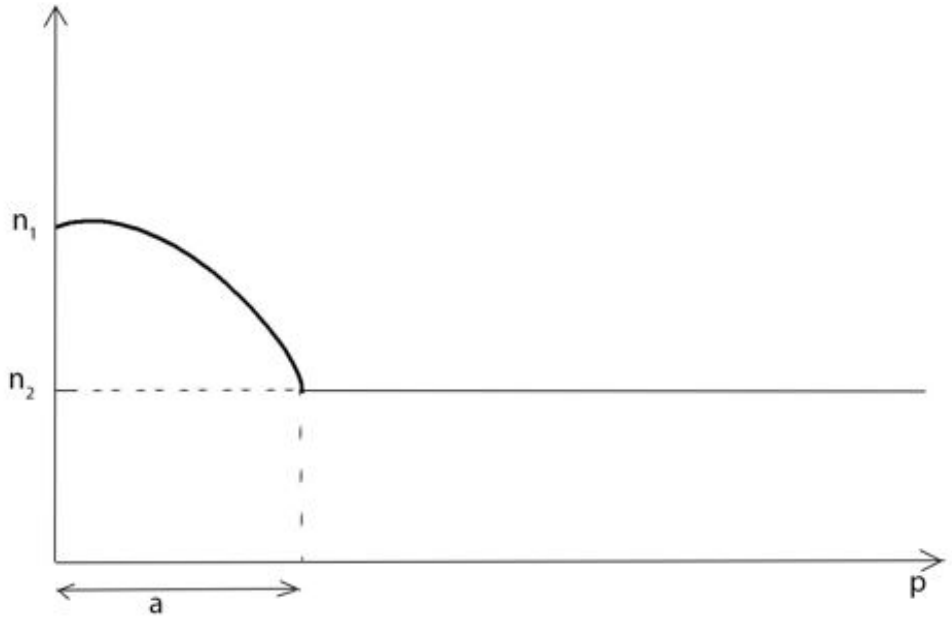

Fig. 7

Let us consider the case of a fiber whose z-independent refractive-index n_ω has the typical dependence on the transverse coordinate r shown in Fig.(7), which is necessary for achieving confinement and guidance of light. A monochromatic electric field propagating inside the fiber obeys the vectorial equation (see Eq.109 of lecture notes on EM propagation in matter)

$$\nabla^2 \mathbf{E}_\perp^{(\omega)}(\boldsymbol{\rho},z)+2\nabla_\perp\{\mathbf{E}_\perp^{(\omega)}(\boldsymbol{\rho},z)\cdot\nabla_\perp ln[n_\omega(\rho)]\}+k^2 n_\omega^2(\rho)\mathbf{E}_\perp^{(\omega)}(\boldsymbol{\rho},z)=0\,, \quad (6)$$

$\nabla_\perp$ representing the transverse component of the "nabla" vector , that is $\nabla_\perp=\hat{\mathbf{x}}\frac{\partial}{\partial x}+\hat{\mathbf{y}}\frac{\partial}{\partial y}$.

The polarization-mixing term can be neglected as long as $(\Delta n/n)(\lambda/a)<<1$, where Δn is the variation of the refractive index n over the fiber radius a ,typically $(n_1-n_2)/n_1 = 10^{-2}\text{-}10^{-3}$, which allows one to rewrite Eq.(6) in the form of a the *scalar Helmholtz equation*

$$\nabla^2 \mathbf{E}_\omega(\boldsymbol{\rho},z)+k^2 n_\omega^2(\rho)\mathbf{E}(\boldsymbol{\rho},z)=0 \quad , \quad (7)$$

having set, to use a simpler notation, $\mathbf{E}_{\perp}^{(\omega)}(\boldsymbol{\rho},z) \equiv \mathbf{E}_{\omega}(\boldsymbol{\rho},z)$.

A general approach to solving the above *linear* equation is to look for particular solutions of the kind

$$\mathbf{E}_{\omega}(\boldsymbol{\rho},z) = \boldsymbol{\varepsilon}_{\omega}(\boldsymbol{\rho})e^{i\beta_{\omega}z} \quad , \quad (8)$$

which possesses , if β_{ω} is a real quantity, the property of being diffraction-free, that is

$$|\mathbf{E}_{\omega}(\boldsymbol{\rho},z)|^2 = |\boldsymbol{\varepsilon}_{\omega}(\boldsymbol{\rho})|^2 .$$

Actually, one looks for solutions to corresponding to *guided propagation*, meaning that $\boldsymbol{\varepsilon}_{\omega}(\boldsymbol{\rho})$ has to go to zero, for $\rho \to \infty$, fast enough that the flux of the Poynting vector vanishes, so that optical energy is not lost to radiation. These solutions, provide they exist, are called *guided modes* of the structure associated to a specific $n_{\omega}(r)$ and have to obey the *eigenvalue equation*

$$\nabla^2\mathbf{E}_{\omega}(\boldsymbol{\rho},z)+(\omega/c)^2 n_{\omega}^2(\boldsymbol{\rho})\mathbf{E}(\boldsymbol{\rho},z) = \beta^2\mathbf{E}_{\omega}(\boldsymbol{\rho},z) \ . \ (9)$$

Typically, this equation admits of a denumerable set of solutions

$$\mathbf{E}_{\omega}^{(n)}(\boldsymbol{\rho},z)= \boldsymbol{\varepsilon}_{\omega}^{(n)}(\boldsymbol{\rho})e^{i\beta_{\omega}^{(n)}z}, \qquad (10)$$

where (n) stands for a set of integers identifying the mode. Assuming that this set of modes forms an *orthonormal complete set* (which is usually characteristic of the above eigenvalue problem), then the most general *guided monochromatic* field can be written, due to the linearity of the propagation equation, as an expansion of the form

$$\mathbf{E}_{\omega}(\boldsymbol{\rho},z,t) = \sum_{(n)} c_{\omega}^{(n)} e^{i\beta_{\omega}^{(n)}z - i\omega t}\boldsymbol{\varepsilon}_{\omega}^{(n)}(\boldsymbol{\rho}) \ , \ (11)$$

where the modes amplitudes $\boldsymbol{\varepsilon}_{\omega}^{(n)}(\rho)$ are orthonormal , that is

$$\int[\boldsymbol{\varepsilon}_{\omega}^{(m)}(\rho)]^{*}\cdot\boldsymbol{\varepsilon}_{\omega}^{(n)}(\rho)d\rho = \delta_{n,m} \ , \quad (12)$$

$\delta_{n,m}$ being the Kronecker symbol.

3.3 Modal dispersion

In general, a non-monochromatic field can be expressed as

$$\mathbf{E}(\rho,z,t) = \sum_{(n)}\int c_{\omega}^{(n)} e^{i\beta_{\omega}^{(n)}z - i\omega t}\boldsymbol{\varepsilon}_{\omega}^{(n)}(\rho)d\omega \ , \ (13)$$

where

$$c_{\omega}^{(n)} = \frac{1}{2\pi}\int d\rho\int dt\ \boldsymbol{\varepsilon}_{\omega}^{(n)}(\rho)^{*}\cdot\mathbf{E}(\rho, z=0, t)e^{i\omega t} =$$

$$\frac{e^{i\omega_0 t}}{2\pi}\int d\rho\int dt\ \boldsymbol{\varepsilon}_{\omega}^{(n)}(\rho)^{*}\cdot\mathbf{E}_0(\rho)A(t)e^{i(\omega-\omega_0)t} \ . \quad (14)$$

The typical spectrum of $c_{\omega}^{(n)}$ looks, for a standard telecommunication application (see Fig.8)

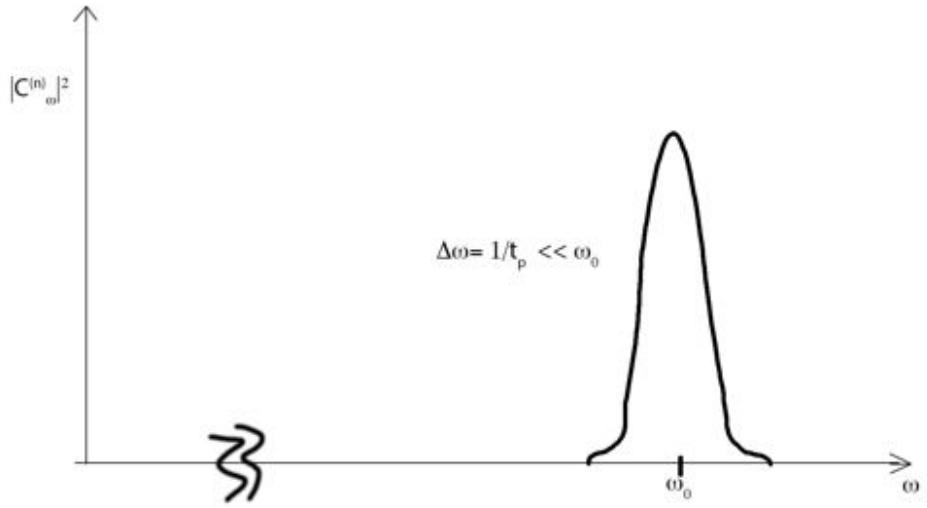

Fig.8

where t_p is the characteristic time of variation of A(t).
According to Eq.(13), we have

$$\mathbf{E}(\rho,z,t) = \sum_n \mathbf{E}^{(n)}(\rho,z,t) \quad , \quad (15)$$

with

$$\mathbf{E}^{(n)}(\rho,z,t) = \int_0^\infty c_\omega^{(n)} e^{i\beta_\omega^{(n)} z - i\omega t} \boldsymbol{\varepsilon}_\omega^{(n)}(\rho) d\omega \cong$$

$$\boldsymbol{\varepsilon}_{\omega_0}^{(n)}(\rho) \int_0^\infty c_\omega^{(n)} e^{i\beta_\omega^{(n)} z - i\omega t} d\omega =$$

$$\boldsymbol{\varepsilon}_{\omega_0}^{(n)}(\rho) e^{i\beta_{\omega_0}^{(n)} z - i\omega_0 t} \int_0^\infty c_\omega^{(n)} e^{i[\beta_\omega^{(n)} - \beta_{\omega_0}^{(n)}] z - i(\omega - \omega_0)t} d\omega \quad . \quad (16)$$

We can finally write, stopping at the first-order term in the Taylor expansion of $\beta_\omega^{(n)}$ around ω_0 ,

$$\mathbf{E}^{(n)}(\rho,z,t) \cong \boldsymbol{\varepsilon}_{\omega_0}^{(n)}(\rho) e^{i\beta_{\omega_0}^{(n)} z - i\omega_0 t} \int_0^\infty c_\omega^{(n)} e^{i[(z/V_g^{(n)}) - t](\omega - \omega_0]} d\omega$$

$$\equiv \boldsymbol{\varepsilon}_{\omega_0}^{(n)}(\rho) e^{i\beta_{\omega_0}^{(n)} z - i\omega_0 t} A(t - z/V_g^{(n)}) \quad , \quad (17)$$

having defined the *group-velocity of the n-th mode* as

$$V_g^{(n)} = (d\beta_\omega^{(n)} / d\omega)_{\omega=\omega_0}^{-1} \quad . \quad (18)$$

The fact that different modes possesses different group-velocity produces a *modal delay* , between any two of them given by

$$T_{n,m} = L \left| \frac{1}{V_g^{(n)}} - \frac{1}{V_g^{(m)}} \right| \quad , \quad (19)$$

where L is the propagation distance. Whenever more than two modes are present, one can estimate the *total modal delay* or *modal dispersion* T_M as the maximum value of $T_{n,m}$ over a group of simultaneously present modes, that is

$$T_M = \max T_{n,m} \text{ over } \{n,m\} \quad (\textit{modal dispersion}). \quad (20)$$

It sets a lower limit to the separation T_p allowed among the carrying-information pulses (see Fig.9)

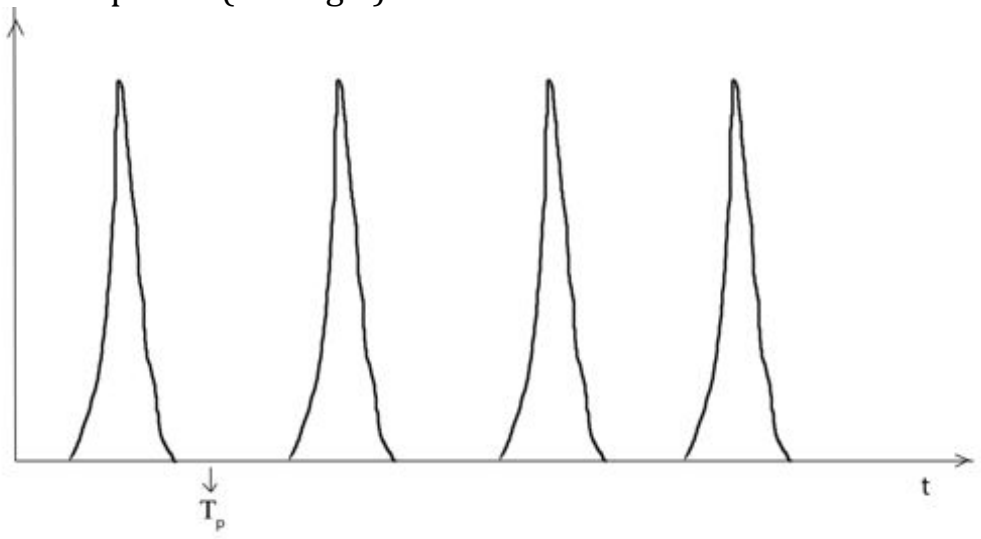

Fig. 9

that is $T_p > T_M$, which limits the number of bits transmissible per second to $1/ T_M$ bits/second.

3.4 Chromatic dispersion

If only one mode is excited, the only source of dispersion is associated with the fact that the group-velocity depends on frequency

$V_g^{(n)} = V_g^{(n)}(\omega)$.

This dependence induces *a delay between any two frequencies* ω' and ω" of the spectrum of the signal, which can be evaluated a

$$T_{cr} = L \left| \frac{1}{V_g^{(n)}(\omega')} - \frac{1}{V_g^{(n)}(\omega'')} \right| = L \left| (d\beta_{\omega}^{(n)}/d\omega)_{\omega=\omega'} - (d\beta_{\omega}^{(n)}/d\omega)_{\omega=\omega''} \right| \cong$$

$$L \left| [(d\beta_{\omega'}^{(n)}/d\omega')_{\omega_0} + (d^2\beta_{\omega'}^{(n)}/d\omega'^{2})_{\omega_0}](\omega' - \omega_0) \right.$$
$$\left. - [d\beta_{\omega''}^{(n)}/d\omega'')_{\omega_0} + (d^2\beta_{\omega'}^{(n)}/d\omega'^{2})_{\omega'=\omega_0}](\omega' - \omega_0) \right|$$
$$= L \left| \left(\frac{d^2\beta}{d\omega^2}\right)_{\omega_0} (\omega' - \omega'') \right| \cong L \left| \left(\frac{d^2\beta}{d\omega^2}\right)_{\omega_0} \right| \Delta\omega \quad , \quad (21)$$

where Δω is the bandwidth of the signal. This expression accounts both for the intrinsic dispersion of the *material* the guide is made of and for its geometry.
If the mode is *strongly confined* inside the core, then the chromatic dispersion is basically that of the core material, that is

$$\beta(\omega) \cong (\omega/c) n(\omega),$$

where n(ω) is the refractive index of the core. By using
$\lambda = 2\pi c/\omega$ instead of ω as an independent variable gets, by performing a simple change of variables,

$$T_{cr} = \frac{L\lambda}{c} \left| \left(\frac{d^2 n(\lambda)}{d\lambda^2}\right)_{\lambda=\lambda_0} \right| \delta\lambda \quad , \quad (22)$$

where $\delta\lambda/\lambda_0 = \delta\omega/\omega_0$, so that the chromatic dispersion is zero for a value of λ_0 such that

$$\left(\frac{d^2 n(\lambda)}{d\lambda^2}\right)_{\lambda=\lambda_0} = 0 \ . \quad (23)$$

A range of typical values of chromatic dispersion is shown in Fig.10. In general, by playing with the dispersion of the material and that of the propagating mode one can move the wavelength value of zero-dispersion in order to avoid losses. (see Fig.5, note that the broken line which corresponds to *Rayleigh scattering* alone, that is to the incoherent sum of the fields scattered by the single atoms, corresponds to unavoidable losses).

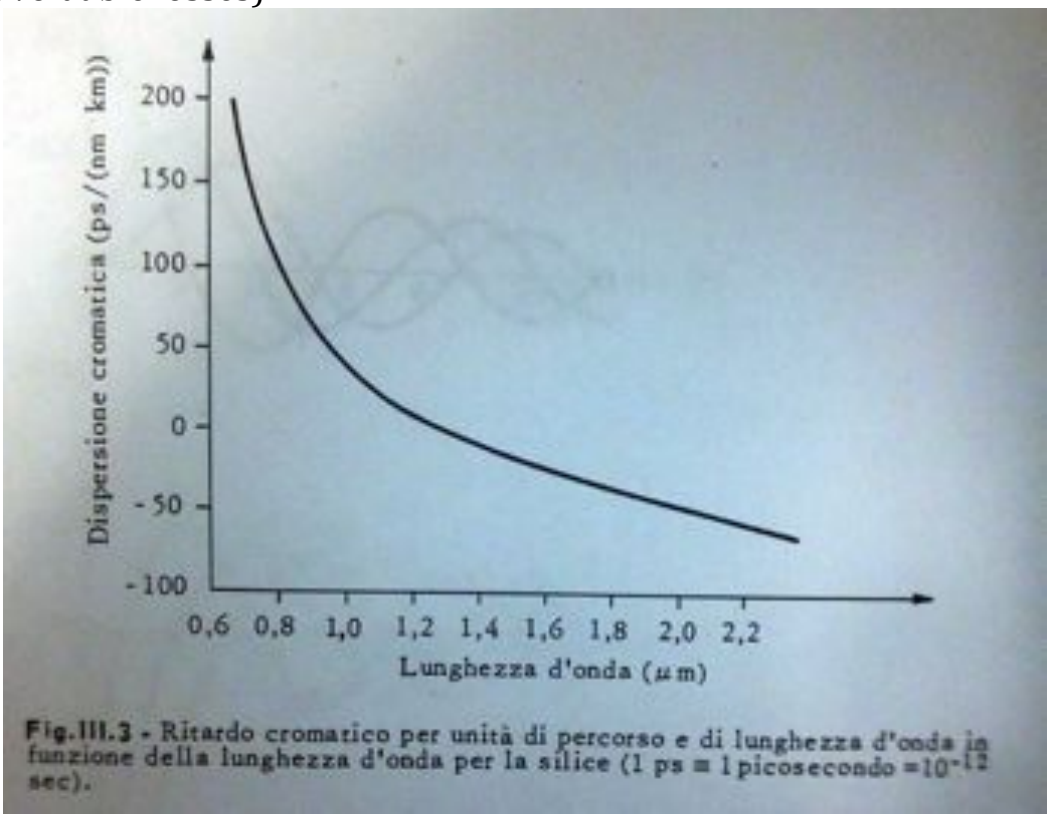

Fig.III.3 - Ritardo cromatico per unità di percorso e di lunghezza d'onda in funzione della lunghezza d'onda per la silice (1 ps = 1 picosecondo = 10^{-12} sec).

Fig.10

3.5 Optical communications: single-mode fibers

From the above considerations it is apparent that, apart from the intrinsic losses of the material, the main limitation to the transmission of a carrying-information optical signal is due to both modal and chromatic dispersion.

Modal dispersion is associated to the possible presence of more than one propagating mode and to their different group-velocity (see Eq.(20)). One way of avoiding the problem seems to excite only one propagation mode, that is to input the fiber with only one of the possible transverse configurations, so that the entire optical power travels on the chosen mode while the other ones are not excited. Actually, this solution is not a realistic one since the unavoidable imperfections present in the fiber structure induce a coupling mechanism among all the guided modes which eventually results (in most cases after few centimeters) in a power-sharing among many propagating modes which produces signal distortion.

The only way out is associated with a remarkable property of dielectric optical fibers: the propagation constants β_ω of all propagating modes but one (the *fundamental mode*) acquire an imaginary part below a certain value $\bar{\omega}$ (*cut-off value*) of the frequency ω. This produces a damping mechanism which eventually takes out of the competition all modes but the fundamental one and thus eliminates modal dispersion.

This behavior is illustrated below for the case of a round fiber whose refractive index has the (ideal) radial dependence presents a discontinuous behavior (*step-index* optical fiber,(see Fig.11).

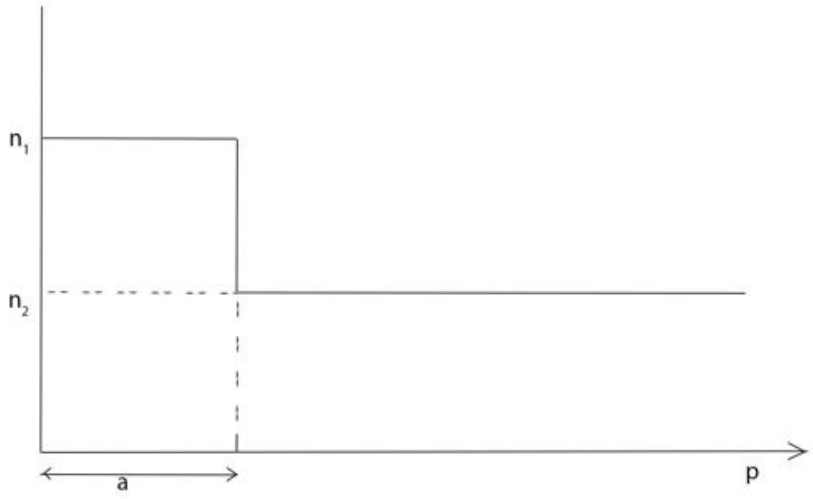

Fig. 11

Since, as it can be checked *a posteriori* , $(n_1 - n_2)/ n_1 = 10^{-2} - 10^{-3} << 1$, the scalar Helmholtz equation

$$\nabla^2 \mathbf{E} + k^2 n^2(\rho)\mathbf{E} = 0 \quad (24)$$

can be considered valid also for values of the radius a of the order of λ, and it is reasonable to adopt a description in which the modes are associated with *linearly polarized fields* (that is, their z-component is neglected), each of them possessing two independent mutually-orthogonal linearly polarized states (LP modes).

The electric field E (E_x or E_y) of a generic mode obeys the equations

$$\nabla_\perp^2 E = -\gamma^2 E \quad \text{for } r < a \,, \qquad \nabla_\perp^2 E = \delta^2 E \quad \text{for } r > a \tag{25}$$

with

$$\gamma = \sqrt{n_1^2 k^2 - \beta^2}, \quad \delta = \sqrt{\beta^2 - n_2^2 k^2} \quad , \; k=\omega/c \; , \tag{26}$$

where $kn_2 \le \beta \le kn_1$ and

$$\nabla_\perp^2 = \frac{\partial^2}{\partial x^2} + \frac{\partial^2}{\partial y^2} = \frac{1}{\rho}\frac{\partial}{\partial \rho}\left(\rho \frac{\partial}{\partial \rho}\right) + \frac{1}{\rho^2}\frac{\partial^2}{\partial \phi^2}.$$

One has to find the solutions of Eq.(25) such that *the field and its normal derivati*ve are continuous at $\rho = a$ and *decrease exponentially* in the cladding for $\rho \to \infty$.

Possible solutions can be written, by separating the variables, in the form (m=0,1,2,....)

$$E(\rho,\phi,z) = B e^{i\beta_\omega z} J_m(\gamma\rho) e^{\pm im\phi} \quad , \; \rho \le a$$
$$E(\rho,\phi,z) = C e^{i\beta_\omega z} K_m(\delta\rho) e^{\pm im\phi} \quad , \; \rho \ge a \tag{27}$$

where B and C are constants , J_m the *Bessel functions of the first kind* and K_m the *modified Bessel function of the second kind* (See Fig.12).
Are there values of β such that the two branches of E and of its radial derivatives can be matched at $\rho = a$?

$$\frac{d^2 f}{d\rho^2} + \frac{1}{\rho}\frac{df}{d\rho} + \left(\chi^2 - \frac{l^2}{\rho^2}\right) f = 0$$

Bessels equation (above) and Bessels functions (below)

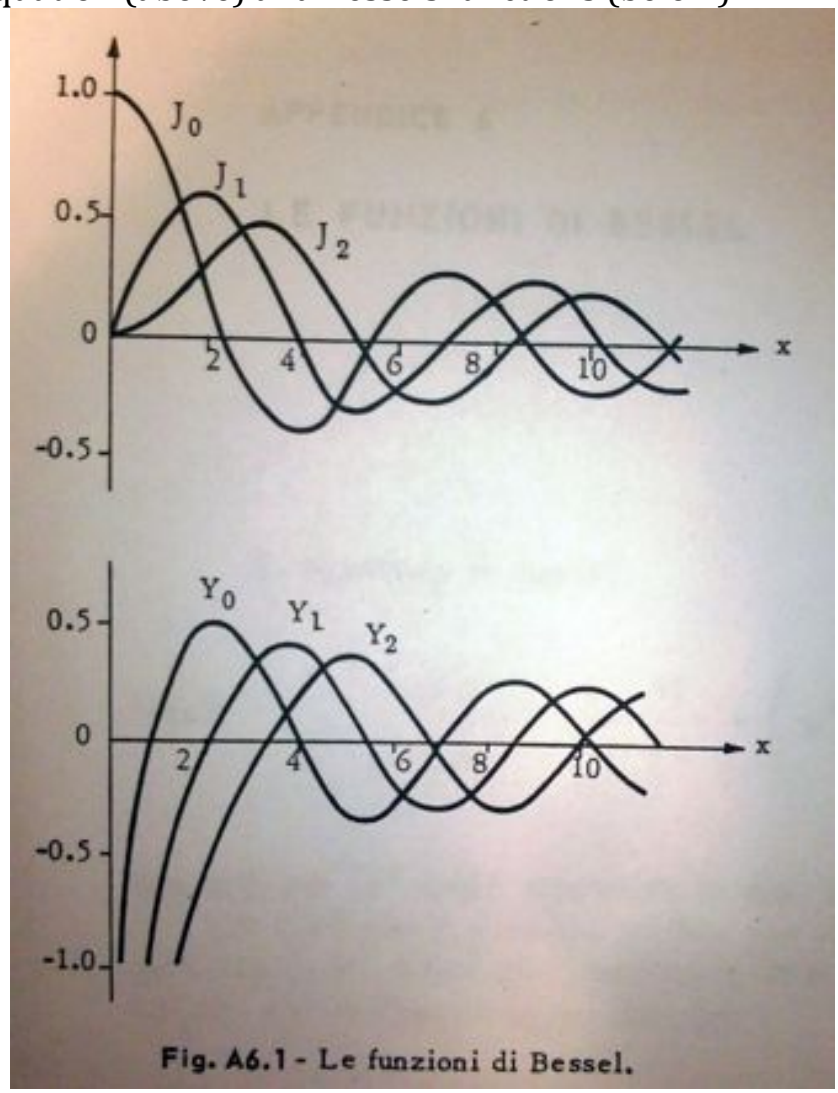

Fig. A6.1 - Le funzioni di Bessel.

Fig. 12

For the simplest case m=0 these two conditions read

$$\begin{aligned} BJ_0(\gamma a) &= CK_0(\delta a) \\ B\gamma J_0'(\gamma a) &= C\delta K_0'(\delta a) \end{aligned} \quad , \qquad (28)$$

where the "prime" stands for derivative with respect to the argument, or

$$\frac{\gamma J_0'(\gamma a)}{J_0(\gamma a)} = \delta \frac{K_0'(\delta a)}{K_0(\delta a)} \quad .$$

Since $J'_0(x)=-J_1(x)$, $K'_0(x)=-K_1(x)$, one gets the transcendental equation

$$\gamma \frac{J_1(\gamma a)}{J_0(\gamma a)} = \delta \frac{K_1(\delta a)}{K_0(\delta a)} \quad . \quad (29)$$

Finally, by using the relation (see Eq.(26))

$$\gamma^2 + \delta^2 = k^2(n_1^2 - n_2^2) = V^2/a^2 \quad , \quad (30)$$

where $V=ka\sqrt{n_1^2 - n_2^2}$ is the normalized frequency, it is possible to write the *characteristic equation* (in γa) relative to our eigenvalue as

$$\gamma a \frac{J_1(\gamma a)}{J_0(\gamma a)} = \sqrt{V^2 - (\gamma a)^2} \; \frac{K_1(\sqrt{V^2 - (\gamma a)^2})}{K_0(\sqrt{V^2 - (\gamma a)^2})} \quad . \quad (31)$$

Once the solutions of Eq.(31) are found, one can get the corresponding

δa and β from Eqs (26) and (31), so that the mode is completely determined (the ratio between B and C can be obtained by Eq.(28)). The solutions have to be looked for in the interval $0<\gamma a<V$ since, otherwise, $V^2-(\gamma a)^2$ is imaginary).
For every value of V, a denumerable set of solutions exists, the corresponding modes being labeled, LP standing for linearly polarized, LP_{01}, LP_{02} , ….., LP_{0q} with q=1,2,3,….
For a generic m>1, the continuity conditions at ρ=a eventually yield

$$\gamma\frac{J'_m(\gamma a)}{J_m(\gamma a)} = \delta\frac{K'_m(\delta a)}{J_m(\delta a)} \ , \ m=0,1,2,\dots \ ,$$

which, by exploiting properties of the Bessel functions, is equivalent to

$$-\gamma a\frac{J_{m-1}(\gamma a)}{J_m(\gamma a)} = \sqrt{V^2-(\gamma a)^2}\ \frac{K_{m-1}(\sqrt{V^2-(\gamma a)^2})}{K_m(\sqrt{V^2-(\gamma a)^2})} \ . \quad (32)$$

The solutions of the above equations provide the *transverse modal configurations*

$$E^{(\omega)}_{mq}(\rho,\phi,z) = Be^{i\beta(\omega)_{mq}z}J(\gamma_{mq}\rho)e^{\pm im\phi} \ , \quad \rho\le a$$
$$E_{mq}(\rho,\phi,z) = Ce^{i\beta_{mq}z}K_m(\gamma_{mq}\rho)e^{\pm im\phi} \ , \rho\ge a, \quad (33)$$

in terms of which the generic monochromatic field propagating in the fiber can be expanded.
A plot of the normalized value of $\beta^{(\omega)}$, that is $b=[\beta/k)-n_2]/(n_1-n_2)$, as a function of the normalized frequency V for some guided modes of the fiber is shown in Fig. 13.

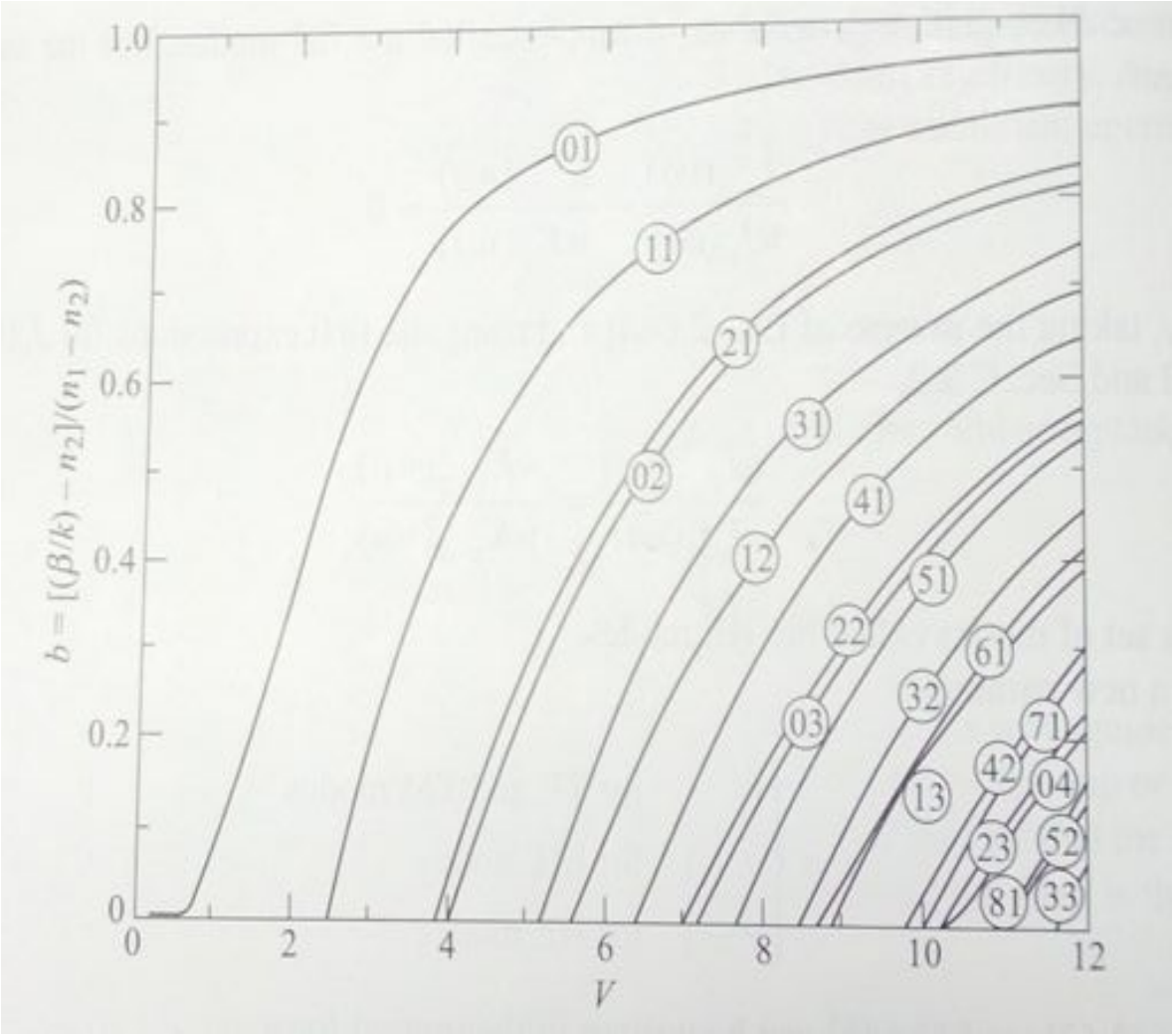

Fig. 13

The propagation constant of any guided mode, except the fundamental one LP_{01}, becomes imaginary at a given value $\bar{V}$ of V, so that if $V < \bar{V}$ the mode is attenuated and disappears (is *cut-off*) after a short distance. The cut-off values of V for some low-order LP can be inferred by the picture..
By looking at Fig.13 is apparent that by choosing the propagation φρεθυενχψ ω in such a way that V<2.405 (the first zero of $J_0(x)$), the only mode with a real propagation constant is LP_{01} , so that the fiber is operating in a *single-mode regime.* As an example, if n_1=1.502, n_2=1.5 and λ= 1.3μm, the fiber becomes single mode when a <6.4μm.
Counting the *number of modes* N *for a given value of* V one finds that, for large V and including the two independent polarization states,

$N \cong V^2/2$, (34)

so that 50 modes are present for V=10.

In the limit of large V one can take advantage of geometrical optics for getting an estimate of the modal delay and find that

$T_M=(L/c)n_1(n_1- n_2)/ n_2$ (for n_1=1.50, n_2= 1.49 , t= 30 nsec/Km). (35)

The geometrical optics picture of fiber propagation suggests that modal delay could be reduced if the refractive-index would decrease from the axis of the fiber to the cladding (see Fig.14)

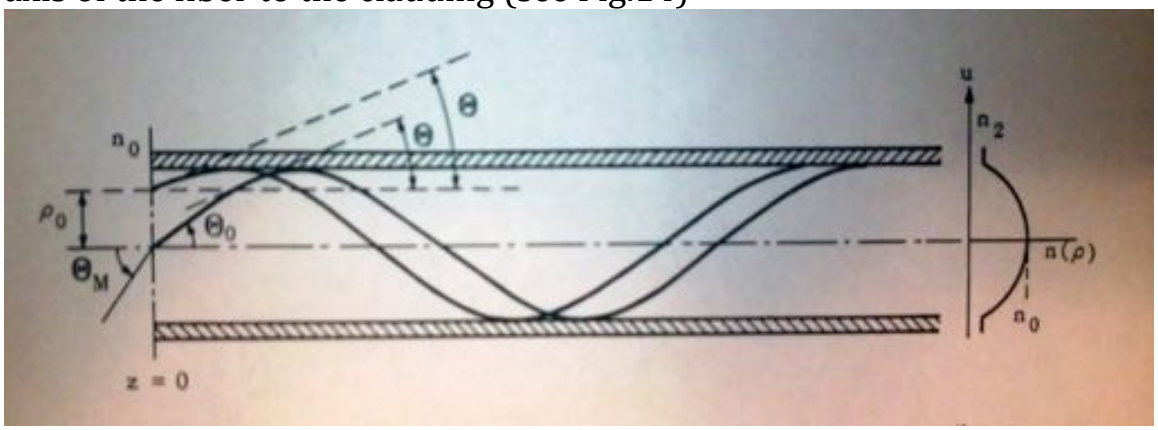

Fig. 14
Guided rays in a graded-index fiber

so that the rays traveling at a higher inclination with respect to the propagation direction, thus traveling a longer distance, would do it at higher velocity. As a result, the modal delay would be reduced with respect to the step-index fiber.
These fibers are called *graded-index fibers* and it can be actually shown that, in the limit of large V, and for a *parabolic profile*,

$T_M=(L/8cn_1)(n_1- n_2)^2$, (36)

to be compared, to advantage, with the above modal delay for a step-index fiber.
It is possible to describe propagation in a graded-index fibers by using the same physical-optics formalism employed for the step-index fiber

and find the corresponding analytic expressions for modal amplitudes and the propagation constants.

3.6 Single mode regime

In the frame of long-distance signal propagation , the fiber has to operate in a single-mode regime and the only source of dispersion is associated with *chromatic dispersion*. While for the modes of a multi-mode fiber far from cut-off it is reasonable to assume

$$\beta(\omega)=n_1(\omega)\omega/c \ , \quad (38)$$

for a single-mode fiber, or when considering modes near cut-off, the above equation becomes questionable since β depends on the modal configuration and on the refractive-index of the cladding, that is $n_2(\omega)$. By playing with the modal profile it is possible to shift the value of ω for which chromatic dispersion has a minimum to spectral regions (e.g., l around 1.55 μm) where the attenuation has a minimum (DS, *dispersion-shifted fibers).* Also, it is possible to achieve low dispersion in a whole interval (DF, *dispersion-flattened fibers*, e.g., between the wavelengths relevant to telecommunications, 1.2 and 1.6μm). Typically, single-mode operation requires small core-radius, a demand which does not allow, during fiber fabrication, a precise control of its refractive-index profile. Luckily, it turns out that both the modal configuration and the propagation constant are quite insensitive to the specific spatial behavior of the refractive index. As an example, a good approximation for the single-mode configuration is

$$\psi(\mathbf{r}_\perp) \cong e^{-r_\perp^2/2r_0^2} \ , \quad (39)$$

where

$$r_0^2=a^2/\ln V \ , \quad \text{for } V>1 \ , \quad (40)$$

a being the core radius.

3.7 Graded-Index Fibers

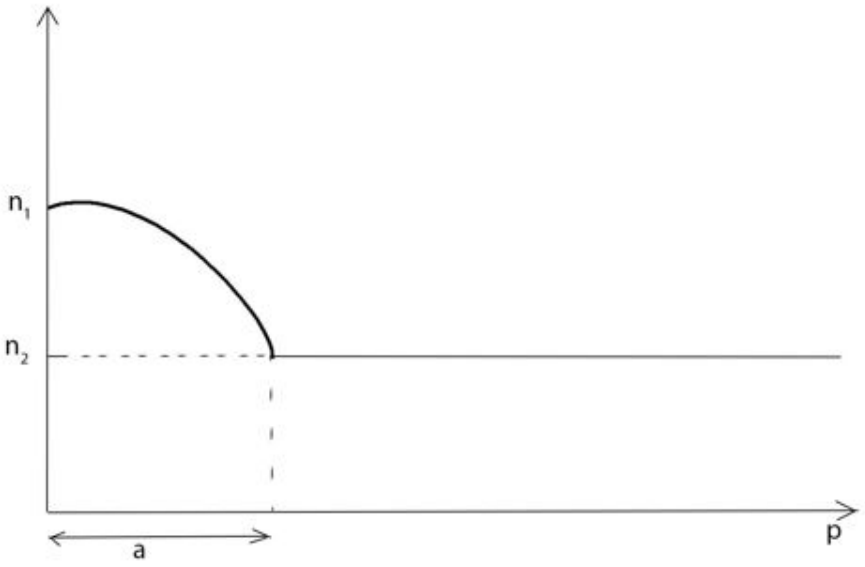

$$n^2(r_\perp) = \begin{cases} {n_1}^2 - ({n_1}^2 - {n_2}^2)\left(\frac{r_\perp}{a}\right)^q & r_\perp \le a \\ {n_2}^2 & r_\perp > a \end{cases} \qquad (41)$$

(for q→∞ one recovers the step-index fiber).

In particular for q=2

$$\begin{cases} n(r_\perp) = n_1\sqrt{1 - \frac{{n_1}^2 - {n_2}^2}{{n_1}^2}(\frac{r_\perp}{a})^2} \cong n_1 - \frac{{n_1}^2 - {n_2}^2}{2n_1}(\frac{r_\perp}{a})^2 & r_\perp \le a \\ n(r_\perp) = n_1 & r_\perp > a \end{cases} \qquad (42)$$

(parabolic profile).

The Helmholtz equation, in polar coordinates reads

$$\left(\frac{\partial^2}{\partial z^2}+\frac{\partial^2}{\partial {r_\perp}^2}+\frac{1}{r_\perp}\frac{\partial^2}{\partial r_\perp}+\frac{1}{{r_\perp}^2}\frac{\partial^2}{\partial \phi^2}+n^2(r_\perp)k^2\right)E(r_\perp,\phi,z)=0 \qquad (43)$$

or , looking for solutions of the kind (*separation of variables*)

$$E(r_\perp,\phi,z)=f(r_\perp)g(\phi)e^{i\beta z},$$

$$\frac{1}{f}\left({r_\perp}^2\frac{d^2f}{d{r_\perp}^2}+r_\perp\frac{df}{dr_\perp}\right)+(n^2k^2-\beta^2){r_\perp}^2+\frac{1}{g}\frac{d^2g}{d\phi^2}=0 \qquad (44)$$

which can be satisfied by choosing

$$\begin{cases}\frac{1}{f}\left({r_\perp}^2\frac{d^2f}{d{r_\perp}^2}+r_\perp\frac{df}{dr_\perp}\right)+(n^2k^2-\beta^2){r_\perp}^2=K\\ \frac{1}{g}\frac{d^2g}{d\phi^2}=-K\end{cases} \qquad (45)$$

where K is a constant. The second equation admits of single valued solutions of the form

$$g(\phi)=e^{\pm is\phi} \qquad s=0,1,2\ldots$$

that is $K=s^2$. For s=0, the first equation reads (for q=2)

$$\frac{d^2f}{d{r_\perp}^2}+\frac{1}{r_\perp}\frac{df}{dr_\perp}+[({n_1}^2-\alpha{r_\perp}^2)k^2-\beta^2]f=0, \qquad (46)$$

where we have set $\alpha^2=\frac{{n_1}^2-{n_2}^2}{a^2}$, $\alpha=\frac{\sqrt{{n_1}^2-{n_2}^2}}{a}$.

It possesses a Gaussian solutions

$$f(r_\perp)=Ae^{-{r_\perp}^2/{w_0}^2} \qquad (47)$$

where A and w_0 are constants, ${w_0}^2=\frac{2}{\alpha k}$ and $\beta=\sqrt{{n_1}^2k^2-2\alpha k}$.

The above represents the solution inside the nucleus ($r_\perp \leq a$) but since for $r_\perp \geq a$ one has

$$e^{-r_\perp{}^2/w_0{}^2} = e^{-\frac{r_\perp{}^2 \alpha k}{w_0}} = e^{-r_\perp{}^2 \frac{(n_1{}^2 - n_2{}^2)^{1/2}}{2a} k} \leq e^{-\frac{ak\sqrt{n_1{}^2 - n_2{}^2}}{2}} = e^{-\frac{a\pi\sqrt{n_1{}^2 - n_2{}^2}}{\lambda}} \ll 1$$

we may assume the Gaussian solution to be a good approximation also for r⊥ > a. In general, one can find more general solutions of the form.

$$E_{ps}(r_\perp, \phi, z) = AL_p{}^{(s)}(2\frac{r_\perp{}^2}{w_0{}^2}) e^{-r_\perp{}^2/w_0{}^2} (\frac{r_\perp \sqrt{2}}{w_0})^s e^{\pm s\phi} e^{i\beta_{ps} z} \qquad (48)$$

where $L_p{}^{(s)}$ are the Laguerre polynomials

$$L^{(s)}{}_0(X) = 1\,, L^{(s)}{}_1(X) = s + 1 - X$$

and

$$L_2{}^{(s)}(x) = \frac{(s+1)(s+2)}{2} - (s+2)x + \frac{x^2}{2}$$

etc., while

$$\beta_{ps} = \sqrt{n_1{}^2 k^2 - 2\alpha k(p + s + 1)}. \qquad (49)$$

If instead of using cylindrical coordinates (r⊥,ϕ) we would have introduced Cartesian coordinates (x,y) the problem would still separable and we would have obtained a different class of solutions, that is

$$E_{l,m}(x, y, z) = AH_l(\frac{x\sqrt{2}}{w_0}) H_m(\frac{y\sqrt{2}}{w_0}) e^{-\frac{x^2 + y^2}{w_0{}^2}} e^{i\beta_{lm} z} \qquad (50)$$

where H_ℓ, Hm are the Hermite polynomials of order ℓ, m and

$$\beta_{lm} = \sqrt{n_1{}^2 k^2 - 2\alpha k(l + m + 1)}$$

The presence of Hermite polynomials increases the transverse width of the transverse configuration. This width , which is approximately $w_0 = \frac{\sqrt{2}}{\sqrt{k}} \frac{\sqrt{a}}{\sqrt[4]{n_1{}^2 - n_2{}^2}}$ for the fundamental mode, can be approximately expressed as $w_0\sqrt{l+1}$ $(or\ w_0\sqrt{m+1})$ for higher order modes and the consistency of the approach requires that the mode amplitude has

become less than a given (small) quantity when $x^2 + y^2 = a^2$. In this way , one can evaluate the number of graded modes, thus getting

$$N = \frac{V^2}{4} \qquad (number\ of\ guided\ modes)$$

Let us now rewrite

$$\beta_{lm} = n_1 k \sqrt{1 - 2\left[\frac{\sqrt{{n_1}^2 - {n_2}^2}}{{n_1}^2 ka}(l + m + 1)\right]}.$$

Assuming a/λ >> 1 and ${n_1}^2 - {n_2}^2 \ll {n_1}^2$ we can expand the above expression and get

$$\beta_{lm} = \left[n_1 k - \frac{\sqrt{{n_1}^2 - {n_2}^2}}{n_1 a}(l + m + 1)\right] - \frac{{n_1}^2 - {n_2}^2}{2{n_1}^3 ka^2}(l + m + 1)^2 \quad (51)$$

The group velocity of the (ℓ ,m) mode is given by

$$V_{lm} = \frac{c}{n_1 + \frac{{n_1}^2 - {n_2}^2}{2{n_1}^3 k^2 a^2}(l+m+1)^2} \qquad (52)$$

The maximum is for ℓ =m=0 and the minimum is in correspondence with the maximum order mode the guide can support. As a first approximation the fiber has no modal delay and as the second approximation, the modal delay τ can be estimated to be

$$T_m = \frac{L}{8cn_1}(n_1 - n_2)^2, \quad (53)$$

to be compared with that of a step-index fiber, which is proportional to (n_2-n_1).

As far as chromatic dispersion of a single mode is concerned, it depends on the propagation constant of a particular mode one is dealing with. For the modes of a multimode fiber for cutoff, it is reasonable to assume that

$$\beta_m(\omega) \cong n_1(\omega)\frac{\omega}{c} \qquad (54)$$

where $n_1(\omega)$ is the core refractive index. For a single mode fiber, or when considering modes near cutoff, the above equation becomes questionable since β depends on the modal configuration and on refractive index in the core, that is $n_2(\omega)$. By playing with the modal profile, if is possible to shift the mimimum of chromatic dispersion to special regions(e.g ., $\lambda \approx 1.55\mu m$) where the attenuation has a minimum (DS , dispersion shifted fibers). Also, it is possible to achieve low dispersion in a whole interval (DF, dispersion flattened fibers),e.g. ,between 1.2 and 1.6μm.

3.8 Planar symmetric dielectric waveguides

Let us consider TE modes (transverse electric)

$$E_y(x,z,t) = E_y(x)\, e^{i(\beta z-\omega t)}$$

$$H_x(x,z,t) = H_x(x)\, e^{i(\beta z-\omega t)}$$

$$H_z(x,z,t) = H_z(x)\, e^{i(\beta z-\omega t)}$$

where

$$H_x(x) = -\frac{\beta}{\omega\mu} E_y(x) \ , \quad H_z(x) = -\frac{i}{\omega\mu}\frac{dE_y(x)}{dx}.$$

Boundary conditions imply that conservation of the tangential components of E and H, that is E_y and H_z, that is of E_y and $\frac{dE_y}{dx}$.

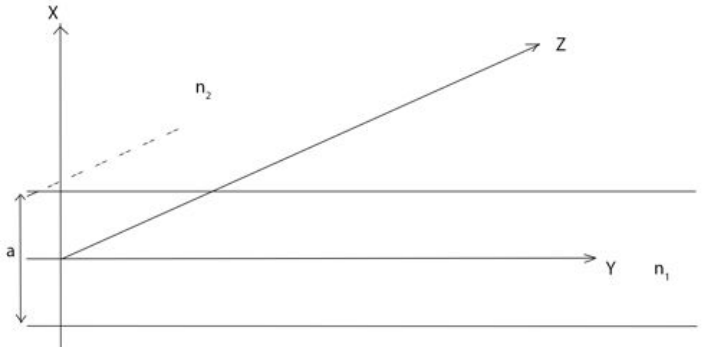

Fig. 1 Dielectric Waveguide

One expects ($K=\omega/c$) the following relation to hold

$$n_2K \le \beta \le n_1K$$

so that the Helmholtz equation reads

$$\begin{cases} \dfrac{d^2E_y}{dx^2} = -\gamma^2 E_y & |x| < a \quad (*) \\ \dfrac{d^2E_y}{dx^2} = \delta^2 E_y & |x| > a \ (**) \end{cases}$$

where γ and δ are the positive real constants given by

$$\gamma = \sqrt{{n_1}^2K^2 - \beta^2} \qquad\qquad \delta = \sqrt{\beta^2 - {n_2}^2K^2}.$$

The solutions of Eq.(*) could be either a sine (odd) or a cosine (even). Let's start with the even ones, that is

$$\begin{cases} E_y(x) = A\cos(\gamma x) & \to |x| < a \\ E_y(x) = Be^{-\delta(|x|-a)} & \to |x| > a \end{cases}$$

Enforcing the continuity of $E_y(x)$ and $\frac{dE_y(x)}{dx}$ at x=±a, we obtain

$$A\cos(\gamma a) = B\ , \qquad A\gamma\sin(\gamma a) = B\delta$$

from which

$$\tan(\gamma a) = \frac{\delta}{\gamma} \qquad (***)$$

If we write now

$$\beta \equiv n_1K(1-\xi^2) \qquad (0 \le \xi \le \frac{n_1 - n_2}{n_1})$$

we have

$$\gamma = \sqrt{{n_1}^2K^2 - {n_1}^2K^2(1-\xi^2)} = n_1K\xi$$

$$\delta = \sqrt{{n_1}^2K^2(1-\xi^2)K - {n_2}^{2^2}} = n_1K\sqrt{1 - \xi^2 - \frac{{n_2}^2}{{n_1}^2}}$$

which, together with Eq.(***) , produces a transcendental characteristic equation in the unknown ξ, that is

$$\tan(n_1 Ka\xi) = \frac{1}{\xi}\sqrt{1-\xi^2-\frac{{n_2}^2}{{n_1}^2}}\,.$$

Once ξ is found, one can derive γ and δ and then the mode structure and B (once A, which remains arbitrary, is fixed).

The previous argument can be repeated for the odd modes by taking

$$\begin{cases} E_y(x) = A\sin(\gamma x) & |x| < a \\ E_y(x) = B\,sign(x)e^{-\delta(|x|-a)} & |x| > a \end{cases}$$

and satisfying the boundary conditions

$$A\sin(\gamma a) = B$$

$$A\gamma\cos(\gamma a) = -B\delta.$$

This procedure allows one to find out both the eigen-vectors and eigen-solutions of the problem. In particular, it is convenient to express the propagation constant β in terms of the normalized quantity defined below as

$$b(V) = \frac{\left[\frac{\beta(V)}{K}\right]^2 - {n_2}^2}{{n_1}^2 - {n_2}^2},$$

with $V = Ka\sqrt{{n_1}^2 - {n_2}^2}$. The mode TE_0 has no cut-off , also if, as V→0, it is less and less confined: for $n_2 \rightarrow n_1$ it becomes a plane wave propagating along the z axis.
In the interval

$$0<V<1.7$$

it is the only propagating mode.

The previous considerations can be extended to the case of asymmetric planar wave guides, rectangular wave guides and so on.

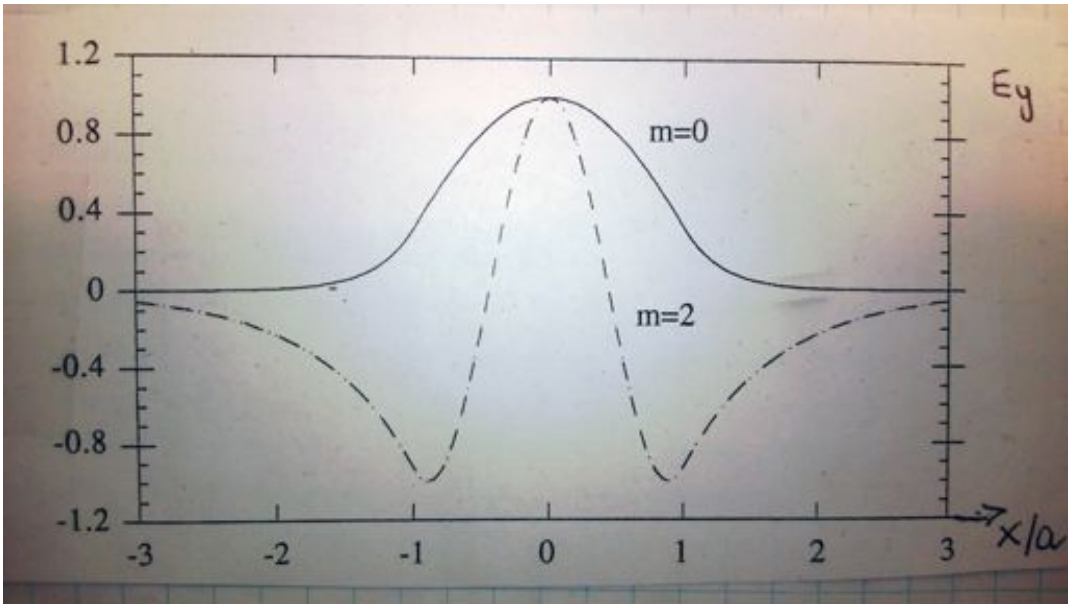

Fig. 2 Even mode profile

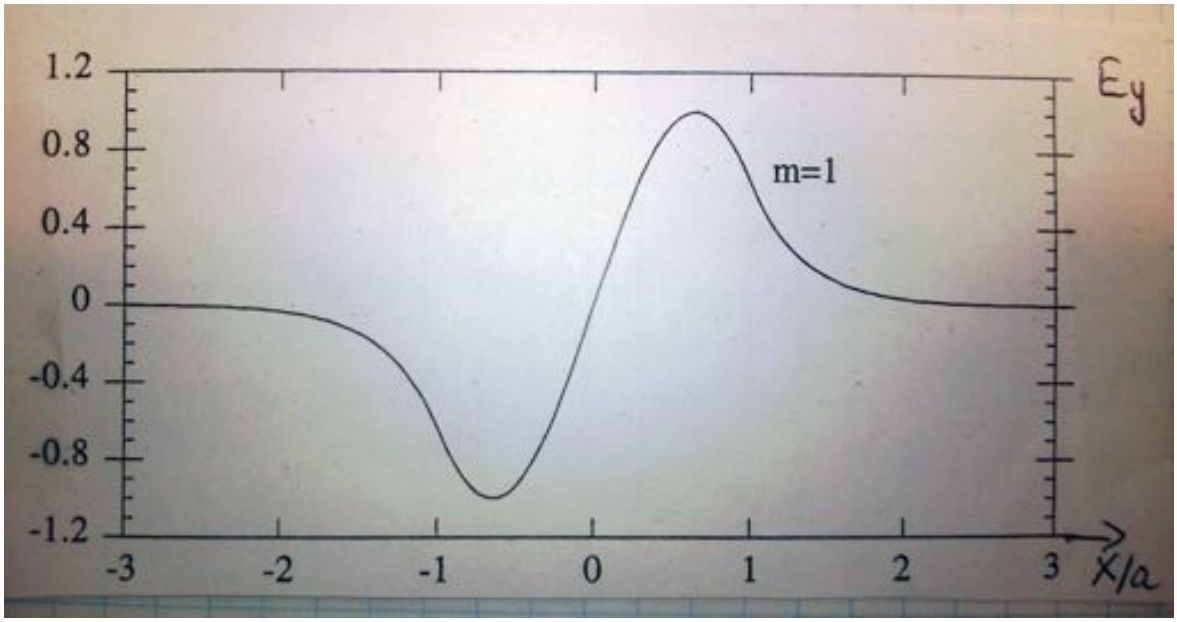

Fig.3 Odd mode profile

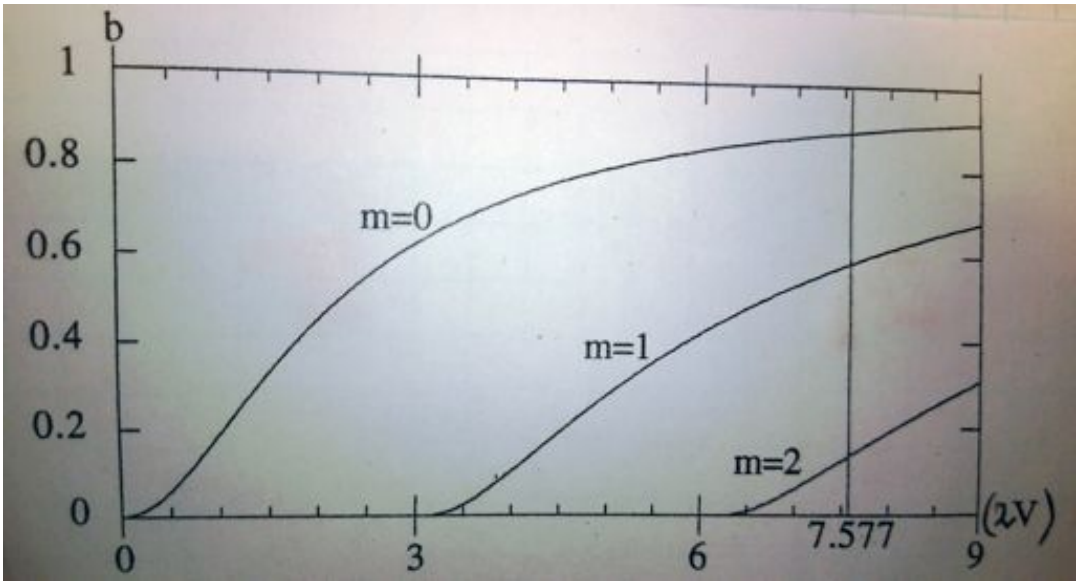

Fig. 4 Normalized propagation constant

4 Nonlinear optics

4.1 Second-order nonlinear optics

In general, in the frame of a phenomenological approach, the polarization per unit volume $\mathbf{P}(\mathbf{r},t)$, induced in a material medium by a propagating electric field, consists of both the sum of a linear term proportional to the propagating field $\mathbf{E}(\mathbf{r},t)$ and of a nonlinear one containing contributions proportional to higher-order powers of the field itself, that is

$$\mathbf{P}(\mathbf{r},t) = \mathbf{P}^{(L)}(\mathbf{r},t) + \mathbf{P}^{(NL)}(\mathbf{r},t) \equiv \mathbf{P}^{(1)}(\mathbf{r},t) + \sum_{m=2}\mathbf{P}^{(m)}(\mathbf{r},t) \ , \quad (1)$$

More specifically, allowing in general the propagation medium to be anisotropic, one has (i=x,y,z),

$$\begin{aligned} P_i(\mathbf{r},t) &= \varepsilon_0 \int_0^\infty dt' \chi_{ij}^{(1)}(\mathbf{r},t') E_j(\mathbf{r},t-t') + \\ &\varepsilon_0 \int_0^\infty dt' \int_0^\infty dt'' \chi_{ijk}^{(2)}(\mathbf{r},t',t'') E_j(\mathbf{r},t-t',t-t'') E_k(\mathbf{r},t-t',t-t'') + \ldots, \end{aligned} \quad (2)$$

where the Einstein's convention of sum over repeated indices is used. Starting from macroscopic Maxwell equations, the wave equation which describes propagation in the presence of the induced polarization $\mathbf{P}(\mathbf{r},t)$ can be written as

$$\nabla^2\mathbf{E}+\frac{1}{\varepsilon_0}\nabla\nabla\cdot\mathbf{P}=\frac{1}{c^2}\frac{\partial^2}{\partial t^2}\mathbf{E}+\mu_0\frac{\partial^2}{\partial t^2}\mathbf{P}^{(L)}+\mu_0\frac{\partial^2}{\partial t^2}\mathbf{P}^{(NL)}. \quad (3)$$

Due to the structure of $\mathbf{P}^{(NL)}$, it is obvious that the usual strategy based on performing the Fourier transform does not work in general. One has, for example,

$$\tilde{P}_i^{(2)}(\mathbf{r},\omega)=\varepsilon_0\int_0^\infty \chi_{ijk}^{(2)}(\mathbf{r},\omega',\omega-\omega')E_j(\mathbf{r},\omega')E_k(\mathbf{r},\omega-\omega')d\omega' , \quad (4)$$

so that one ends up with an integro-differential equation and it is no longer possible, as in the linear case, to take advantage of the concept of refractive index. Note that $\tilde{P}_i^{(2)}(\mathbf{r},\omega)$ is zero for material media exhibiting *inversion symmetry*, that is invariant under the inversion $\mathbf{r}\rightarrow -\mathbf{r}$, i.e., $P_i \rightarrow -P_i$ and $E_j \rightarrow -E_j$. When this property, which implies $\tilde{P}_i^{(2)}(\mathbf{r},\omega)=0$, is not present, typically in a crystal, the second-order term is non zero and gives rise to the so-called *second-harmonic generation*.

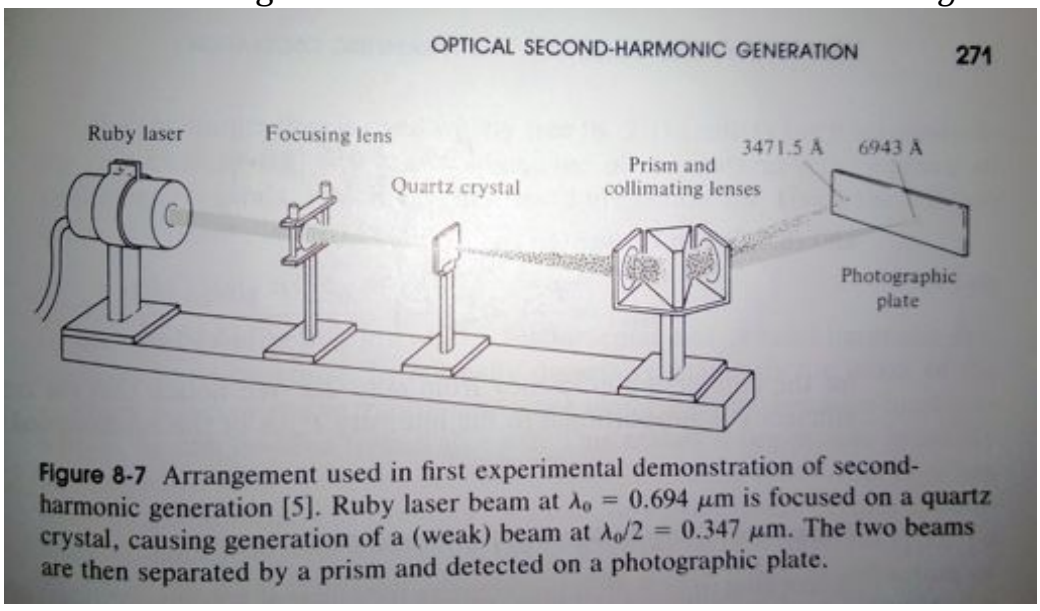

Figure 8-7 Arrangement used in first experimental demonstration of second-harmonic generation [5]. Ruby laser beam at $\lambda_0 = 0.694\ \mu m$ is focused on a quartz crystal, causing generation of a (weak) beam at $\lambda_0/2 = 0.347\ \mu m$. The two beams are then separated by a prism and detected on a photographic plate.

Fig. 1

To describe this process, it is convenient to adopt a simple heuristic approach in which initially the only a monochromatic field present

$$\mathbf{E}_1(t)=\mathbf{E}_1(\omega_1)e^{i\omega_1 t}+\mathbf{E}_1^*(\omega_1)e^{-i\omega_1 t} \quad (5)$$

gives rise to a nonlinear polarizability vibrating at a frequency $2\omega_1$ (as easily seen by inserting Eq.(5) into Eq.(2))

$$P^{(NL)}(t)=\varepsilon_0\hat{\chi}^{(2)}_{ijk}(\omega_1,\omega_1)E_j(\omega_1)E_k(\omega_1)e^{2i\omega_1 t}+c.c.= \quad (6)$$
$$q_i(2\omega_1)e^{2i\omega t}+c.c.$$

where $\hat{\chi}^{(2)}_{ijk}(\omega_1,\omega_1)$ is the *double* Fourier transform of $\chi^{(2)}_{ijk}(t',t'')$. This polarization generates in turn an electric field of the kind

$$\mathbf{E}_2(t)=\mathbf{E}_2(\omega_1)e^{i\omega_1 t}+\mathbf{E}_2^*(\omega_2)e^{-i\omega_2 t}, \quad \omega_2=2\omega_1, \quad (7)$$

which adds up to $\mathbf{E}_1(t)$ to produce a *total* field

$$\mathbf{E}(t)=\mathbf{E}_1(t)+\mathbf{E}_2(t)\ . \quad (8)$$

This field gives, in turn, rise to a nonlinear polarizability containing terms vibrating at the frequencies $\omega_1,\ 2\omega_1, 3\omega_1$ and $4\omega_1$, generating fields 0scillating at the same frequencies which add up to produce

$$\mathbf{E}(t)=\mathbf{E}_1(t)+\mathbf{E}_2(t)+\mathbf{E}_3(t)+\mathbf{E}_4(t), \quad ,$$

and so on. However, as one can check *a posteriori* , this possibility does not practically materialize unless specific conditions are met, so that, as shown later, *only the fields at* ω_1 *and* $\omega_2=2\omega_1$ *are able to survive*. Under

these circumstances, the nonlinear polarizability consists of only two terms:

$$P_i^{(NL)}(t) = \varepsilon_0[\hat{\chi}^{(2)}_{ijk}(-\omega_1;2\omega_1)E^*_j(\omega_1)E_k(2\omega_1) +$$

$$\hat{\chi}^{(2)}_{ijk}(2\omega_1;-\omega_1)E_j(2\omega_1)E^*_k(2\omega_1)]e^{i\omega_1 t} + c.c. \qquad (9)$$

$$\equiv p_i(\omega_1)e^{i\omega_1 t} + c.c.\,,$$

and the one (see Eq.(6)) vibrating at $2\omega_1$, *mutually exchanging energy* through the nonlinear interaction. Once they are inserted into the wave equation, one gets the two *coupled-equations*

$$\nabla^2 E_j(\omega_1) + \frac{\omega_1^2}{c^2\varepsilon_0}\varepsilon_{ij}(\omega_1)E_j(\omega_1) = -\mu_0\omega_1^2 p_i(\omega_1)$$

$$\nabla^2 E_i(2\omega_1) + \frac{(2\omega_1)^2}{c^2\varepsilon_0}\varepsilon_{ij}(2\omega_1)E_j(2\omega_1) = -\mu_0(2\omega_1)^2 q_i(2\omega_1) \qquad (10)$$

where $\varepsilon_{ij}(\omega)/\varepsilon_0 = \delta_{ij} + \hat{\chi}^{(1)}_{ij}(\omega)$, with the *boundary conditions*

$E_i(\omega_1, \mathbf{r}_\perp, z=0)$ and $E_i(2\omega_1, \mathbf{r}_\perp, z=0)=0$.

After writing

$$E_i(\omega_1, \mathbf{r}_\perp, z) = A_i(\omega_1, z)e^{-ik_1 z}\,,$$
$$E_i(2\omega_1, \mathbf{r}, z) = A_i(2\omega_1, z)e^{-ik_2 z},$$

where

$$k_1^2 = \frac{\omega_1^2}{c^2}[1+\hat{\chi}^{(1)}(\omega_1)] = \frac{\omega_1^2}{c^2} n^2(\omega_1) ,$$
$$k_2^2 = \frac{(2\omega_1)^2}{c^2}[1+\hat{\chi}^{(1)}(2\omega_1)] = \frac{(2\omega_1)^2}{c^2} n^2(2\omega_1), \quad (11)$$

and adopting the Slowly Varying Approximation described in connection with paraxial optics, the coupled system of Eqs.(10) becomes first order id d/dz.
If we further assume the second-harmonic field to remain a small fraction of that at ω_1 (*pump field*), we have, in this *no-depletion approximation*,

$$\frac{d}{dz} A_i(2\omega_1,z) = -i\sqrt{\mu_0/\varepsilon(2\omega_1)}(2\omega_1)\varepsilon_0 \hat{\chi}^{(2)}_{ijk}(\omega_1;\omega_1)\times$$
$$A_j(\omega_1;z-=0)A_k(\omega_1;z-=0)e^{i(k_2-2k_1)z} , \quad (12)$$

valid as long as $|A_i(2\omega_1,z)| << A_j(\omega_1,z=0)$.
The growth of $A_i(2\omega_1,z)$ is strongly influenced by the phase-factor

$$e^{i(k_2-2k_1)z} = e^{i\Delta kz} \rightarrow \Delta k = (k_2-2k_1) = k(2\omega_1) - 2k(\omega_1), \quad (13)$$

the maximum efficiency of the process corresponding to the *phase-matching condition* $\Delta k \cong 0$. Integrating Eq.(12) one gets

$$A_i(2\omega_1,z) = -\frac{1}{(2\omega_1)nc}\sqrt{\mu_0/\varepsilon(2\omega_1)}(2\omega_1)\varepsilon_0 \hat{\chi}^{(2}_{ijk}(\omega_1;\omega_1)\times$$
$$A_j(\omega_1;z-=0)A_k(\omega_1;z-=0)\frac{e^{i\Delta kz}-1}{i\Delta k} , \quad (14)$$

so that the ratio between the power at $2\omega_1$ and that at ω_1, over a crystal of length L, reads

$$\frac{P(2\omega_1)}{P(\omega_1)} = F\omega_1^2 I(\omega_1) L^2 \frac{\sin^2(\Delta kL/2)}{(\Delta kL/2)^2} \quad , \ (15)$$

where F is a factor dependent on the material and $I(\omega_1)$ the intensity of the pump field. Note that $\Delta k \cong 0$ implies

$$k(2\omega_1) \cong 2k(\omega_1) \rightarrow \frac{2\omega_1}{c} n(2\omega_1) = 2\frac{\omega_1}{c} n(\omega_1) \rightarrow n(2\omega_1) = n(\omega_1) \ , (16)$$

a condition which cannot be realized in the frame of *normally dispersive materials* where the index of refraction increases with ω.
The coherence length ℓ_c of the process , defined as the maximum crystal length useful to produce second-harmonic power, is given by

$$\ell_c = \frac{2\pi}{\Delta k} = \frac{2\pi}{k(2\omega_1) - k(\omega_1)} \quad , \quad (17)$$

and typically is of the order of 50 μm. In order to enhance it, one can take advantage of the *natural birefringence* of anisotropic crystals where different polarizations can have different values of the refractive-indices In this case one can, under certain circumstances, satisfy the condition required by Eq.(16) by choosing two different kind of waves.
More precisely (see,e.g., A. Yariv, Optical Electronics in Modern Communications) , one can describe propagation in a uniaxial crystal in a *principal axes* system x, y, z such that the relation between the polarizability **P** and the em field **E** reads

$$P_X = \varepsilon_0 \chi_{11} E_X, \ P_Y = \varepsilon_0 \chi_{11} E_Y, \ P_Z = \varepsilon_0 \chi_{33} E_Z \ , \quad (18)$$

z being the crystal *optical axis*.
One can have a wave, polarized in a direction orthogonal to z, behaving as a wave in an isotropic medium of refractive index

$n=n_0(1+\chi_{11})^{1/2}$ (*ordinary wave*), and one, (*extraordinary wave*) propagating at an angle θ with respect to z, possessing an effective refractive index $n_e(\theta)$ obeying the relation

$$\frac{1}{n_e^2(\theta)}=\frac{\cos^2(\theta)}{n_0^2(\omega)}+\frac{\sin^2(\theta)}{n_e^2(\omega)}, \qquad n_e(\omega)=1+\sqrt{1+x_{33}(\omega)} \quad . \text{(19)}$$

If $n_e(2\omega)<n_0(\omega)$, there is an angle θ_m such that

$$n_e(2\omega,\theta_m)=n_0(\omega) ,$$

which, according to above, is given by

$$\sin^2(\theta_m)=\frac{[n_0(\omega)]^{-2}-[n_0(2\omega)]^{-2}}{[n_e(2\omega)]^{-2}-[n_0(2\omega)]^{-2}} \quad . \text{(20)}$$

4.2 Soliton propagation

The third order nonlinear term of polarizability approximately reads, for a fast responding isotropic material (like glass)

$$P^{(3)}(t)=\varepsilon_0\bar{\chi}^{(3)}E^3(t)=\frac{\varepsilon_0\bar{\chi}^{(3)}}{8}(\hat{E}(t)+\hat{E}^*(t))^3 \quad \text{(21)}$$

where E is the linear polarized propagating field.

If the field is narrow-band, we can approximately write

$$\hat{E}(t)=A(t)e^{i\omega_0 t}, \qquad \text{(22)}$$

where A(t) is a slowly-varying (over a scale comparable to $1/\omega_0$) function of time. Accordingly, one obtains

$$P^{(3)}(t) = \frac{\varepsilon_0 \bar{\chi}^{(3)}}{8}[A^3(t)e^{3i\omega_0 t} + A^{*3}(t)e^{-3i\omega_0 t} + 6|\hat{E}(t)|^2 E(t)]$$

so that, neglecting the terms vibrating at very high frequencies (which tend to average to zero unless special conditions, like phase matching , are met) one has

$$P^{(3)}(t) = \frac{3}{4}\varepsilon_0 \bar{\chi}^{(3)}\left|\hat{E}(t)\right|^2 E(t)\,. \quad (23)$$

Taking now the Fourier transform of both sides (in the frequency interval relevant to the propagating field bandwidth) one gets

$$P^{(3)}(\omega) = \frac{3}{4}\varepsilon_0 \bar{\chi}^{(3)}\left|\hat{E}(t)\right|^2 E(\omega), \quad (24)$$

so that , formally , it is still possible to introduce a (time-dependent) dielectric constant of the medium ε(ω).

4.3 Optical Kerr effect

The general propagation equation of the field reads

$$\nabla^2 \boldsymbol{E} + \frac{1}{\varepsilon_0}\nabla\nabla.\boldsymbol{P} = \mu_0\varepsilon_0 \frac{\partial^2 \boldsymbol{E}}{\partial t^2} + \mu_0 \frac{\partial^2 \boldsymbol{P}^{(L)}}{\partial t^2} + \mu_0 \frac{\partial^2 \boldsymbol{P}^{(NL)}}{\partial t^2}\ , \quad (25)$$

where

$$\boldsymbol{P}^{(NL)} = \boldsymbol{P}^{(3)} = \frac{3}{4}\varepsilon_0 \bar{\chi}^{(3)}\left|\widehat{\boldsymbol{E}}(\boldsymbol{r},t)\right|^2 \boldsymbol{E}(\boldsymbol{r},t). \quad (26)$$

Taking the Fourier transform of both sides we can still introduce a time –dependent refractive index from the relation

$$D_\omega = \varepsilon_0 E_\omega + P_\omega = \varepsilon_0\left(1 + \chi^{(1)}{}_\omega\right)E_\omega + \frac{3}{4}\varepsilon_0 \bar{\chi}^{(3)}\left|\hat{E}(t)\right|^2 E_\omega$$

$$\frac{\varepsilon(\omega)}{\varepsilon_0} = \left(1 + \chi^{(1)}{}_\omega\right) + \frac{3}{4}\bar{\chi}^{(3)}|\hat{E}|^2,$$

that is

$$n = \sqrt{\frac{\varepsilon(\omega)}{\varepsilon_0}} = n_1(\omega)[1 + \frac{3}{4}\frac{\overline{\chi}^{(n)}}{n_1}|\hat{E}(t)|^2]^{1/2} \quad (27)$$

or, after introducing the *nonlinear refractive index coefficient* n_2,

$$n \cong n_1 + n_2\left|\hat{E}(t)\right|^2, \qquad n_2 = \frac{3}{8n_1}\bar{\chi}^{(3)}. \quad (28)$$

Recalling that

$$I(t) = intensity = \frac{1}{2}\frac{n_1}{Z_0}|\hat{E}(t)|^2, \quad Z_0 = \sqrt{\frac{\mu_0}{\varepsilon_0}} \approx 377 ohms,$$

one can finally write

$$n = n_1 + 2\frac{n_2}{n_1} z_0 I \equiv n_1 + \tilde{n}_2 I \quad (Optical\ Kerr\ effect). \quad (29)$$

Intuitive approach

Kerr nonlinearity is responsible for:

1) Self-focusing (or defocusing)
2) Self phase modulation .

1) <u>Self-focusing</u>

$$n(\omega, r_\perp) = n_1(\omega) + \tilde{n}_2 I(r) \ , \quad (30)$$

resulting in *self-induced waveguide* $n(\omega, 0) > n(\omega, r_\perp)$ (and eventually catastrophic collapse), or defocusing if $\tilde{n}_2 < 0$.

2) <u>Self-phase modulation</u>

$$E(z,t) = E_0 e^{i\omega t - i\frac{\omega}{c}n_1(\omega)z - i\frac{\omega}{c}\tilde{n}_2 I(t)z} \quad (31)$$

resulting, for $\tilde{n}_2 > 0$, in a frequency-shift

$$\delta\omega = \frac{d\Phi}{dt} = -\frac{\omega}{c}\tilde{n}_2 z \frac{dI(t)}{dt} = \begin{cases} < 0 & for\ \frac{dI}{dt} > 0 \\ > 0 & for\ \frac{dI}{dt} < 0 \end{cases}$$

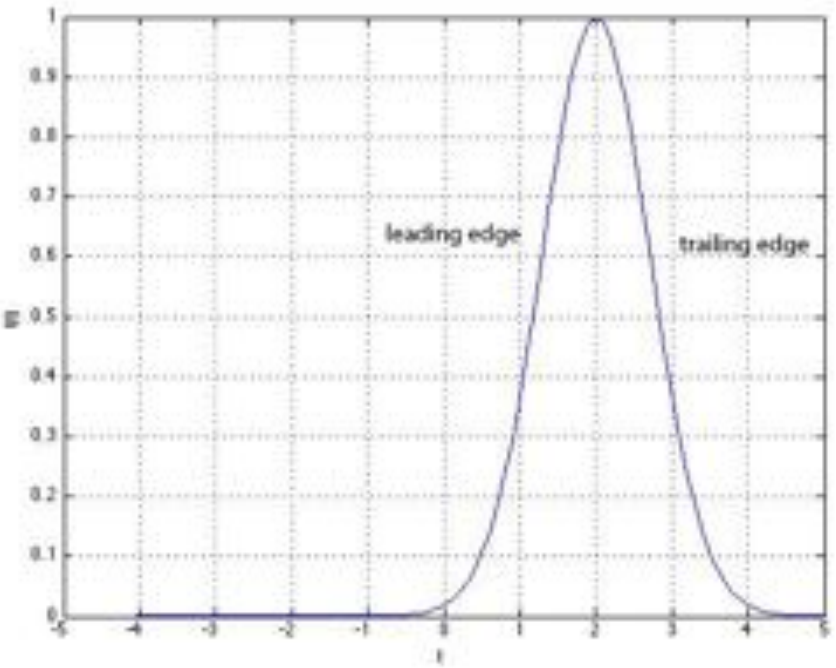

Fig. 1 Leading edge of the pulse in downshifted, trailing edge of the pulse is up-shifted.

If $dV_g(\omega)/d\omega > 0$ (positive group-velocity dispersion) the leading edge is slowed down while the trailing edge is accelerated: the pulse is compressed (self-compression).

If $dV_g(\omega)/d\omega < 0$ (negative group-velocity dispersion) the leading edge is accelerated while the trailing edge is slowed down: the pulse is broadened (self-broadening).

Since

$$\frac{d^2k}{d\omega^2} = \frac{d}{d\omega}\frac{dk}{d\omega} = \frac{d}{d\omega}\frac{1}{V} = -\frac{dV/d\omega}{V^2} \quad , \qquad \left(V = V_g = \left(\frac{dk}{d\omega}\right)^{-1}\right),$$

compression can be achieved if $\frac{d^2k}{d\omega^2} < 0$ (for $\lambda \geq 1.3\mu$ in silica)

broadening occurs if $\frac{d^2k}{d\omega^2} < 0$ (for $\lambda < 1.3\mu$ in silica).

The analytic solution of the problem can be sought for by using the propagation equation valid in the paraxial and slowly varying approximation (see Eq. (135) of the first part of lecture notes), that is, after writing

$$E(r_\perp, z, t) = A(r_\perp, z, t)e^{i\omega_0 t - ik(\omega_0)z},$$

$$(\frac{1}{V}\frac{\partial}{\partial t} + \frac{\partial}{\partial z} + \frac{i}{2k_0}\nabla^2{}_\perp - \frac{i}{2}(\frac{d^2k}{d\omega^2})_{\omega_0}\frac{\partial^2}{\partial t^2})A(r_\perp, z, t) = -ik_0\frac{\delta n}{n_1}A(r_\perp, z, t),$$

or, after introducing the change of variable $t' = t - z/V$,

$$(\frac{\partial}{\partial z} + \frac{i}{2k_0}\nabla^2{}_\perp - \frac{i}{2}\left(\frac{d^2k}{d\omega^2}\right)_{\omega_0}\frac{\partial^2}{\partial t'^2})A(r_\perp, z, t') = -ik_0\frac{\delta n}{n_1}A(r_\perp, z, t'). \quad (32)$$

In the case of the third order Kerr nonlinearity, the above equation takes the form

$$(\frac{\partial}{\partial z} + \frac{i}{2k_0}\nabla^2{}_\perp - \frac{i}{2}\left(\frac{d^2k}{d\omega^2}\right)_{\omega_0}\frac{\partial^2}{\partial t'^2})A(r_\perp, z, t') =$$
$$-ik_0\frac{n_2}{n_1}|A(r_\perp, z, t')|^2 A(r_\perp, z, t') . \quad (33)$$

One can now work separately the case of a plane-wave solution (that is, $A(r_\perp,z,t')=A(z,t')$) and that of a monochromatic wave , that is $A(r_\perp,z,t')=A(r_\perp,z)$ (in particular $A(r_\perp,z,t')=A(x,z)$)).

The associated *nonlinear propagating equation* , usually referred to as Nonlinear Schroedinger Equation (NLS), reads

$$\left[\frac{\partial}{\partial z} - \frac{i}{2}\gamma\frac{\partial^2}{\partial t'^2}\right]A(z,t') = -ik_0\frac{n_2}{n_1}|A(z,t')|^2A(z,t') \qquad (34)$$

and

$$\left[\frac{\partial}{\partial z} + \frac{i}{2k_0}\nabla_\perp{}^2\right]A(z,t') = -ik_0\frac{n_2}{n_1}|A(r_\perp,z)|^2A(r_\perp,z)\,, \quad (35)$$

where $k_0=(\omega_0/c)n_1(\omega_0)$ and we have set $\gamma = \left.\frac{d^2k}{d\omega^2}\right|_{\omega=\omega_0}$ (for silica, $n_2\approx10^{-22}$(m/Volts)^2, $\tilde{n}_2$=5x10^{-16} cm^2/Watts).

An equation completely analogous to Eq.(34) can be derived for propagation in a *single-mode fiber* after writing, ($\varepsilon(r_\perp)$ being the modal spatial configuration,

$$E(r_\perp,z,t) = \varepsilon(r_\perp)e^{i\omega_0 t - i\beta(\omega_0)z}A(z,t).$$

The only difference is the substitution of $k(\omega_0)\frac{n_2}{n_1} \rightarrow k(\omega_0)\frac{n_2}{n_1\sigma}$, where σ represents the <u>effective area</u> of the fiber mode, that is

$$\frac{1}{\sigma} = \frac{\int_{-\infty}^{\infty}\varepsilon^4(r_\perp)dxdy}{\int_{-\infty}^{\infty}\varepsilon^2(r_\perp)dxdy}\,, \quad (36)$$

having assumed the mode to be normalized,

$$\int_{-\infty}^{\infty}\varepsilon^2(r_\perp)dxdy = 1.$$

In general, Eq. (34) and Eq. (35) do not admit of analytic solutions if both the diffusive (diffractive) and nonlinear terms are included. If one of the two is neglected then the solutions of Eq.(34) (something analogous holding for Eq.(35)) read, respectively , (t' = t-z/V_g)

$$A(z,t) = \left(\frac{-i}{2\pi z\gamma}\right)^{\frac{1}{2}}\int_{-\infty}^{\infty}e^{\frac{i}{2z\gamma}[t"-t']^2}\,A(z=0,t'')dt'' \quad (37)$$

(chromatic-dispersion dominated)

and

$$A(z,t) = e^{-\left[ik\frac{n_2}{n_1}\left|A(z=0,t')\right|^2 z\right]}A(z=0,t') \quad (38)$$

(nonlinearity dominated) .

The dispersion dominated regime corresponds to the temporal spreading due to chromatic dispersion. The nonlinearity dominated regime corresponds to self-phase modulation. The interplay between the two regimes can lead in the case of $\gamma<0$ (anomalous dispersion) to an exact compensation between the two effects, thus producing solutions which propagate without distortion called "bright" temporal solitons.

Same argument holds if " dispersion" is replaced by "diffraction", the distortion-less solution of Eq.(35) being referred to as a "bright" spatial soliton.

In the case of a temporal solutions, in order to prove their existence, we write

$$A(z,t') = e^{i\alpha z}A(t') \,,$$

which, inserted into Eq.(34) yields the eigen-value equation

$$\alpha A(t') - \frac{1}{2}\gamma\frac{d^2}{dt'^2}A(t') = -\frac{kn_2}{n_1}|A(t')|^2A(t') \quad (39)$$

By direct integration, it can easily be proved that the solution of Eq. (39) results in the temporal soliton

$$A(z,t') = A_0 e^{\frac{i\gamma z}{2T^2}}\,\mathrm{sech}\left(\frac{t'}{T}\right) \quad , \qquad (40)$$

the hyperbolic secant (sech(x)) being the inverse of the hyperbolic cosine (cosh(x), that is sech(x)=1/cosh(x), provided that

$$-\frac{\gamma}{T^2} = \frac{k_0 n_2}{n_1} |A_0|^2 \,. \qquad (41)$$

Note that we have assumed $n_2>0$, so that γ has to be negative ($\gamma<0$, anomalous dispersion)).
The same approach can be used for *spatial propagation*, looking for solutions of the kind

$$A(x,z) = A_0 e^{-\frac{iz}{2k_0 l^2}} \operatorname{sech}\left(\frac{x}{l}\right) \qquad (42)$$

whose existence condition reads

$$\frac{1}{k_0^2 \ell^2} = \frac{n_2}{n_1} |A_0|^2 \quad , \ (43)$$

or, equivalently,

$$\frac{1}{(2\pi)^2}\left(\frac{\lambda}{l}\right)^2 \approx \frac{1}{(2\pi)^2} tan^2(\theta_D) = \frac{\tilde{n}_2}{n_1} I \quad ,$$

where θ_D is the diffraction angle. This shows how to use optical Kerr effect to compensate for a not too large diffraction angle θ_D. However, a large intensity is usually required in silica and similar materials, whose nonlinear response is basically associated with the electronic cloud. Conversely, the peak-power(P) required to generate a temporal soliton in a single mode optical fiber is quite reasonable (for λ=1.55 μm and T=10 psec one finds P=50mW), this being due to the strong confinement associated with the small traverse area of the fiber. Note that the procedure followed to prove the existence of 1-D spatial solitons *cannot* be trivially extended to the 2D case where things become more complicated. Also, soliton-like solutions of the NLS exist whenever the input field is N times (N integer) the field generating the fundamental soliton, that is (see Eq. (41))

$$A(z=0,t) = NA_0 \operatorname{sech}\left(\frac{t}{T}\right) \quad . \quad (44)$$

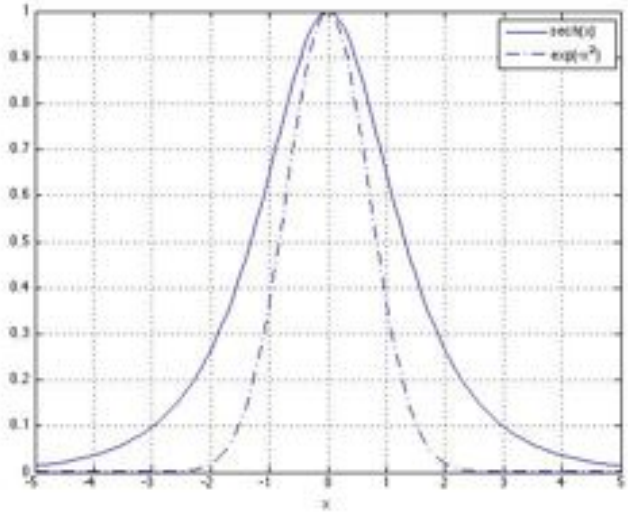

Fig.2 Plot showing the different behavior of the Gaussian and Hyperbolic Secant function.

They are not shape-invariant but periodic (see Figs. 4 and 5) , with a spatial period

$$z_0 = \pi T^2 |A_0|/2$$

A typical value of z_0 can be of the order of 8km, for the case of a single-mode fiber.

The fundamental solutions described above are called bright solitons. It is also possible to propagate *absence of light* (*darkness*), thus getting fundamental dark solitons ($n_2<0$, $\gamma>0$) by the change sech(x) → tanh(x) (see figure below). However, they carry an infinite amount of energy and cannot correspond to a realistic case if not approximately.

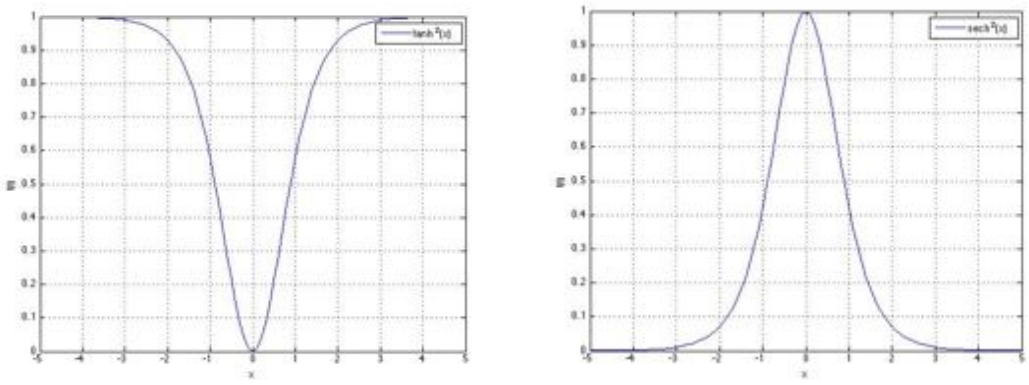

Fig.3 Dark and bright solitons

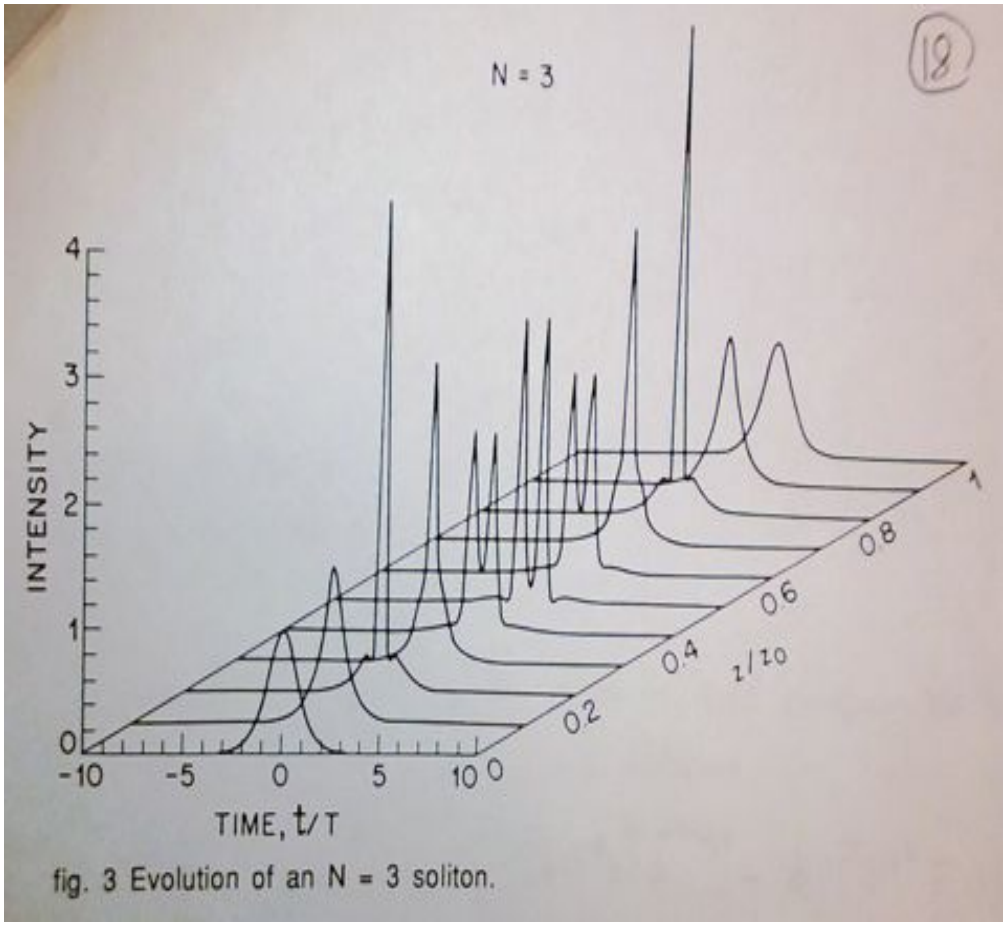

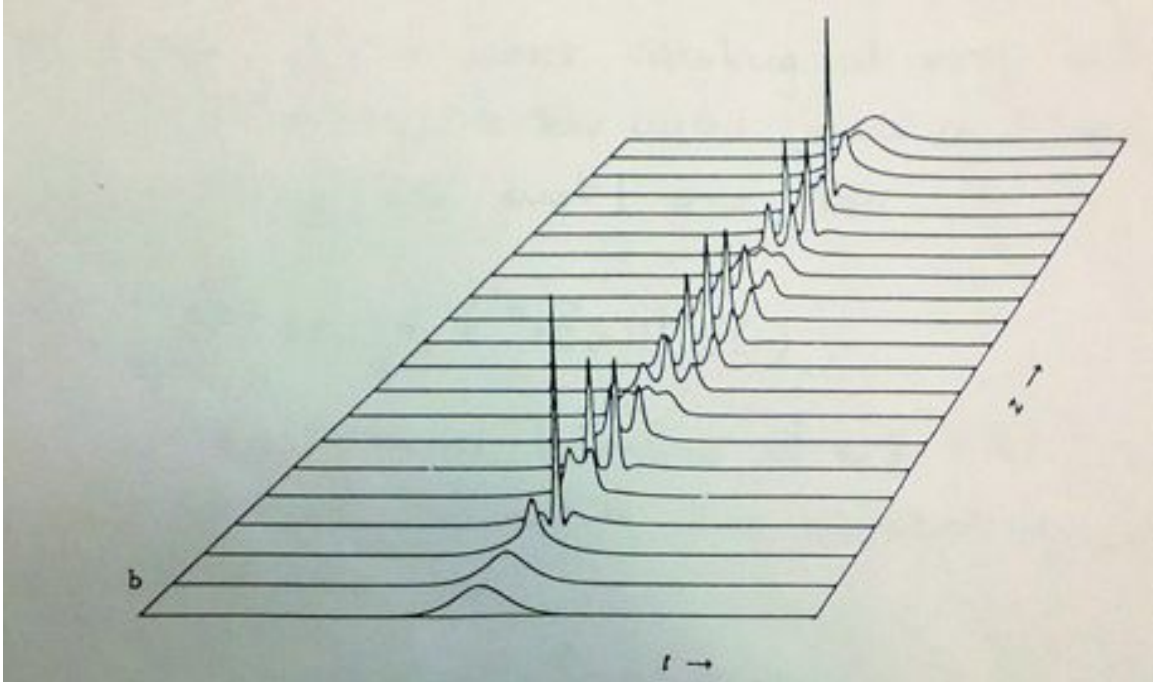

fig. 4 Evolution of an N = 4 soliton.

ACKNOWLEDGMENTS
The author wishes to thank Abhiram Moturi for his precious help in editing these lecture notes